

AFIT/GAE/ENY/92M-01



# AN EXAMINATION OF WING ROCK FOR THE F-15

THESIS

Michael T. Davison, Capt, USAF

AFIT/GAE/ENY/92M-01

Approved for public release; distribution unlimited



AFIT/GAE/ENY/92M-01

# AN EXAMINATION OF WING ROCK FOR THE F-15

THESIS

Presented to the Faculty of the School of Engineering

of the Air Force Institute of Technology

Air University

In Partial Fulfillment of the

Requirements for the Degree of

Master of Science in Aeronautical Engineering

Michael T. Davison, B.S.

Captain, USAF

February 1992

Approved for public release; distribution unlimited



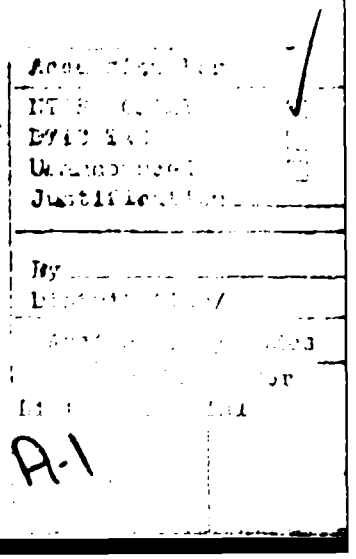

## Preface

The purpose of this study was to examine the some of the problems encountered in high angle-of attack flight, namely wing rock. This was done both analytically, through bifurcation analysis and computer simulation, and experimentally, through flight test. In all phases of the research, I am indebted to those who have lent invaluable assistance.

First off, I would like to thank Capt Jim Planeaux, without whose assistance this study would not be possible. He kept this research on track during its beginning phases. His knowledge of aircraft dynamics and the problems experienced in bifurcation analysis was indispensable, as were the simulation and driver programs he lent me. I would also like to thank Capt Jeff Beck, who developed both the 12 and 35 state driver models for the bifurcation analysis, for lending assistance when the research was snagged by a problem with the driver programs or with the AUTO software. I would also like to thank Capt Dan Baumann, for his insights on the aerodynamic model he developed.

In the flight test portion, I owe a great deal of gratitude to Capt Paul Lockhart and Capt Bob Mlnarik (USMC), who suffered through my attempts at managing a test, and flew the majority of the test missions. I know both of them found flying the F-15D difficult. I would also like to thank the 3246th Test Wing at Eglin AFB FL,

and most notably Maj Mark "Roman" Polansky and Maj Randy Neville, who graciously loaned us the F-15D, and worked hard to make this research a success. Finally, I would like to thank Maj Dan Gleason, who guided me throughout the two years both AFIT and TPS and without whose support this research would never have been completed.

TABLE OF CONTENTS

## List of Figures

## List of Tables

## List of Symbols

$\alpha$ : angle of attack, degrees
$\beta$ : sideslip angle, degrees
c : control parameter
$\phi$ : bank or roll angle, degrees
$\psi$ : heading angle, degrees
$\theta$ : pitch angle, degrees
b : wing span, feet
$C_L$ : lift coefficient
$C_l$ : rolling moment coefficient
$C_{l_\beta}$ : dihedral effect
$C_{l_p}$ : roll damping
$C_m$ : pitching moment coefficient
$C_n$ : yawing moment coefficient
$C_{n_\beta}$ : directional stability
$C_x$ : x axis force coefficient
$C_y$ : y axis force ccefficient
$C_z$ : z axis force coefficient
C.G. : center of gravity
f : vector function describing system or aircraft dynamics
g : gravitational constant, 32.174 ft/sec$^2$
I : aircraft inertia tensor
$I_x$ : moment of inertia about x axis, slug ft$^2$
$I_y$ : moment of inertia about y axis, slug ft$^2$
$I_z$ : moment of inertia about z axis, slug ft$^2$
$I_{xz}$ : product of inertia in x and z direction. slug ft$^2$
L : rolling moment, ft lbf
M : pitching moment, ft lbf
M : Mach number
m : aircraft mass, slugs
N : yawing moment, ft lbf
p : roll rate, radians/second
q : pitch rate, radians/second
q : dynamic pressure, lbf/ft$^2$
r : yaw rate, radians/second
S : wing planform area, ft$^2$
T : thrust force, lbf
TAS : true airspeed, ft/sec
t : time, seconds
u : vector of system or aircraft states
$V_{tr}$ : true airspeed, ft/sec

## Abstract

Wing rock in the F-15 was examined both analytically and experimentally. Using a previously developed model for the F-15, bifurcation analysis and continuation techniques were used to map out the periodic wing rock solutions and the equilibrium solutions leading up to wing rock. This was done for four maneuvers; a 1 g stall, rudder sweeps, constant bank turns and a symmetric pullup. To supplement this research, time history simulations were used to examine the time history of wing rock. A study of stability derivatives was also done, to determine the critical parameters in wing rock. Bifurcation was also used to study candidate feedback architectures used to suppress wing rock. It was found that feeding back roll rate was effective in delaying wing rock onset and suppressing the subsequent motion, but this made the aircraft more departure prone.

The results from the 1 g stall, constant bank turns, and the symmetric pullup were experimentally tested through flight test. Wing rock onset differed 4 degrees AOA from predicted in all maneuvers but the symmetric pullup, where the flight mach number correlated with the computer model's flight condition. Wing rock was found to be highly random and non periodic, directly contradicting computer predictions and prior research.

# I. Wing Rock Analysis of the F-15

Throughout the history of aviation, man has been extending the performance capabilities of fighter aircraft. Traditionally this was done by increasing the aircraft's speed, altitude, range, and armament, all while keeping the aircraft's turning radius as small as possible. While flight envelopes have grown, certain regions in the flight envelope have been off-limits, namely the region on the lift curve approaching stall. As aviation evolved into the high performance jet fighters of today, this region held particular dangers for the pilots: aircraft departed violently, sometimes rolling or yawing viciously as they stalled, leaving the pilots in unrecoverable flat spins. Thus, the region near stall became a very dangerous region that was best avoided.

Despite the tremendous increase in speed brought about by even more advanced turbojet engines, combat experience showed that dogfighting between two opposing aircraft was still prevalent. This was graphically borne out in the Vietnam conflict, where heavier and sluggish F-4's and F-105's were forced to engage the slower, yet more nimble MiG-17's and MiG-21's.

Dogfighting, or Air Combat Maneuvering (ACM) involves often tight turns that push the fighters operational capability. One of the boundaries reached by fighter

aircraft in the ACM environment is the limit of useful angle of attack (AOA). Often, this is exceeded in ACM, with disastrous results. The aircraft with a wider AOA envelope gives the pilot an advantage over his adversary.

Before stall and departure are reached in combat aircraft however, a variety of nonlinear phenomena are encountered, leading to a degradation of the aircraft's flying qualities. The first of the nonlinear phenomena encountered is wing rock. Wing rock is defined as a lightly damped rolling motion, and is exhibited in many combat aircraft as angle of attack is increased (1:1). Wing rock imposes tracking limitations on aircraft at high AOA, and can cause other safety and flying qualities problems. For example, wing rock can be easily excited by lateral control inputs, and severe pilot induced oscillations (PIO) can be experienced, resulting in controllability problems ranging from degradation of tactical effectiveness during combat maneuvers to flight safety during landing (2:3).

Wing rock may be experienced throughout the entire velocity envelope, but the root causes of the phenomenon vary over the flight envelope. In slow, subsonic, high AOA flight, wing rock can be triggered by the interaction of the aircraft forebody flow with the downstream components; i.e. non symmetrical vortex shedding off the forebody and impinging on the vertical stabilizer. As Mach number is

increased however, the onset AOA decreases and the flow asymmetry changes. For example, in the F-5 aircraft at transonic speeds, wing rock is driven by shock induced separation, and is a completely wing dominated phenomenon. This characteristic is not unique to the F-5, as many current combat aircraft exhibit wing rock over a wide range of flight conditions in which the character of the motions and the aerodynamics that cause them vary significantly (2:5).

## Overview of Investigation

The purpose of this investigation is to analytically study the wing rock phenomena of the F-15, using bifurcation and continuation techniques. The validity of the analysis and aerodynamic model was then verified through a series of flight tests performed at the Air Force Test Pilot School at Edwards AFB CA. To support the objectives, the high AOA aerodynamic model developed by Baumann (10) is combined with the control system models developed by Beck (13) for a realistic model of the aircraft dynamics.

The F-15 was picked for this investigation primarily due to the work previously done by Beck and Baumann on the control models and aerodynamics of the F-15. These models lend themselves to a thorough analysis of the wing rock phenomenon because they need only further refinement, and

not a full development, which can be a research project in and of itself.

There are four distinct areas that this investigation covers:

I. Investigation of wing rock throughout the F-15 maneuvering envelope. This involves three different maneuvers: 1-g approach to stall, steady state turns, and steady pullups. The 1-g approach to stall flight condition was investigated in reference 13, so it provides a good starting point as well as a check to the current investigation. The other two flight conditions were chosen as they represent maneuvers commonly encountered in flight, and especially in ACM.

A specific flight test program then investigate wing rock during these maneuvers, with flight parameters set as close as possible to model parameters, in an effort to validate and expose any weaknesses in the analytical work done on the phenomena.

II. Investigate the effects of the F-15 Control Augmentation System (CAS) on wing rock. There is evidence in reference 13 that a slightly modified CAS system has a profound effect on suppressing

wing rock. This is further investigated by modeling the F-15 with and without its CAS system.

III. Investigate the changes in aerodynamic coefficients as AOA is increased. It is known that roll damping is an important parameter in wing rock and the roll damping derivative is the primary determinant of dutch roll damping at high AOA. By observing what changes occur to the critical stability derivatives as a computer simulator of the aircraft approaches and enters wing rock, the dominant parameters can be identified, in the hope that the results will yield additional insight into the previous research in this area, and aid in selecting an adequate flight control scheme to solve the problem.

IV. Investigate control system solutions to wing rock. This phase consists of researching the literature for existing high AOA flight control data and applying this data to the F-15 model, to find candidate feedback architectures that will suppress the wing rock problem. Simple model feedback architectures will be developed in

conjunction with the results of section three and the literature search, to modify the coefficients that are most greatly affected by the limit cycles.

## Overview of Thesis

The following chapter reviews some of the basic principles of bifurcation theory, to orient the reader with the terminology and the basic principles of this new analysis method. Chapter 3 reviews the research done on wing rock, covering some of the basic aerodynamics driving the phenomena, reviewing past research, and covering some of the benefits of suppressing wing rock. Chapter 4 goes into greater depth on the structure of wing rock, using computer simulation to analyze the dynamics of the F-15B as it enters wing rock. The bifurcation model is also introduced as a way to detect the onset of wing rock, as well as the length and stability of the periodic branch that maps wing rock. Furthermore, flight test results are compared to both the computer simulation of wing rock dynamics and the prediction of wing rock onset point as modeled by the bifurcation method. Covered at the end of the chapter is an analysis of some of the more important stability derivatives that previous researchers have identified as important, to see how they contribute to the phenomena in the F-15B. This part of the analysis is aided

by comparing the F-15B to a variety of other aircraft that exhibit the same phenomena, to see if there is one stability derivative dominant in wing rock.

Chapter 5 examines wing rock in maneuvering flight. This expands on the 1-g stall that served as the basis for previous studies of wing rock by examining the limit cycle solutions that occur while the aircraft is performing basic maneuvers, such as steady turns and pullups. Computer models are compared to flight test results to examine how close both correlate. Also examined is when wing rock is encountered as only the rudder is varied.

Chapter 6 covers various simple feedback architectures that were tried to examine their effect on wing rock. Both roll rate feedback to the aileron and differential tail are examined as well as angle of attack and roll rate feedback to the rudder. Also examined is the 35 state reduced order model of the F-15 control augmentation system (CAS) to examine the effects of a modified (but still realistic) F-15 flight control system on high angle of attack aerodynamics.

Finally Chapter 7 covers the results of the research, and makes recommendations as to what directions future research could take.

# II. Bifurcation Theory

To understand how an aircraft transitions from equilibrium flight to the steady periodic motion known as wing rock, this study has used bifurcation theory. Bifurcation theory is the classical mathematical discipline that treats non-linear phenomena (20:xi). This chapter is to orient the reader on some of the basic principles and terminology of this discipline that was applied to this research. Most of this chapter is derived from Seydel (20), which the reader is referred to for an excellent discussion on this topic. The driver program used in this research, AUTO, will also be outlined.

## Equilibrium and Stability

The motion of non-time dependent systems can be mathematically written as

$$\dot{u} = f(u) \tag{1}$$

where **u** is the state vector. This system would said to be in equilibrium if

$$0 = f(\mathbf{u}) \tag{2}$$

Physically, equilibrium represents a system at rest or in uniform motion, such as an aircraft with no translational or angular accelerations, and with its roll and pitch

angles constant. The points that satisfy equation (2) are known as **equilibrium points**.

The **stability** of a system is determined by its behavior near an equilibrium point. The system is considered **stable** if the response to a small perturbation is small as time goes to infinity. If the response goes to zero as time goes to infinity then the system is said to be **asymptotically stable**. A system that gets large over time is considered **unstable**. A system that does not grow or go to zero as time goes to infinity is said to be **neutral**.

Stability of a system can be found by linearizing the system around the equilibrium point. The stability of the system can then be found by looking at the eigenvalues of the resulting Jacobian matrix of the linear system. The system is considered stable if the eigenvalues reside in the left-half plane; i.e. if they are negative or zero. The nature of the eigenvalues determines the type of equilibrium point and the behavior of trajectories near the equilibrium point.

Parameter Dependence

The dependence of a system on some parameter can be found by varying the parameter and finding any new equilibrium points. Equation (1) can be rewritten as

$$\dot{u} = f(u, c) \tag{3}$$

where c is the control parameter, and is called the **bifurcation parameter**. In an aircraft model, these parameters would be such things as thrust, weight, or control surface deflections. By plotting the bifurcation parameter versus a state variable of interest, it is possible to obtain a qualitative idea of the system's dependence on this parameter. This plot is known as a **bifurcation diagram**. An example of this would be an aircraft model with elevator deflection as the bifurcation parameter. As the elevator is deflected from one stop to another, the bifurcation diagram provides a global view of the aircraft's behavior. Unfortunately, bifurcation diagrams only provide stability information, and do not give information of the aircraft's dynamic response over time. For time response information, the researcher still has to resort to more traditional methods, such as numerical integration schemes to obtain this information.

Limit Points

One of the branch points that occur when an eigenvalue of the Jacobian is zero is a **limit point** (or **turning**

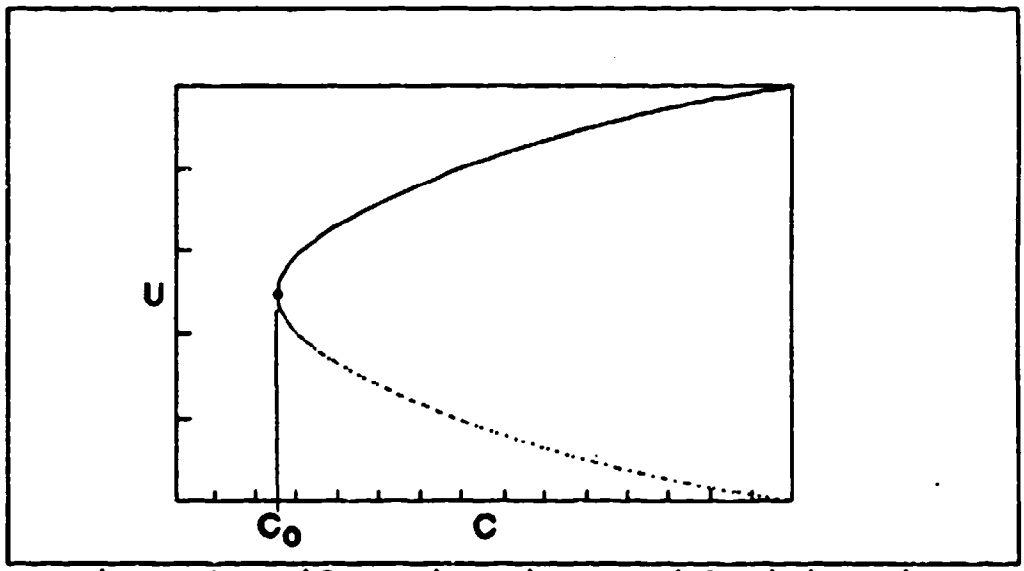


**Figure 1. Bifurcation Diagram with Limit Point**

**point**). Figure 1 represents a bifurcation diagram of a limit point. Limit points are characterized by having two solutions on one side of $c_0$ and none on the other side of $c_0$, where $c_0$ is the value of the parameter at the limit point.

Because the limit point occurs as a real eigenvalue moves across the imaginary axis, it represents a change in stability. At least one portion of the branch departing the limit point is unstable. Typically, in bifurcation diagrams stable portions are represented with solid lines and unstable portions are shown with dashed lines.

Sometimes, a branch loses stability at one limit point, only to become stable at another limit point. This is known as **hysteresis**, and an example of this is shown in figure 2. The

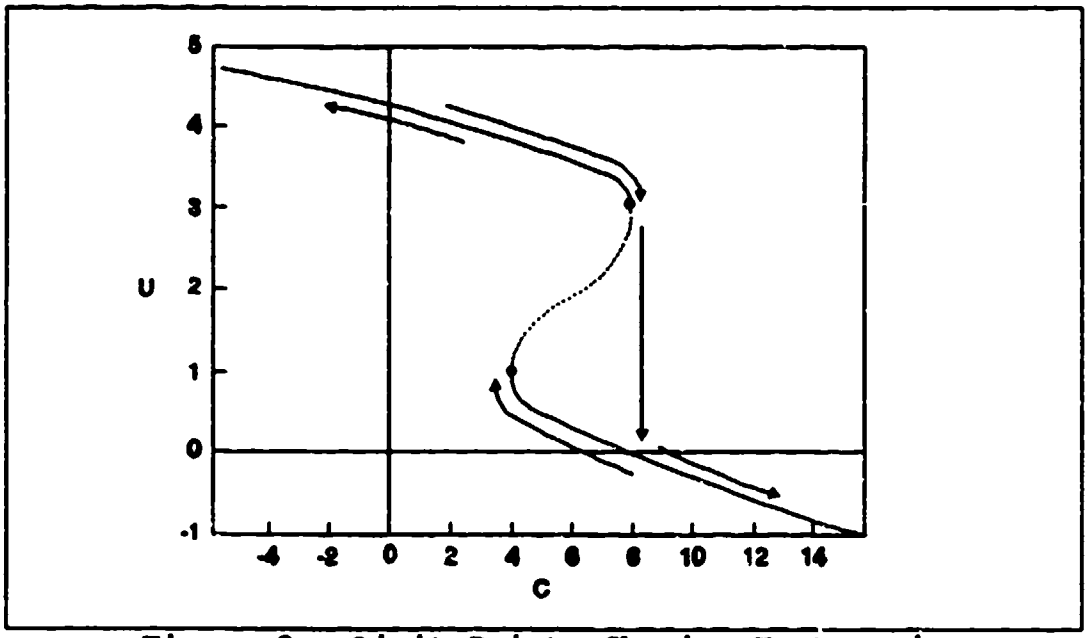


**Figure 2. Limit Points Showing Hysteresis**

arrows indicate the path the equilibrium solution takes as **c** is increased or decreased. Each limit point has two equilibrium solutions that it can exist at, and the transition between these two solutions is called a **jump**. Other types of equilibrium points can exist when the Jacobian Matrix has a zero eigenvalue, but these are beyond the scope of this research. The interested reader is referred to (20) for further information.

Limit Cycles and Hopf Bifurcation Points

Sometimes, systems tend towards a periodic or cyclic motion instead of an equilibrium point. A system described by a limit cycle is one that remains in a cyclic motion with period T, such that $\mathbf{u}(t) = \mathbf{u}(t+T)$ where $\mathbf{u}(t)$ is a solution to equation (1). Some typical limit cycles are those describing "nerve impulses, currents in electrical circuits, vibrations in violin strings, the flutter of panels and laser light. " (20:22) Figure 3 shows the trajectory of a system described by the Van der Pol equation.

$$\ddot{a} - \sigma(1 - a^2)\dot{a} + a = 0 \tag{4}$$

with

$$\sigma = 1$$

$$u_1 = a$$

$$u_2 = \dot{u}_1$$

The system is leaving an unstable focus and approaching a limit cycle. Note that for stable limit cycles, trajectories approach from the inside and the outside. Limit cycles are of particular interest in this study as wing rock is described by limit cycles.

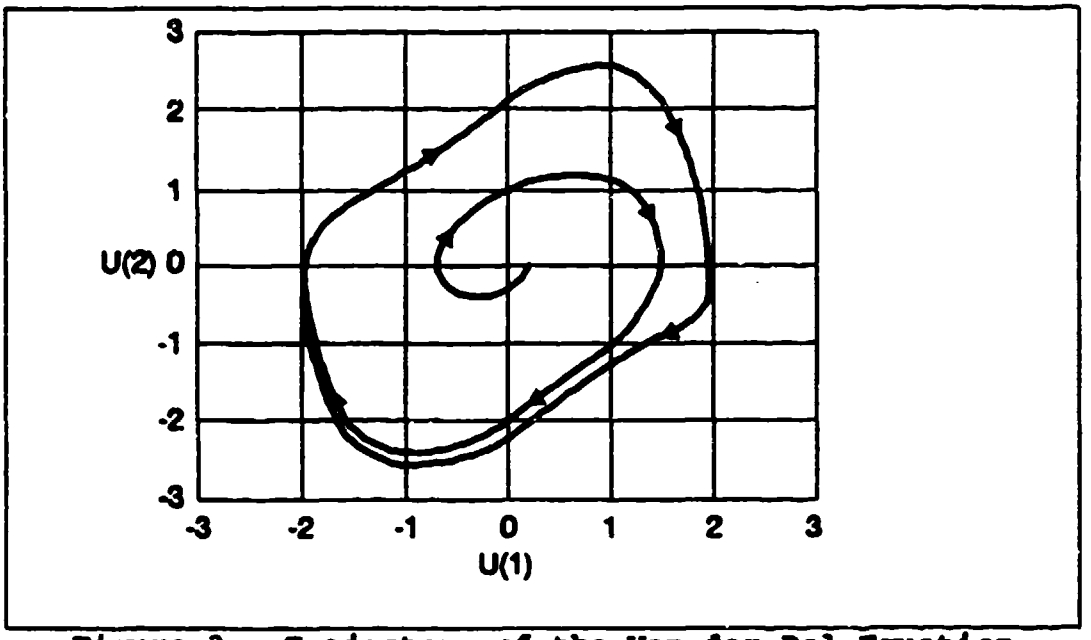


**Figure 3. Trajectory of the Van der Pol Equation**

Limit cycles are detected on bifurcation diagrams through **Hopf** points. A Hopf point is the point where the periodic motion emanates from a branch of stable equilibrium. Hopf bifurcations occur when a complex conjugate pair of eigenvalues crosses the imaginary axis.

Figure 4 shows a typical Hopf bifurcation. The branch is represented by plotting the maximum value of the state attains during the limit cycle. Closed circles represent stable values and open circles represent unstable portions. Other bifurcations that occur from limit cycle branches are beyond the scope of this review.

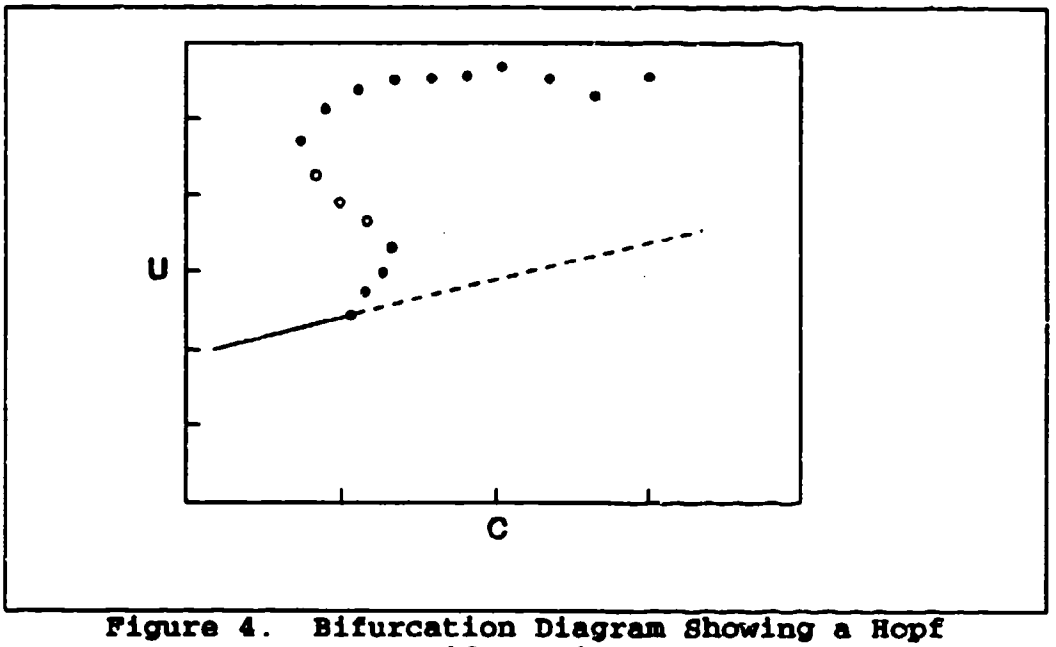


**Figure 4. Bifurcation Diagram Showing a Hopf Bifurcation**

AUTO Software

The software package used in this research to trace out the equilibrium branches and find the limit cycles is the program AUTO written by E. Dodel (11). From a known equilibrium condition which satisfies equation (3), Dodel uses pseudo arc length continuation to complete the equilibrium branches for each new value of the bifurcation parameter. The pseudo arc length technique varies the stepsize along the branch and using the direction vector (u,ċ) a predictor-corrector method algorithm finds the next solution. The predictor-corrector method algorithm used is the Newton method. The pseudo arc length technique allows the algorithm to be scaled so it can compute near and past limit points where the direction vector is infinite. AUTO

also incorporates adaptive stepsize, to ease computation time when the solution is converging rapidly. If the solution is not converging, the stepsize is halved until a minimum stepsize is reached. If convergence still does not occur, the program will also signal non-convergence.

Bifurcation and limit points are identified in AUTO by monitoring the Jacobian matrix at each solution and identifying sign changes in the eigenvalues. Using bifurcation analysis, these changes are identified as limit points, bifurcation points, or Hopf points. AUTO has the capability to calculate branches emanating from bifurcation points, and compute limit cycles that emanate from Hopf bifurcations. More information on the capabilities of AUTO can be found in the AUTO user manual (11).

# III. Overview of Wing Rock

As modern fighter aircraft engage in combat, they are pushed to their operational limits. One limit commonly encountered during the violent turns that occur in the air combat arena is the AOA limit, beyond which the aircraft begins to exhibit undesirable nonlinear behavior, potentially leading to departure or spin. To gain a maneuverability advantage, many modern aircraft designers are trying to eliminate this undesirable behavior at high AOA. The first undesirable phenomenon encountered as AOA is increased is "wing rock." It is a common phenomenon found in many low aspect ratio aircraft, including such aircraft as the F-5, T-38, F-14, F-15 and the AV-8B Harrier.

Wing rock is defined to be an uncommanded rolling motion that occurs as angle of attack is increased. It builds up to a limit cycle, in which the aircraft will roll in one direction, stop, begin rolling back to the opposite direction until a maximum roll angle is reached and then reverse direction and roll back. In studies done on the F-14, this limit cycle developed with amplitudes on the order of ±35°/sec roll rate and ±10° of side slip. This limit cycle had a period of ~4.5 sec, indicating that it was seen and felt by the pilot (1:150).

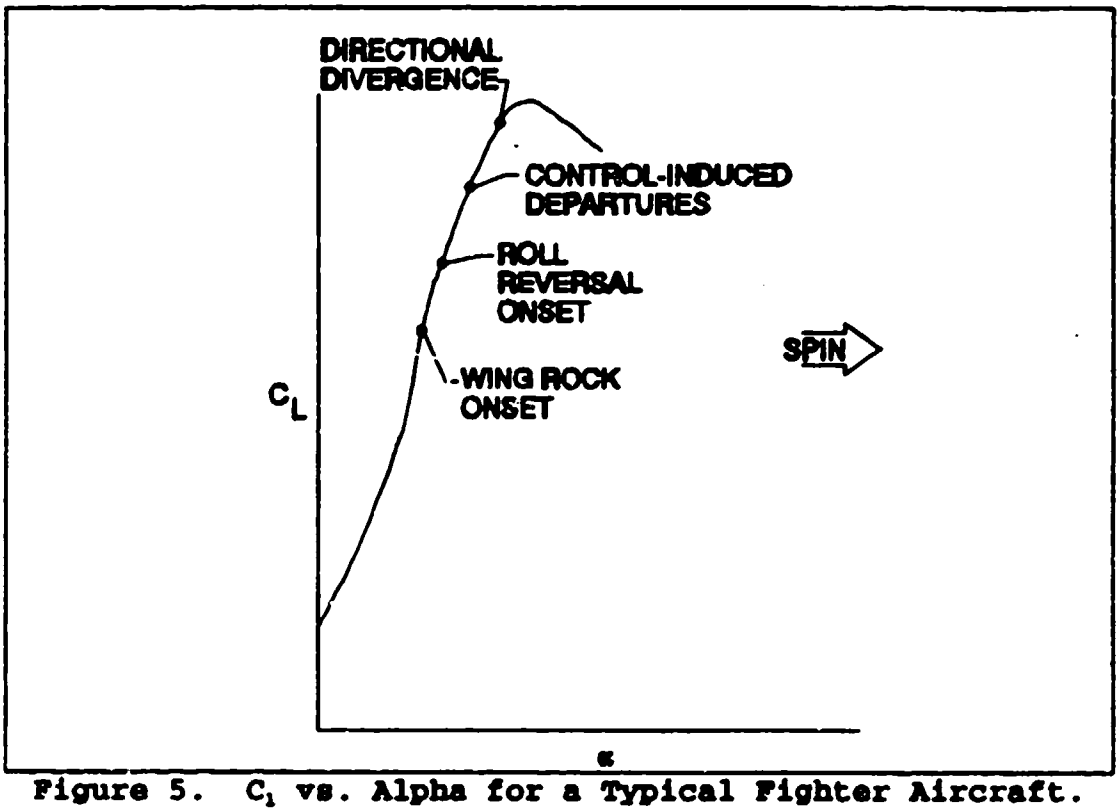


**Figure 5. $C_L$ vs. Alpha for a Typical Fighter Aircraft. (1:164)**

As indicated by figure 5, wing rock onset occurs well before $C_{L_{MAX}}$ is reached, effectively limiting the useful AOA of the aircraft. Wing rock occurs at a lower AOA than the other non-linear phenomena, and the AOA of wing rock onset is often the indication that maximum useful lift has been reached (2:3).

One problem brought on by wing rock is the loss of tracking performance, with possible PIO encountered as the pilot tries to track the target in the region where wing rock exists. An example of this is outlined in reference 1, which describes an F-14 in ACM. As the pilot pulled up into the wing rock region, he encountered PIO as he

attempted to maintain the target aircraft in his gunsight. Although the amplitudes were not large, they were enough to measurably degrade tracking performance (1:158).

Wing rock can also cause flight safety problems in other regions of flight. If it is encountered in landing, the potentially high roll rates (as high as 50°/sec) and large bank angles (±90°) could lead to severe PIO close to the ground (3:3). Furthermore, the existence of wing rock can cause problems in flight control systems that are designed for enhancement of flying qualities at high AOA. For example, use of a high gain aileron-to-rudder interconnect for elimination of adverse yaw at high AOA can aggravate and amplify the wing rock motions to the extent that the airplane/pilot combination becomes tactically ineffective (3:3).

Wing rock does have one advantage in certain configurations; it serves as a natural stall warning mechanism. Wing rock is the first phenomenon encountered as AOA is increased, and as previously indicated, onset of wing rock is the indication that maximum useful lift has been reached. An excellent example of this is the T-38A aircraft. The buffet boundary proceeding the high sink rate characteristic of stall in this aircraft is too wide to use as a stall warning. However, as the aircraft gets close to stall, a moderate wing roll off (wing rock) and lateral oscillations occur just prior to the development of

the high sink rate with full back stick. The wing rock lateral oscillations provide a satisfactory stall warning, in both cruise and landing configuration in this aircraft (4:11).

Despite this potential benefit, studies have shown that the elimination of wing rock can lead to greater tactical effectiveness in a high AOA ACM environment. Reference 1 describes one such study. In this test two F-14 aircraft, one with a special high AOA stability and control system, and one without were engaged in one-on-one ACM. Despite various initial conditions of the engagement, it eventually evolved into a low speed, high AOA turning fight in which each aircraft was attempting to gain an advantageous position. For comparison, these evaluations were flown with and without the stability and control system engaged. The overall results obtained reconfirmed earlier studies which have consistently shown that a properly designed high AOA control system can provide substantial benefits during high AOA ACM in terms of reduced pilot workload, lower skill requirements, and increased pilot confidence. Figure 6 (1:179) illustrates this improvement. Shown are the time histories from two simulated engagements made with and without the high AOA control system. The Basic system data indicate poor control of roll and sideslip as the airplane was maneuvered above about 20° AOA. Under very similar conditions, much

better control is indicated with the system active (1:158-159). Of course, this system is not exclusively designed to solve the wing rock problem, but by eliminating the wing rock problem and improving control effectiveness at high AOA, the aircraft's maneuvering envelope, and tactical effectiveness, is improved.

Although wing rock is found throughout the subsonic and transonic flight regimes, the aerodynamics driving the phenomenon vary in these two velocity ranges. Subsonic wing rock, or the wing rock that occurs in the absence of appreciable compressibility effects is by far the more researched of the two types of wing rock. The mechanics of the phenomenon are described by Hsu and Lan (5:921):

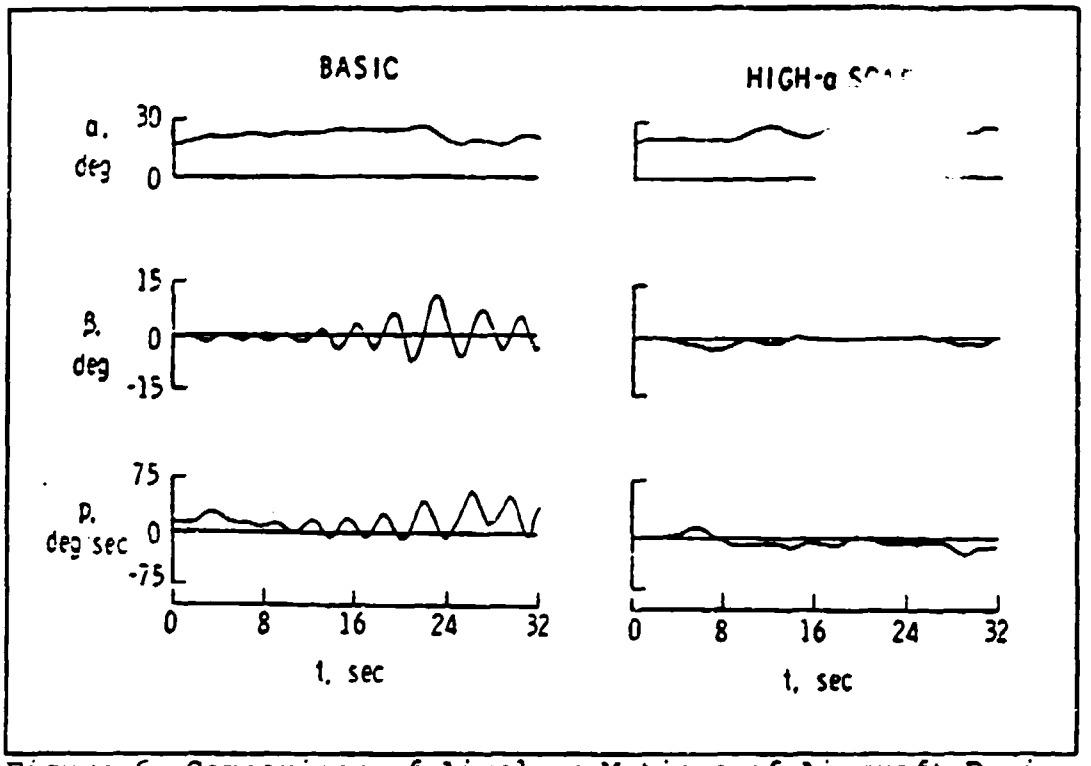

Figure 6. Comparison of Airplane Motions of Aircraft During Simulated ACM With and Without SCAS (1:179)

"Wing rock is an uncommanded roll-yaw oscillation dominated by roll motion oscillating with constant amplitude. It may be initiated either with a sideslip or during a zero sideslip flight with some flow asymmetries over the aircraft flying at high angles of attack. Once the asymmetric flow starts, a rolling oscillation amplitude will keep building up if the roll damping is negative. The transient amplitude of wing rock will grow gradually over some oscillation cycles because of roll instability and negligible dihedral effect at low roll angle.

Although the roll damping is negative at small roll angles, it is positive at larger roll angles for a sustained wing rock. Both the effective dihedral effect and positive roll damping via aerodynamic non-linearities at large roll angles will gradually reduce roll rate. As these restoring moments become stronger, the aircraft will reach a threshold roll angle and finally switch the rolling direction."

This description of wing rock hits upon a number of important points. First, it is driven by flow asymmetries at high angle of attack. These flow asymmetries are configuration dependent. For aircraft with long, slender forebodes, such as the F-5A or X-29, the wing rock is caused by asymmetrical vortex shedding from the forebody and interacting with the downstream components. For aircraft with low to moderate sweep, such as the F-14, the wing rock is driven by wing stall. Airfoil sections experiencing leading edge stall cause a negative damping in plunge. This will cause a moving wall effect that promotes separation and loss of lift, generating a rolling moment that drives the motion. The delayed stall due to the downstream moving wall effects on the opposite wing adds to the rolling motion. Finally, when the roll angle is increased to the point where $\alpha_{eff} < \alpha_{stall}$ on the down going

wing half, the flow reattaches, providing the lift needed to produce the restoring rolling moment (6:49). For a more complete explanation of these aerodynamic drivers of wing rock, the reader is referred to Reference 6.

As previously mentioned, wing rock is an uncommanded roll-yaw oscillation dominated by roll. There has been some thought that significant yaw occurs in wing rock, but the roll observed is greater than any yawing motion. An example of this is found in the T-38A aircraft. T-38A flight test results (appendix D) repeatedly showed that roll rate was at least five times the magnitude of yaw rates in developed wing rock for all maneuvers flown. Pilot observations correlate this data; no yaw was observed in the developed wing rock limit cycles for the T-38A aircraft (18:5).

From this description it is observed that wing rock manifests itself in limit cycle oscillations. After onset, the oscillations begin and eventually build up to constant amplitude oscillations. This characteristic of wing rock lends itself to bifurcation analysis, as the onset is easily predicted by the detection of Hopf points and the calculation of the wing rock periodic branch. This will comprise the majority of the theoretical research of this thesis.

## Conclusions

Wing rock is a highly complex, non-linear phenomenon that is largely configuration and Mach number dependent. Despite this, wing rock appears to the pilot to be an uncommanded roll, appearing to be the same phenomenon throughout the flight envelope, even though it can be driven by radically different aerodynamics. In air combat, the aircraft with the lower angle of attack capability will be at a disadvantage, with wing rock defining the effective maximum lift available. Wing rock destroys tracking and can prove to be a flight safety hazard in landing. Thus, it becomes important to mathematically predict this phenomena, and study what the dominant aircraft states are so that effective feedback mechanisms can be developed to suppress wing rock.

# IV. The Structure of Wing Rock

To fully examine the phenomenon of wing rock, two different analysis techniques have been employed in this study: bifurcation analysis and computer simulations of the aircraft dynamics. The dynamic simulations give the researcher a means to visualize the motion of the aircraft during wing rock, and the bifurcation analysis completes the picture by providing a concise way of finding the onset point, the envelope of stable solutions and the amplitude of the periodic solutions. Bifurcation analysis also more easily lends itself to analysis of feedback architectures to suppress wing rock.

The aircraft being analyzed in this study is the F-15B, the two place, air superiority fighter currently in the Air Force inventory. The following configuration was put into the aircraft model:

1. The aircraft was modeled in cruise configuration with landing gear, flaps up and speedbrake in.

2. No stores, pylons, or conformal fuel tanks were modeled on the aircraft.

3. There was no external test equipment modeled on the aircraft, such as test pitot booms or spin chutes.

4. Aircraft Command Argumentation Systems (CAS) was modeled as being off.

5. There were no fuel asymmetries modeled.

A full description of the aircraft, complete with physical dimensions, is given in Attachment A.

The aerodynamic model employed in this study was developed by Baumann, and represents the aircraft flying at M=0.6, 20,000 ft pressure altitude (PA). The aerodynamic model was formed by fitting the values of the aircraft stability derivatives to polynomials, so that the aerodynamics formed a smooth curve over the entire AOA region. This was done because the bifurcation driver program, AUTO, cannot work with functions or derivatives of functions that have discontinuities. A more complete description of the aerodynamic model can be found in (10).

For the simulation, these aerodynamic derivative approximations were used with a numerical integration

scheme to obtain the full aircraft dynamic simulator. The aerodynamics were fed into an eight state dynamic model, and integrated in time to produce the aircraft dynamics. The dynamics are changed from the initial aircraft steady state by increasing the aircraft's elevator deflection steadily by simulating an infinitely slow pull on the stick by the pilot. At -29 degrees, the elevator hits its lower stop and stays at its final value. This decrease in elevator deflection causes an increase in AOA, and when the simulator hits the critical onset value, the dynamics simulate wing rock.

The bifurcation analysis was run using the AUTO bifurcation software package developed by E. Dodel (11). This was run with a driver program developed by Beck (13), which was a 12 state model representing the dynamics of the F-15. This was generated from an expansion of Newton's laws of motion. By assuming a rigid aircraft, constant air density, constant gravity and a flat earth, and by transforming the force and moment equations from the inertial frame to the body axis frame, the order of the model is reduced to nine. By assuming the xz plane is a plane of symmetry, the following equations are formed (Ref 24)

$$\begin{aligned}\dot{\alpha} = q + \left(\frac{\bar{q}S}{mV}C_z + \frac{g}{V}\cos\theta\cos\phi - p\sin\beta\right)\cos\alpha\sec\beta \\ - \left(\frac{\bar{q}S}{mV}C_x - \frac{g}{V}\sin\theta + r\sin\beta\right)\sin\alpha\sec\beta\end{aligned} \tag{5}$$

$$\dot{\beta} = \left(\frac{\bar{q}S}{mV}C_y + \frac{g}{V}\cos\theta\sin\phi\right)\cos\beta - \left[\left(\frac{\bar{q}S}{mV}C_x - \frac{g}{V}\sin\theta\right)\sin\beta + r\right]\cos\alpha - \left[\left(\frac{\bar{q}S}{mV}C_z + \frac{g}{V}\cos\theta\cos\phi\right)\sin\beta - p\right]\sin\alpha \tag{6}$$

$$\frac{\dot{V}}{V} = \left(\frac{\bar{q}S}{mV}C_x + \frac{g}{V}\sin\theta\right)\cos\alpha\cos\beta + \left(\frac{\bar{q}S}{mV}C_y + \frac{g}{V}\cos\theta\sin\phi\right)\sin\beta + \left(\frac{\bar{q}S}{mV}C_z + \frac{g}{V}\cos\theta\cos\phi\right)\sin\alpha\cos\beta \tag{7}$$

$$\dot{p} = -\left[\left[\frac{I_z - I_y}{I_x} + \frac{I_{xz}^2}{I_x I_z}\right] + \bar{q}\frac{Sb}{I_x}\left[C_l + \frac{I_z}{I_z}C_n\right] + \left[1 - \frac{I_y - I_x}{I_z}\right]\frac{I_{xz}}{I_z}pq\right]\left[1 - \frac{I_{xz}}{I_x I_z}\right]$$

(8)

$$\dot{q} = \frac{I_x - I_z}{I_y}pr + \bar{q}\frac{Sc}{I_y}C_m + \frac{I_{xz}}{I_y}(r^2 - p^2) \tag{9}$$

$$\dot{r} = \left[\left[\frac{I_{xz}^2}{I_x}\frac{I_z - I_y}{I_z}\right]pq + \bar{q}\frac{Sb}{I_z}\left[C_n + \frac{I_{xz}}{I_x}C_l\right] - \left[1 + \frac{I_z - I_y}{I_x}\right]\frac{I_{xz}}{I_z}qr\right]\left[1 - \frac{I_{xz}^2}{I_x}I_z\right]^{-1} \tag{10}$$

$$\dot{\theta} = q\cos\phi - r\sin\phi \tag{11}$$

$$\dot{\phi} = p + (q\sin\phi + r\cos\phi)\tan\theta \quad (12)$$

$$\dot{\psi} = (q\sin\phi + r\cos\phi)\sec\theta \quad (13)$$

Equation (13) was eliminated, since the other equations of motion did not depend on it. A 12 state model was developed, using these equations. Eight of the states were dynamic parameters of the F-15 ($\alpha, \beta, p, q, r, TAS, \theta, \phi$) and the last four states represented the control surface deflections: aileron, rudder, stabilator and differential stabilator. While the dynamics of the 12 state model are identical to the eight state model developed by Barth (12), the 12 state model proved to be easier to use when running simple feedback experiments. These experiments, as well as the more complicated thirty five state model developed by Beck (13) will be discussed later.

The main difference between the 12 state model used in this study and the 12 state model used in reference 13 is the incorporation of the Baumann aerodynamic model. This is the same aerodynamic model of the F-15 used in the dynamic simulator, and it represents a significant improvement over the aerodynamic model developed by Barth (12).

## Flight Test Program

A flight test program was developed at the Air Force Test Pilot School to experimentally verify the bifurcation

program and computer dynamic simulation. For details of the test plan see (21). The tests employed an uninstrumented F-15D, flown in cruise configuration, with no stores, pylons, or conformal fuel tanks. The aircraft was flown as close as possible to the conditions modeled in the bifurcation analysis. The flight test techniques used are found in appendices F, and the tolerance on each test point is found in appendix G. Three basic maneuvers were flown, a 1 g stall, steady banked turns, and a symmetric pullup. The results for the 1 g stall are below, and the results for the other maneuvers can be found with their theoretical analysis in the following chapter.

One note about the flight test. The F-15D AOA gauge is not calibrated in degrees, but is calibrated in units. The exact calibration of the gauge in the test aircraft is unknown, so all flight test results are reported in units. To compare the analytical results to the flight test results, the calibration between the production AOA gauge and the pitot boom AOA gauge found in reference 7 (7:45) was used before the flight test program was initiated to obtain predictions on wing rock 10° difference. In the body of the text, computed AOA is presented in degrees with the corresponding cockpit units following in parentheses. All graphs are left in degrees, due to the fact that some of the scales exceed the range of the F-15 production gauge,

and it would be inaccurate to extrapolate the calibration beyond the gauges upper limit of 45 units AOA.

1 g Stall Results

The 1 g stall was the first maneuver studied, and it provides a good comparison to prior research (13). Bifurcation analysis was initially used to plot the stable equilibrium branch of the aircraft motion, and detect the region of wing rock. At 20 degrees (30 units) AOA, a Hopf bifurcation point was detected, signalling the onset of wing rock. The periodic branch, which is represented in figure 7 by the circles shows the trace of the wing rock branch. Each circle on the periodic branch represents the maximum amplitude in AOA that the periodic solution reaches on that cycle. This representation also shows the stability limits of the branch. Beyond an elevator deflection of -27 degrees the periodic solution is unstable. Since unstable solutions are physically unrealiazible, the solution "jumps" to a higher solution, which in this case is a flat spin. The flat spin results are not presented here, mostly because the bifurcation runs concentrated on AOA < 60 degrees. The spin phenomena is explored in greater detail in references 10 and 14, which deal extensively with this phenomena in the F-15B.

At the onset of wing rock, the equilibrium branch changes stability, with no equilibrium solutions existing

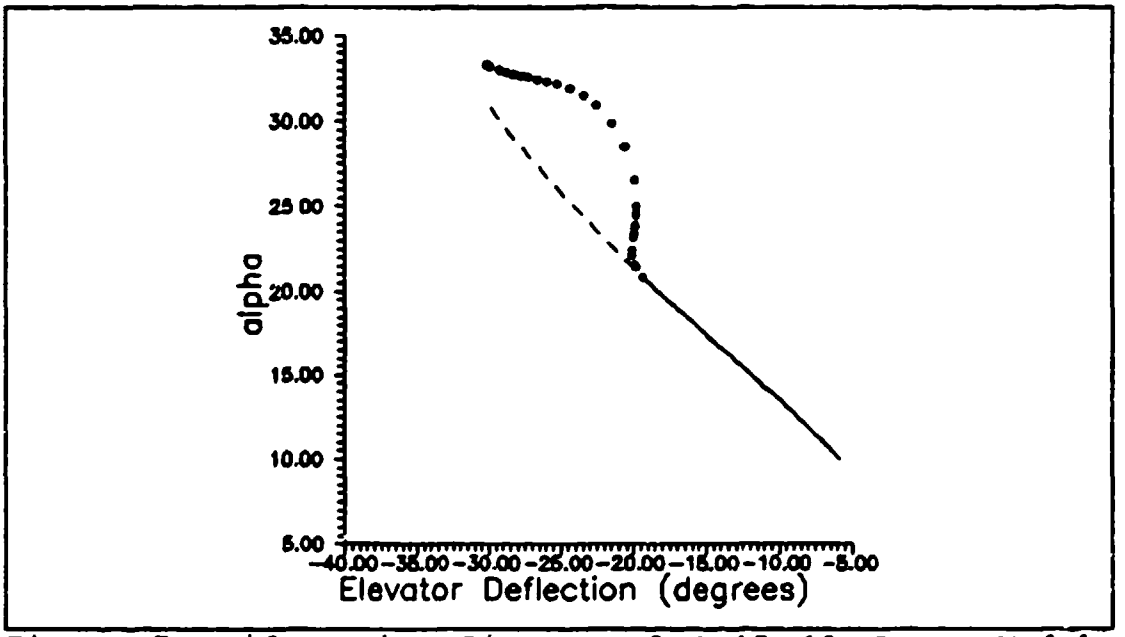


Figure 7. Bifurcation Diagram of F-15 12 State Model, Emphasizing the Periodic Solution

at higher angles of attack for the F-15B. Thus, the bifurcation analysis demonstrates some previously well known facets of wing rock. At flight conditions up to 20 degrees (30 units) AOA, the aircraft can be flown with impunity. Beyond 20 degrees (30 units) AOA non-linear dynamics make it impossible to fly without degrading the tracking performance of the aircraft. And, like most modern fighter aircraft, it is the first non-linear phenomena encountered as the angle of attack is increased.

An attempt was made to validate the above analysis and validate it through flight test using an F-15D. Physically, the F-15D is no different than the F-15B, except it is capable of carrying more internal fuel and has improved engines. The differences between the two aircraft

are outlined in appendix A. The F-15D was flown in cruise configuration, with landing gear and flaps up, and speedbrake in. The aircraft was flown at 20,000 ft PA, but not at M=0.6, as it was realized that the aircraft would slow down as it approached stall. However, it was assumed that the aerodynamic differences between M=0.6 and the mach number where the aircraft stalled would be small enough to neglect and that there would be no mach effects on any wing rock characteristics.

It was discovered during this flight test that the onset of wing rock occurred consistently four units below what was predicted by the bifurcation model. This was attributed to the difference between the aerodynamic coefficients at M=0.6, where the computer model was valid, and the mach number where wing rock onset occurred. The model aerodynamics were only valid at M=0.6, and the aircraft exhibited wing rock at lower mach numbers (around M=0.35) revealing a potential flaw in the bifurcation model. While the eight state equations were capable of accurately modeling the aircraft bleed rate during a 1 g stall, the aerodynamics were still only valid for M=0.6. As a result, the stability map generated by bifurcation in a 1 g stall was not physically realizable. Flight test, however did correlate with some results of the theoretical analysis, and gave some valuable insight into wing rock.

Despite the wing rock being primarily roll, the presence of as much as 8 to 10 degrees of yaw in some wing rock motion has led researchers to classify wing rock as a "dutch roll" type motion (2:2; 19:366) and is often described by pilots as such (16:5; 7:17). However, in the F-15B/D, wing rock is primarily a rolling motion. This is evident in figure 8, which plots both
roll and yaw rate for the F-15B versus time based on numerical simulation. In the plot, roll rate builds up much faster than yaw rate, and achieves much higher magnitudes. This was further verified during flight testing in both the F-15D and the T-38A aircraft. The motion was primarily a rolling motion, with no yaw observed in the F-15D and little yaw recorded in the T-38A ( see appendix D). As a result, the motion in these two aircraft did not exhibit the classic "dutch roll" motion.

Also evident in figure 8 is the "limit cycle" behavior of the wing rock.

This limit cycle behavior was not apparent in flight test, however. Bifurcation did accurately detect an unsteady motion, but flight test showed it was not periodic. Flight test data revealed developed wing rock limit cycles to be erratic, non-symmetric, and inconsistent. A review of qualitative pilot comments on the established wing rock limit cycle confirmed that the magnitude of roll oscillations about an equilibrium AOA

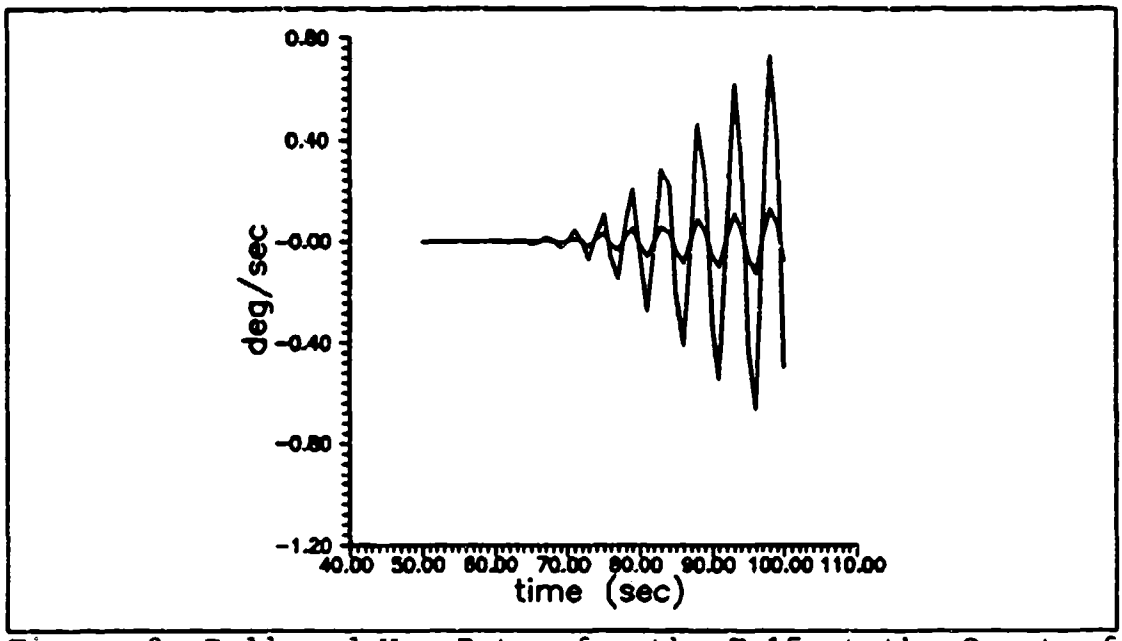

Figure 8. Roll and Yaw Rates for the F-15 at the Onset of Wing Rock

were not constant. The F-15D would oscillate at some roll angle about the equilibrium angle of bank (AOB), and if allowed to persist, would eventually change to a new equilibrum AOB. The direction of this magnitude change was also random. Pilot comments included observations such as, "...aircraft is rocking back and forth, and direction it wishes.." and "...initial symmetrical wing rocking motion did not last long. As AOA reached 30 units, the motion grew in amplitude, remained low in frequency, and became unpredictable" (18:7).

This unpredictability of the motion made it impossible to calculate period, frequency, and in some cases, amplitude. The amplitudes recorded were found in appendix E. Often the wing rock motion experienced more than one amplitude at a fixed angle of attack; in one case during

the 1 g stall (Table E1) four different amplitudes were observed, with bank angle oscillations ranging from $\pm$5 degrees to $\pm$20 degrees.

As previously mentioned, this randomness of the motion was not predicted by either bifurcation or the dynamic simulator. Nor was it expected from prior research. Numerous sources (1;2;5;15) cite that wing rock is a limit cycle oscillation. Hsu and Lan, quoted previously, describe wing rock as " a roll motion with a constant amplitude" (5:921). This behavior is found in the Folland Gnat, whose wing rock " can become a sustained oscillation of near constant amplitude, which can be held for several cycles." (15:5) Also, this behavior is found in the F-5 aircraft (2:2,10), which is similar to the T-38A.

Stability Derivative Study

The F-15B simulator program was used to calculate values of the aerodynamic stability coefficients as a function of angle of attack, in an attempt to correlate these derivatives with wing rock. Previously, attempts have been made by many researchers (1;2;15) to correlate wing rock with one or more stability derivatives, particularly roll damping, $C_{l_p}$. The three stability derivatives most extensively studied are $C_{l_\beta}$ (dihedral effect), $C_{l_\beta}$ (directional stability), and $C_{l_p}$ (roll damping).

Of the three aforementioned stability derivatives, roll damping has been most closely linked with wing rock. In a large number of aircraft, such as the F-14A (1), the Folland Gnat (15), and the static model of the X-29A (16) the loss of roll damping is seen as a main contributor to the wing rock phenomenon. In the X-29 and Gnat aircraft, roll damping changes from positive to negative damping (a sign change from negative to positive) and remains negative throughout the wing rock region, whereas in the F-14A the roll damping remains stable, but gets very small in the wing rock region. This has led many researchers to postulate that a loss of roll damping is an indication of wing rock. (2;5)

Figure 9 shows the F-15B simulator mathematical model of roll damping versus angle of attack. This figure represents a curve fit of tabular data at M=0.6, 20,000 ft PA. As evident by this figure the idea that roll damping hits a critical low value at the onset of wing rock does not apply to the F-15B, as roll damping never changes sign (loses stability) and decreases significantly long before the onset of wing rock. Following the hypothesis that the roll damping hits a critical value upon onset of wing rock, would lead one to believe that onset would occur at an AOA of 15 degrees (15 units). Flight test (Table E1) indicates onset at 16 degrees (26 units) AOA for a 1 g stall at M=0.6, 20,000 ft PA. Similar mathematical studies on the

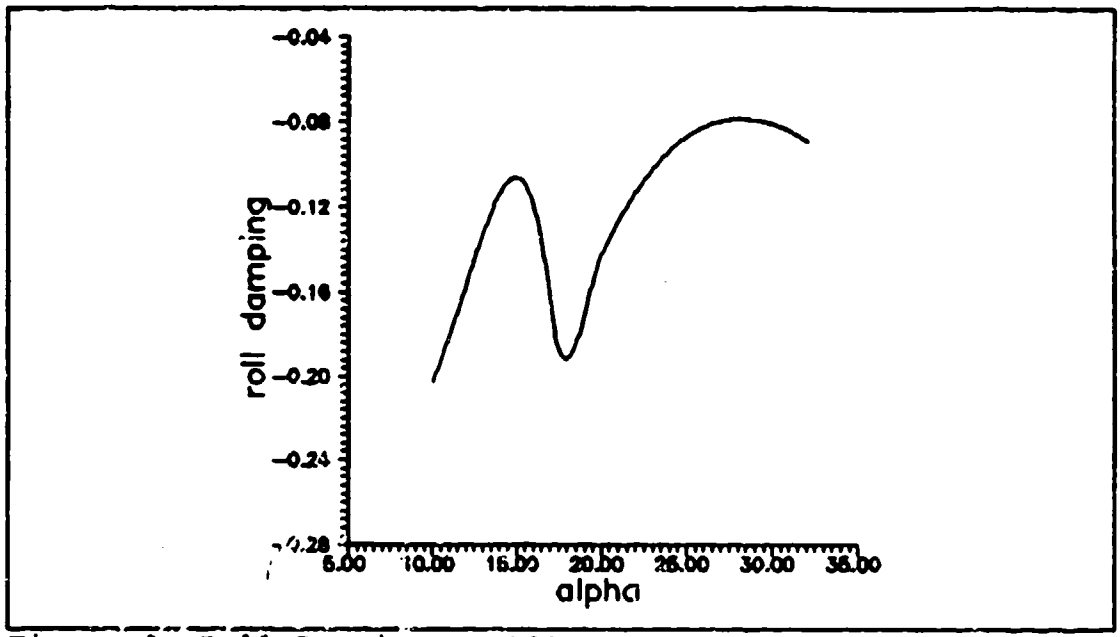

Figure 9. Roll Damping vs AOA

F-4J also exhibit wing rock without drastic loss in roll damping (16:14). In fact, the mathematical model for roll damping in the F-4J is increasing throughout the wing rock region, and while it hits a minimum at onset (onset occurring at approximately 18 degrees AOA) it is still fairly large, (-.1) and since roll damping is increasing with AOA, wing rock should die out. This does not happen in flight, and wing rock occurs until the departure angle of attack is reached. This concludes that roll damping alone cannot be used as an indication of wing rock, for while a loss of roll damping has been associated with wing rock in some configurations, a similar loss of roll damping in the F-15B/D and F-4J cannot be linked to the wing rock phenomena. In the F-15B/D, wing rock occurs some 1 unit after a local maximum in roll damping and occurs at values

much lower than that maxima. In the F-4J, wing rock occurs at a local maxima in the roll damping derivative, but the increase in roll damping throughout the wing rock region would intuitively lead to a damping out of this motion, something not demonstrated in flight test (16:6). Therefore, aircraft with apparently good roll damping still exhibit wing rock.

While some aircraft exhibit wing rock with apparently benign roll damping, it is well documented that artificially increasing roll damping through feedback or arbitrarily increasing the derivative, as in reference 16 and 17, eliminates the wing rock. This aspect of wing rock will be discussed later.

Figure 10 is the dihedral effect, $C_{l_\beta}$, versus angle of attack for the F-15B. Note that at the onset of wing rock, 20 degrees, dihedral effect is -0.0070.

Figure 11 shows $C_{n_\beta}$ versus angle of attack for the F-15B. Figure 11 shows a decreasing trend and negative directional stability beyond 19 degrees (29 units) angle of attack.

High dihedral and a loss of directional stability are two of the reasons that the wing rock is primarily a rolling motion. Reference 16, which details the aerodynamic model of the F-4J, notes that $C_{n_\beta}$ passes through zero at about 20 degrees AOA, while at the same point $C_{l_\beta}$ is still relatively large. This is credited with making the

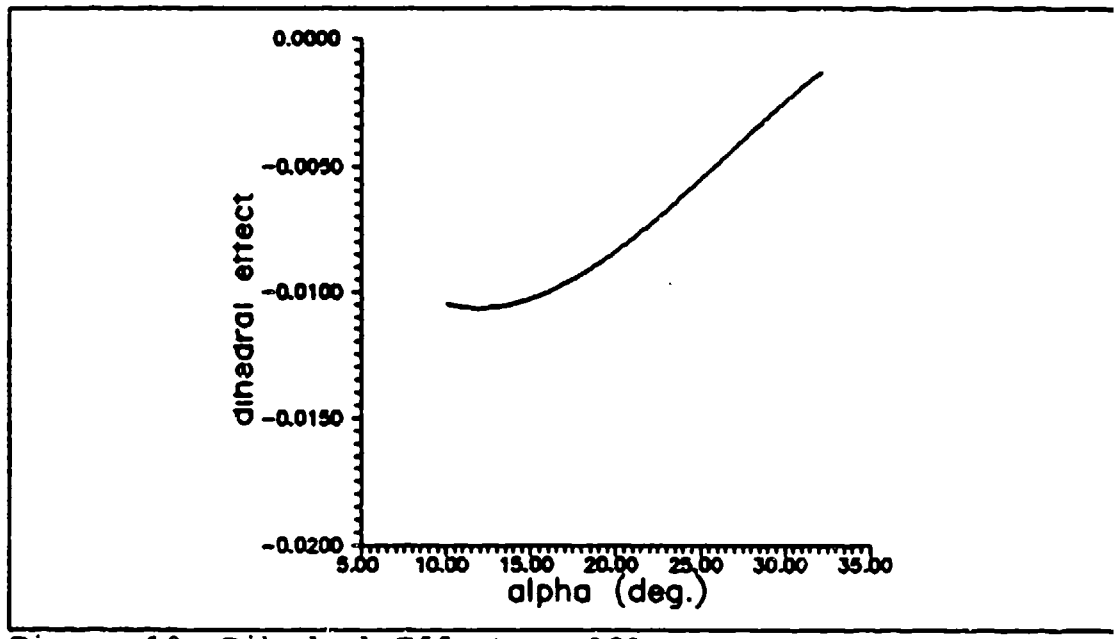

Figure 10. Dihedral Effect vs AOA

dutch roll motion largely a rolling motion, namely wing rock (16:43). Reference 1 says the same thing for the F-14A. The high level of dihedral effect, combined with essentially no directional stability and further combined with a high ratio of Iz/Ix results in the oscillation being almost entirely about the roll axis with very little yaw motion (1:150). Since the F-15B has similar characteristics, it is expected that the F-15B's wing rock would be primarily roll, which is what was found in the simulation runs. Also, like the F-14, both the F-15 and the F-4J also have high yaw-to-roll ($I_z/I_x$) moment of inertias (5 for the F-15 and 6.12 for the F-4J). These factors combine to make the wing rock that occurs in the F-15 a rolling motion. This high dihedral effect, combined with a high yaw-to-roll moment of inertia, and a directionally

unstable aircraft, combine to make wing rock in the F-14A, F-4J, and the F-15B primarily a rolling motion.

## Conclusion

It has been shown that the wing rock experienced by the F-15 is primarily a rolling motion, with much smaller excursions in yaw. This is verified by dynamic simulator runs of the F-15B and through flight test. During the wing rock region, the F-15B aerodynamic model shows the dihedral effect remaining high, with the aircraft becoming directionally unstable at the onset of wing rock. These factors, combined with the aircraft's high yaw-to-roll moment of inertia, makes the wing rock primarily a rolling motion.

Bifurcation analysis predicted the onset point of the wing rock and mapped the branch of the periodic solutions. This prediction of the wing rock onset was 4 units off from the actual flight test data.

Finally, important stability derivatives in the F-15B were reviewed to examine their effects on wing rock. Roll damping, while important, remains high when wing rock onset occurs. This leads to the conclusion that an airframe with good roll damping can still exhibit wing rock, and that an aircraft's wing rock susceptibility cannot necessarily be explained by examining roll damping alone.

# V. Wing Rock During Maneuvering Flight

Up to this point, the wing rock that has been studied has concentrated the airplane flying in a steady, straight and level flight. The elevator is then increased, and the aircraft approaches a 1-g stall. This is useful in studying the wing rock phenomena, but it is a flight condition that is seldom encountered in the combat arena, as it leaves the aircraft vulnerable to opposition. What is most encountered in air to air combat are more dynamic maneuvers, such as turns, and abrupt pullups. It makes some sense, therefore, to model the aircraft in these maneuvers, to see if wing rock occurs, and to check at what point it occurs. In this regard, the airplane was studied in three flight conditions; a rudder sweep, in which the elevator was held fixed and the rudder was swept from one side to the other, steady turns, in which the aircraft is initially in a steady turn, and then the elevator is increased, and a pullup, in which the pitch rate, q, is non-zero, and the elevator is increased to increase the pullup. Bifurcation diagrams are presented for each case, mapping out the stability of each flight condition. Again, flight test is used to verify the bifurcation model in the steady turns and pullup maneuver.

Rudder Sweeps

The first case studied was a rudder sweep. In this maneuver the aircraft is fixed at a certain angle of attack by fixing the elevator deflection. The rudder is then varied, both positive and negative, and the point at which wing rock is noted and the periodic branch is mapped out. It should be noted that this is not a practical maneuver, as it is the classic way to enter a spin. However, it does serve as a good starting point for the study of wing rock in maneuvering flight. Four runs were made, at elevator deflections of -16.72, - 10.255, -19.12, and one at -14.88 degrees and are shown in figures 11,12, 13, 14. Despite the different initial elevator

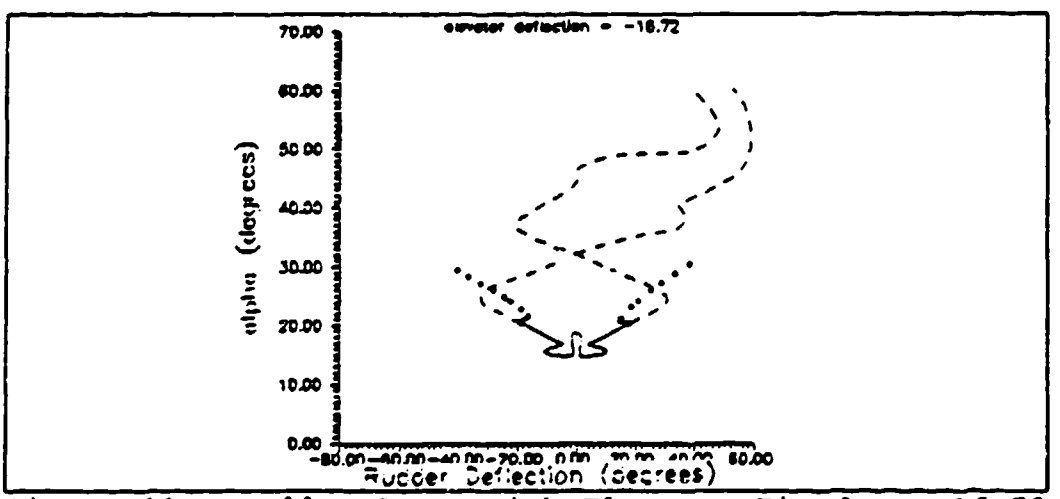


Figure 11. Rudder Sweep with Elevator Fixed at -16.72 Degrees

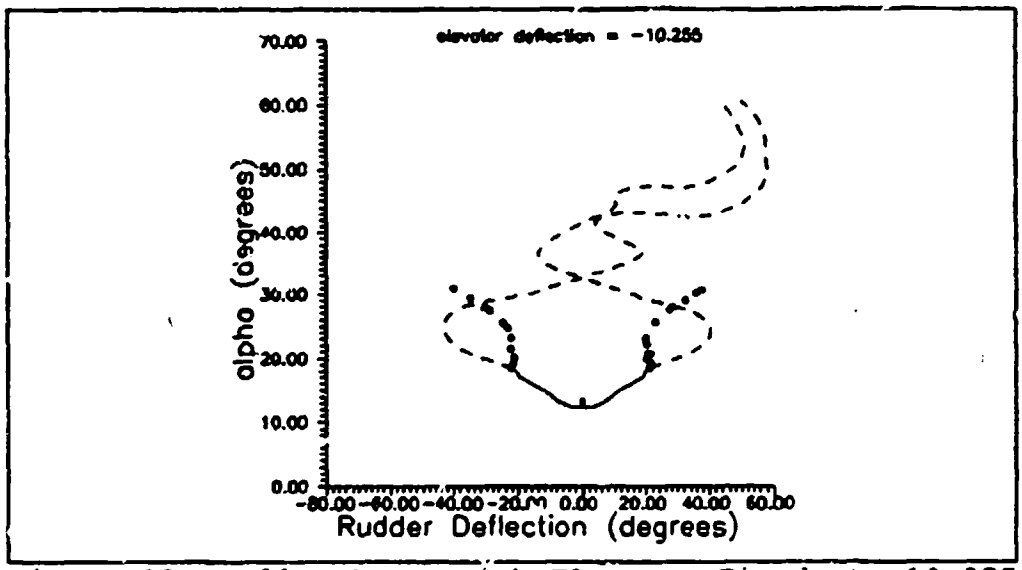


Figure 12. Rudder Sweep with Elevator Fixed at -10.255 Degrees

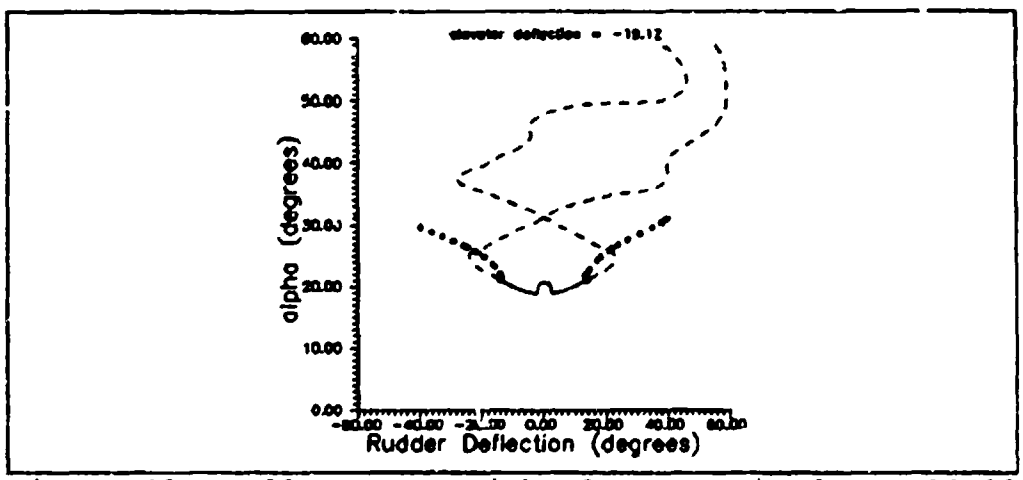


Figure 13. Rudder Sweep with Elevator Fixed at -19.12 Degrees

deflections, the onset point of the wing rock remains relatively unchanged, occurring at 20±1 degrees (30±1 units) AOA. Also, all periodic branches extend to 30

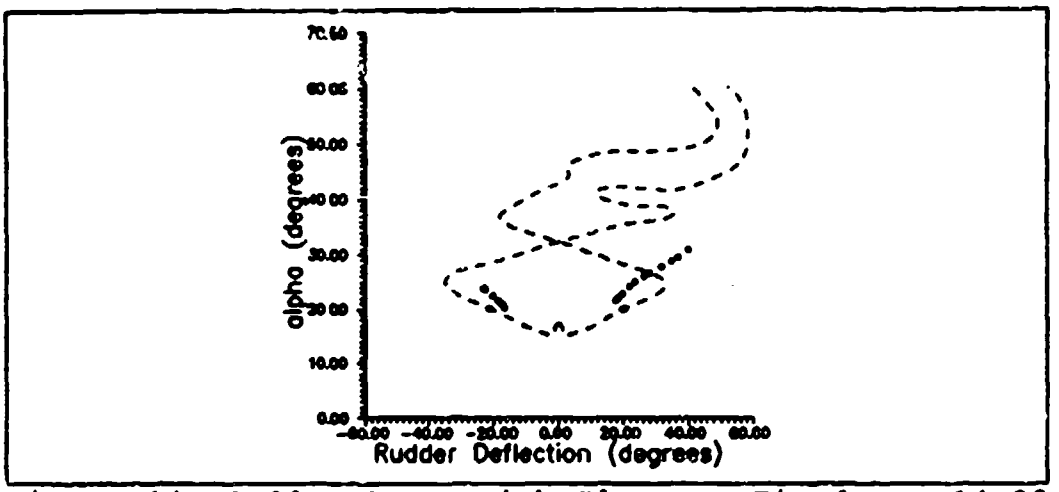

Figure 14. Rudder Sweep with Elevator Fixed at -14.88 Degrees

degrees angle of attack, where they terminate. (The stable solution then "jumps" to the stable spin solutions. For clarity, these are not shown.) So, despite the different initial elevator settings onset occurs at the same point (20±1 degrees), and the periodic branches extend over the same angle of attack range.

Steady Turns

While pure rudder sweeps are something that a pilot wouldn't normally do unless he was entering a spin, steady turns are commonly encountered, and the ability to turn quickly is important in gaining an advantage over an adversary in air to air combat. Since optimum turning flight utilizes the maximum useable lift, wing rock is often encountered in very steep turns, when maximum useable lift is exceeded.

Turning flight poses a problem in that solving for the starting point is a great deal more difficult than rectilinear flight. Given that the stability derivatives for one flight condition are known, it is possible to solve for the three control surface deflections, angle of attack, and sideslip. However, since the stability derivatives in the bifurcation model are functions of the control surface deflections, angle of attack, and sideslip, it becomes impossible to solve for these values using traditional methods. But, through continuation, it is possible to find a steady turn solution by varying the control surface deflections. This is how it is done: first, the aircraft, which is in rectilinear flight, is given an aileron sweep. The aileron sweep begins to roll the aircraft. To get the aircraft in a steady turn, a rudder sweep is then done, and the aircraft enters a turning spiral, with each continuation step increasing the bank angle. At selected bank angles, the change in altitude is calculated, and if the change in altitude is less than 100 ft for the entire turn (which, at M=0.6, can cover several miles) then the turn is taken to be a steady turn. At this point, the elevator deflection is then increased, to simulate the pilot pulling the nose to follow a target, while the airplane was turning. Three turns were analyzed, a shallow turn of 10 degrees bank angle, a moderate turn of 30 degrees, and a steep turn of 70 degrees.

One other parameter that was varied was thrust. It was found early in the investigation that too much thrust with too little bank angle would produce a climbing turn, and without enough thrust, the aircraft would not be able to pull the nose up to a position where a Hopf point could be detected. Thrust was not varied like the other parameters, but instead was set as a constant before the initial aileron sweep. Using these thrust values, and the initial values of the states at these thrust values, it was possible to achieve steady turns with different bank angles. This allowed more of the turning envelope to be explored, for only one steady turn was available at the value of thrust fixed at 8300 lbs.

The next three figures (15, 16, 17) represent the bifurcation diagrams for the three different turns previously mentioned. What is interesting is that all three onset points are identical, and all are identical to the onset point for the 1-g approach to stall. (20 degrees, or 30 units AOA) Also, all periodic branches extend to about the same

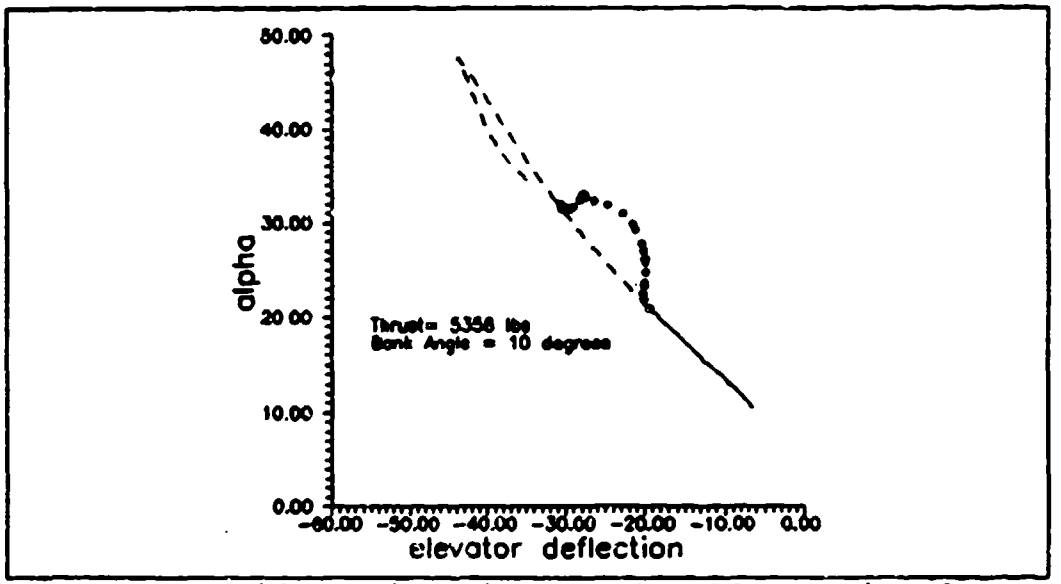


Figure 15. Bifurcation Diagram of F-15 Starting from a 10 Degree Banked Turn

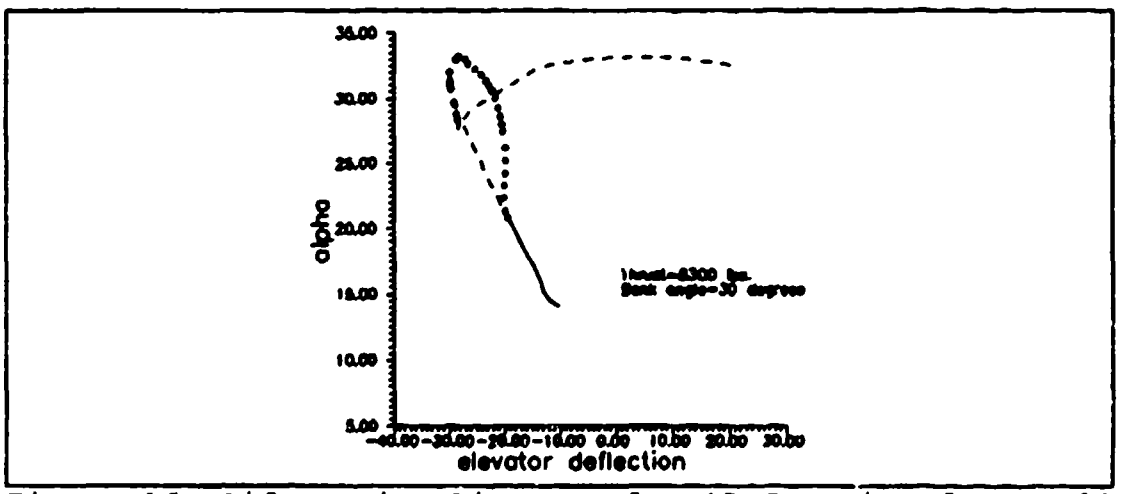


Figure 16. Bifurcation Diagram of F-15 Starting from a 30 Degree Banked Turn

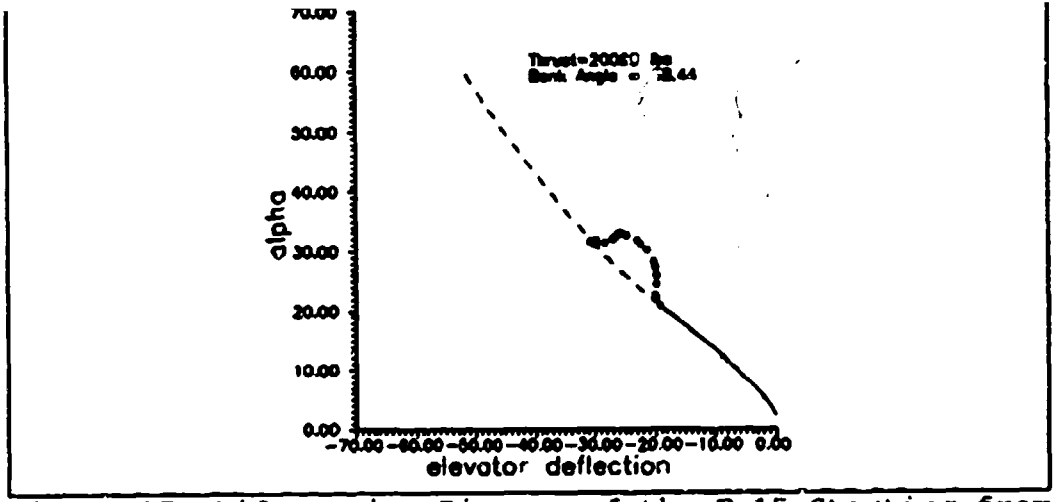

Figure 17. Bifurcation Diagram of the F-15 Starting from a 68 Degree Banked Turn

maximum point, about 33.5 degrees (43.5 units), and none of the periodic branches reattach to the equilibrium branch. Despite the difference in the initial starting maneuvers, all wing rock branches are remarkably similar, with neither the different bank angles or thrust values having a significant effect on the periodic branch.

Flight test results of the same bank angles modeled through bifurcation analysis revealed onset points 4 units lower than predicted by bifurcation. Like the 1 g approach to stall, wing rock onset for these three points occurred at a lower mach number than was strictly valid for the computer model. Table E1 shows the flight test onset points for the four maneuvers, and the mach numbers at which onset occurred. The mach numbers varied from 0.32 to 0.44, different from the 0.6 mach modeled in the F-15

aerodynamics. This reveals that it may not be possible to extrapolate the aerodynamics of the model down to lower mach numbers. Even though the onset points are identical at each point, like the bifurcation model, no conclusions can be drawn from this because of the different mach numbers that occurred during flight test of the wing rock onset points.

Steady Pullup

Another commonly encountered flight condition is the steady pullup, in which the aircraft pitch rate, q , is non-zero. This flight profile is encountered in a split-s maneuver, common in air to air combat. Also, since it is a quasi-steady condition, it easily lends itself to bifurcation analysis.

In this study, only one pullup was studied, for it was assumed that the pitch rate would have no effect on the onset or development of the wing rock cycles. To perform the analysis, though, a modification to the 12 state model had to be made for the steady pullup case to work. This change was to neglect gravity, for it was found that gravity had no effect on the onset point of the wing rock, although it did have an effect on the amplitudes in the developed periodic branch. Gravity was neglected because with it the equilibrium assumption in the theta dot equation is violated, making the regular 12 state model

unsolvable. By removing gravity, the theta dot and phi dot equations become uncoupled, and theta becomes independent, since it is multiplied by gravity in all the equations. This approximation makes the equations solvable with the non-zero pitch rate because the remaining equations no longer rely on pitch attitude, which is transient during this maneuver. As a result, the order of the model is reduced by two states.

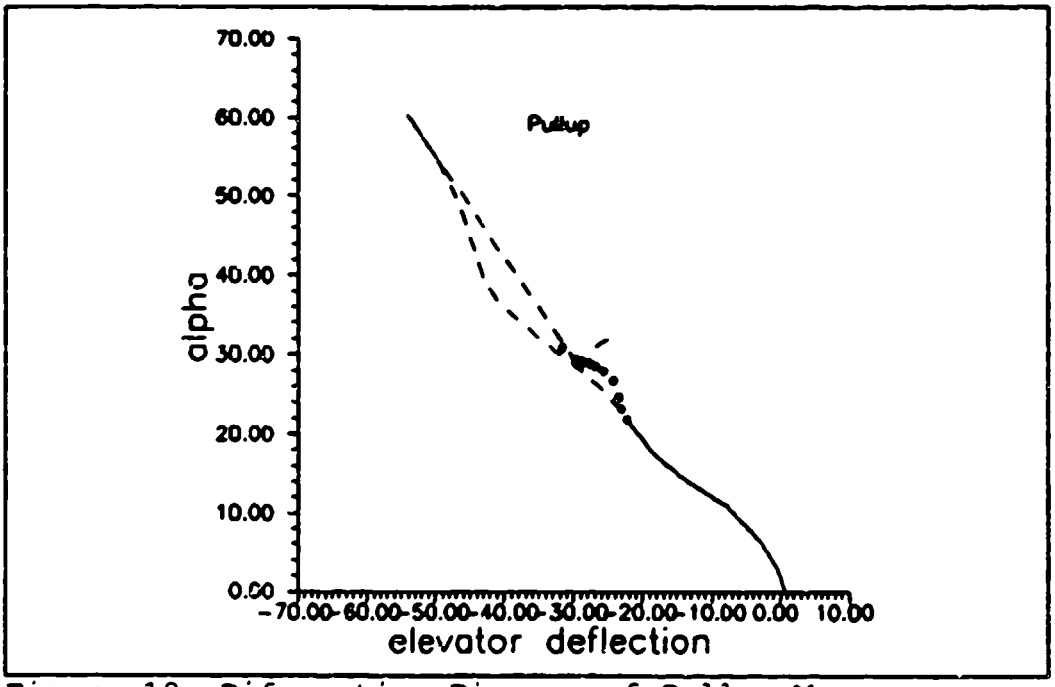


Figure 18. Bifurcation Diagram of Pullup Maneuver

Figure 18 shows the results of the bifurcation analysis for the steady pullup. As seen on the diagram, onset occurs at 21 degrees (31 units) AOA. The fact that q, the pitch rate is non-zero does not effect the onset of wing rock. The amplitude of the periodic solutions are not as pronounced as the 1-g approach to stall or turn cases,

but this is because gravity is neglected. In the pullup case, the maximum AOA achievable is 30 degrees (40 units), slight lower than both turning flight and 1 g stall.

This was the one maneuver that could be flight tested at M=0.6, and as a result, was the one maneuver in which flight test results for wing rock onset correlated well with the prediction of bifurcation analysis. Flight test results revealed onset at 30 $\pm$ 1 units which is what was predicted within the fidelity of the AOA gauge.

## Conclusions

It was found from the flight test that there is a four unit difference between the flight test and the bifurcation model for the wing rock onset point. This discrepancy from the bifurcation model to the flight test is believed to be caused by the differing aerodynamics at the mach numbers modeled (M=0.6) and the mach numbers actually flown.

It should be fully determined what is causing the discrepancy between the flight test results and the model.

# VI. Flight Control Solutions to Wing Rock

In previous research, two solutions to the wing rock problem have been explored; aerodynamic solutions and flight control solutions. The aerodynamic solutions involve shaping either the forebody or leading edge extensions of the aircraft. Although this method has proven successful on such aircraft as the F-20 Tigershark, it involves extensive fluid dynamics research, as well as potentially extensive modifications to the airframe. Both of these methods are expensive to implement, and do not easily lend themselves to computer simulations. As a result this research did not investigate aerodynamic solutions to the problem, concentrating on the flight control solutions.

This study is theoretical, with no flight test to supplement the theoretical research. This is primarily due to the inherent safety risks involved in implementing the simple control structures studied: there are solutions of such limited stability that once wing rock was reached, the aircraft may depart with only the slightest increase in angle of attack. In actuality, such control systems would employ a complex series of washouts, which would prevent the aircraft from departing.

F-14A High AOA Flight Control System

Before examining the F-15B, this chapter will examine the research done on the F-14A high angle of attack flight control system (1). It serves as a good starting point for the F-15B in that it incorporates a simple feedback strategy, while also compensating for the control induced departures that this type of feedback strategy presents. Furthermore, this system was successfully flight tested.

Wing rock suppression was accomplished by feeding back roll rate to the differential tail. This augmented roll damping, which decreased significantly prior to the wing rock region (1:152). This has a side benefit of quickening the roll mode, which helps with the roll reversal problem. However, this feedback architecture, which employs a high gain roll damper, has been shown to be very detrimental to departure/spin characteristics under certain conditions (1:153). To prevent departure/spin, a series of washout circuits were incorporated to prevent the roll damper being employed in a departure situation. The first washout employed was Mach limited, washing out the roll damper where it was not needed (For M>0.77).

Another problem encountered was the use of the roll damper during maneuvering flight at high angles of attack. A common way to roll an aircraft at a high angle of attack is with rudder. With the roll damper employed, however, the flight system will apply opposite roll control

to damp the motion. As a result, the classical crossed, prospin controls are obtained which can cause a departure to occur. To avoid this problem, a pedal fadeout was employed such that the roll damper is deactivated for large pedal inputs (1:153). Finally, a fadeout was employed that deactivated the roll damper at high angle of attack, ($\alpha$>35 degrees), to prevent the system from applying inputs which could aggravate departure should one occur. As it is, precise tracking is no longer possible in this region, and the roll damper is not needed (1:153).

F-15B Flight Control System

Like the F-14, the F-15 also has roll rate feedback to the differential tail, but it is washed out prior to the onset of wing rock. This is not without merit, as it was found in the initial flight testing of the F-15 that the roll damper was applying adverse (prospin) control inputs during both wing rock and departure; i.e. the differential stabilator feeds inputs that are opposite the roll rate (7:10). As a result, one of the initial recommendations implemented was a washout of the roll damper to prevent such inputs that would lead to spin.

Also in the F-15 is an aileron-rudder interconnect, which is capable of controlling the aircraft during wing rock, because of the rudder's ability to roll the aircraft in this region. Unfortunately, The aileron rudder

interconnect is connected to a washout circuit that filters out low frequency oscillations, such as wing rock. As a result of the two washout circuits, the F-15 has minimal flight control system employed at the angle of attack where the wing rock occurs.

Overview of Flight Control Study

To study the feedback effects on wing rock, two approaches are taken. The first is to study the effects of simple feedback strategies on the 12 state model. Three feedback strategies are employed: feedback of roll rate to the aileron, feedback of roll rate to the differential tail, and feedback of angle of attack and roll rate to the rudder. The first two methods are to supplement the roll damping for the F-15, and the last feedback strategy is to employ the effectiveness of the rudder at moderately high angles of attack.

The other approach is to study the effects of a reduced order model of the actual control system on the F-15 developed in (13). This model is presented with and without the roll damper limiter engaged, to show what the current flight control system can do and to show what realistic modifications can do to solve the wing rock problem.

Roll Rate to Aileron Feedback

The first simple feedback strategy studied was the roll rate to aileron feedback. Feedback to the aileron makes sense; it is the classical lateral control, and is successfully employed to damp wing rock in the X-29 (8:6). The feedback strategy employed is -60*K*p, with four different gains studied. Figure 19 and 20

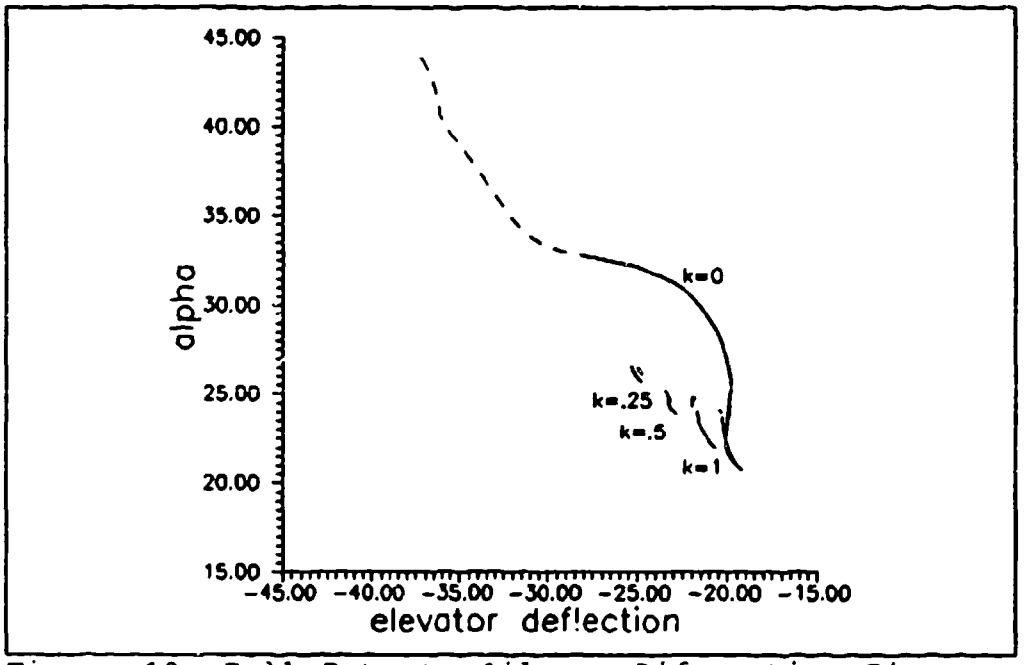


Figure 19. Roll Rate to Aileron Bifurcation Diagram, Showing the Periodic (Wing Rock) Solutions

shows the effect of this feedback on the periodic branch. (The equilibrium branch leading up to the Hopf point is not shown, and for simplicity the traditional representation of the bifurcation analysis is abandoned. In the following cases studied, a solid line indicates a stable periodic solution, a dashed line an unstable one.)

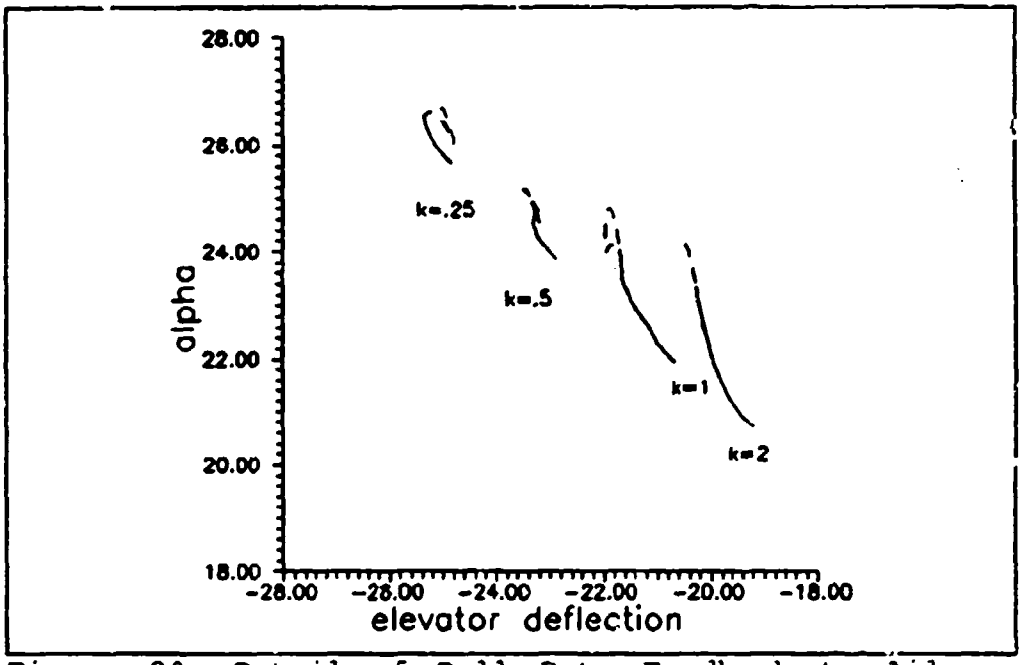


Figure 20. Detail of Roll Rate Feedback to Aileron Bifurcation Diagram

Two things are immediately evident: first, the Hopf point is initially delayed with gain, and secondly, and perhaps more importantly, the length of the periodic branch is greatly reduced as gain is increased. For example, in the no feedback case, the stable wing rock region extends from an angle of attack of 20 degrees to an angle of attack of 33 degrees. But for the case where the feedback gain equals 0.25 the stable wing rock region extends only one degree before departure. As the gain is increased, the wing rock region is increased, but the onset point also decreases, until the onset point is back to the no gain case when K=2. Thus, this simple feedback strategy exposes the danger of feeding back roll rate to suppress wing rock;

it greatly increases the chance of departure. This yields mathematical support to the results that a high gain roll damper aggravates the divergence susceptibility of the aircraft. It also shows that for a successful design, there has to be a tradeoff between the onset of wing rock and the stability of the solution. As clearly shown in figure 21, the onset can be delayed up to 26 degrees AOA,

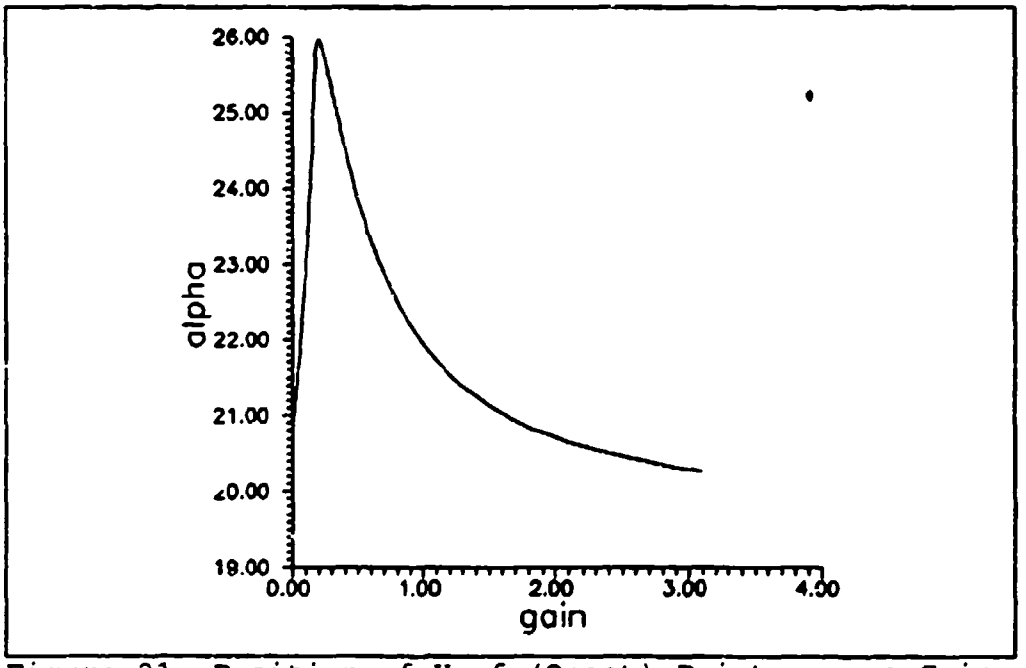


Figure 21. Position of Hopf (Onset) Point versus Gain Aileron Feedback Case

but the stable branch is so small that an effective washout circuit has to be employed to prevent the aircraft from diverging. The area of effective gain is small, as beyond K=2 the onset point decreases beyond the case of no

feedback, with a substantial decrease in the length of the stable region of the branch.

Roll Rate to Differential Tail

Figure 22 shows the analysis of the roll rate feedback to the differential tail. Like the roll rate to aileron feedback case, the increase in gain initially delays the onset of wing rock, but also decreases the stable wing rock region. (For clarity, the zero feedback case is not shown.) The feedback delays the onset point in a similar fashion to the roll rate to aileron feedback case, with the longest delay occurring at K=0.5 (see Figure 23).

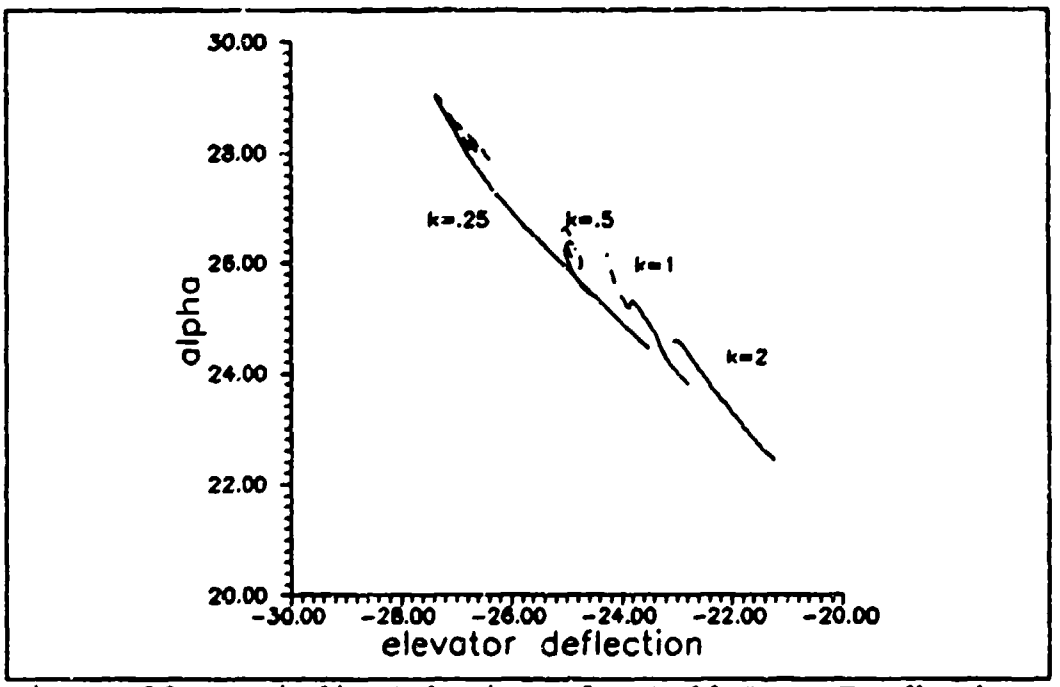


Figure 22. Periodic Solutions for Roll Rate Feedback to Differential Tail

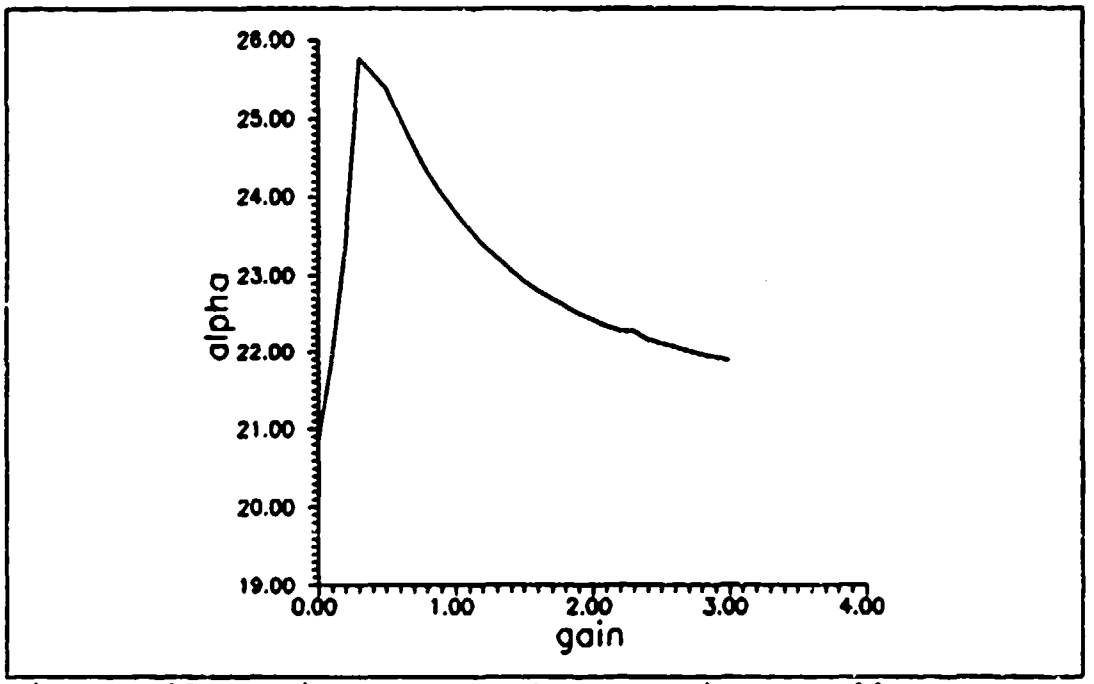

Figure 23. Gain versus Onset Point, Roll Rate to Differential Tail Feedback

Likewise, as gain is increased beyond the optimum point, the onset point decreases back to, and beyond the onset point for no feedback.

It is known that roll rate feedback delays the onset point, but what does the feedback do when the aircraft enters wing rock? The answer is that the lateral motion that is characteristic of wing rock gets damped out. Figure 24 provides an example of this, as roll angle is plotted against angle of attack, for a typical limit cycle. As gain is increased the excursions in roll angle go from 50 degrees in the zero feedback case to 5 degrees in the K=0.2 feedback case. Thus as gain is increased the excursions on both angle of attack and roll angle are greatly damped. Therefore, not only is it possible to move

the onset point almost five degrees AOA as gain is increased, but the wing rock that does occur is greatly damped over the zero feedback case.

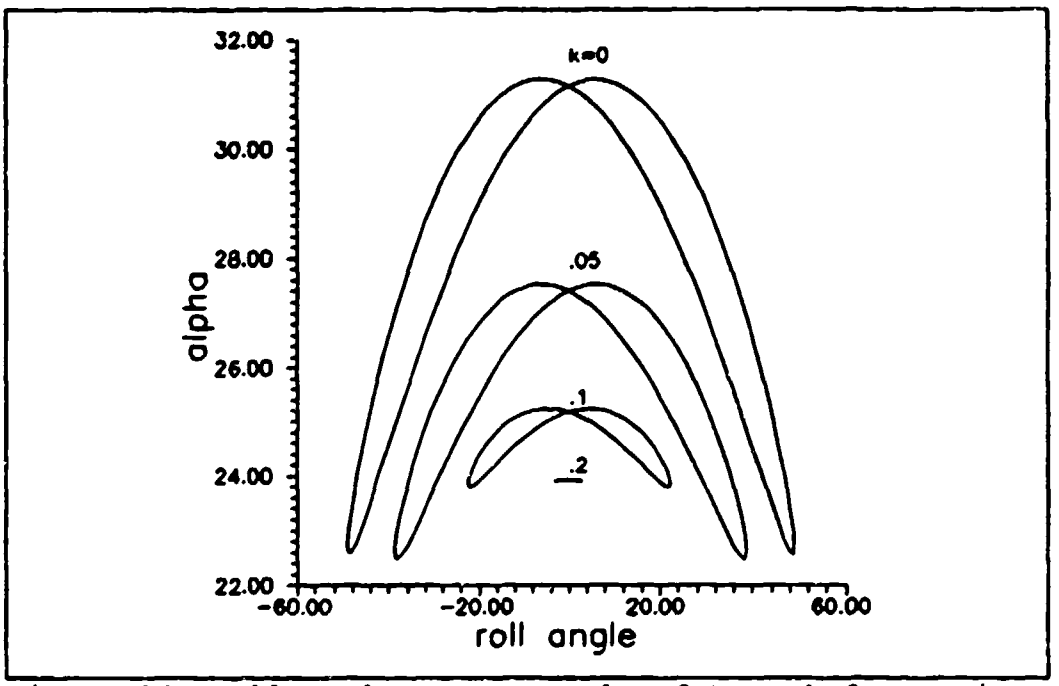


Figure 24. Roll Angle versus Angle of Attack for Various Gains in to the Differential Elevator

Augmenting the roll damping in the F-15 greatly suppresses the wing rock motion, and can give the F-15 six to seven additional degrees of angle of attack. However, as pointed out in (7), care must be taken so that the roll damper does not induce prospin inputs in the high AOA region. As a result, any flight control scheme to give the F-15 a wider angle of attack envelope would have to include the necessary washouts to prevent pro spin inputs and to allow the pilot to control the aircraft.

Angle of Attack and Roll Rate Feedback to the Rudder

As stated previously, the rudder is often used to roll the aircraft at high angles of attack. Thus, some sort of feedback to the rudder is logical to improve control of the aircraft at high AOA. In this analysis the feedback architecture used was $-\alpha*K*p$. This was chosen as it represents the aileron-to-rudder interconnect that is found in the F-15. Unfortunately, in the F-15 this interconnect is attached to a washout circuit (s/s+1) that filters out all low frequency inputs, such as wing rock. As a result, the aileron-to-rudder interconnect, which is capable of suppressing wing rock, is not effective in the wing rock region.

Figure 25 shows the periodic solutions for this type of feedback structure. Like all of the other feedback structures, an increase in gain widens the equilibrium angle of attack envelope, but also lowers the stable range of solutions. Figure 26 shows the position of the Hopf (onset) point with different gains. Unlike the two previous solutions, this feedback structure can accept higher gains.

Despite the increased gain, this feedback strategy basically gives the same performance in moving the onset

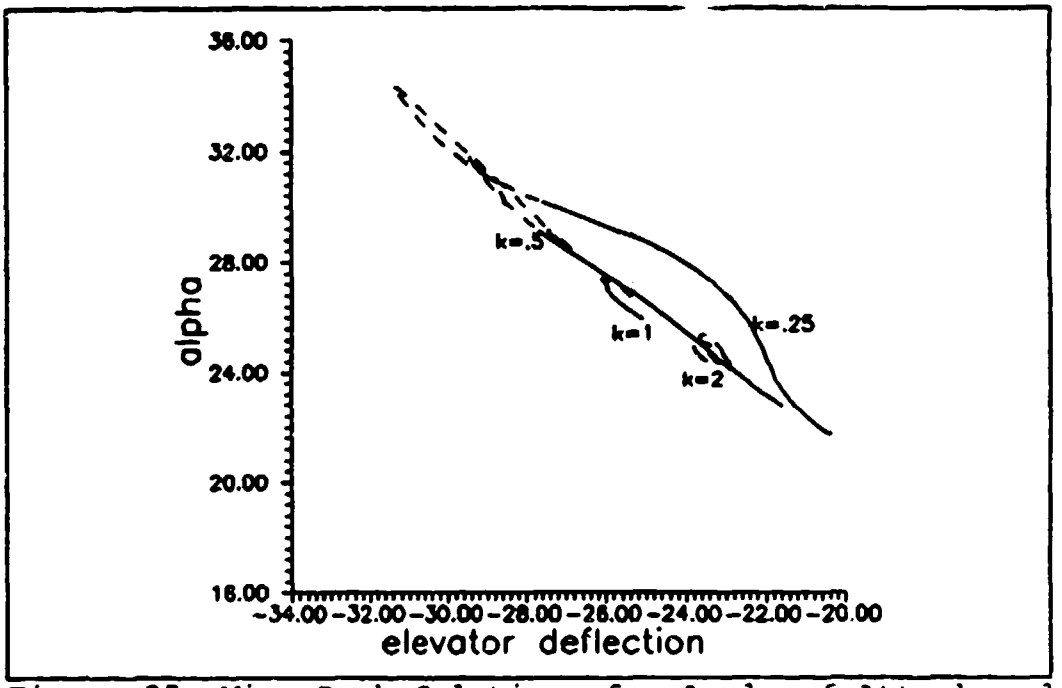


Figure 25. Wing Rock Solutions for Angle of Attack and Roll Rate Feedback to the Rudder

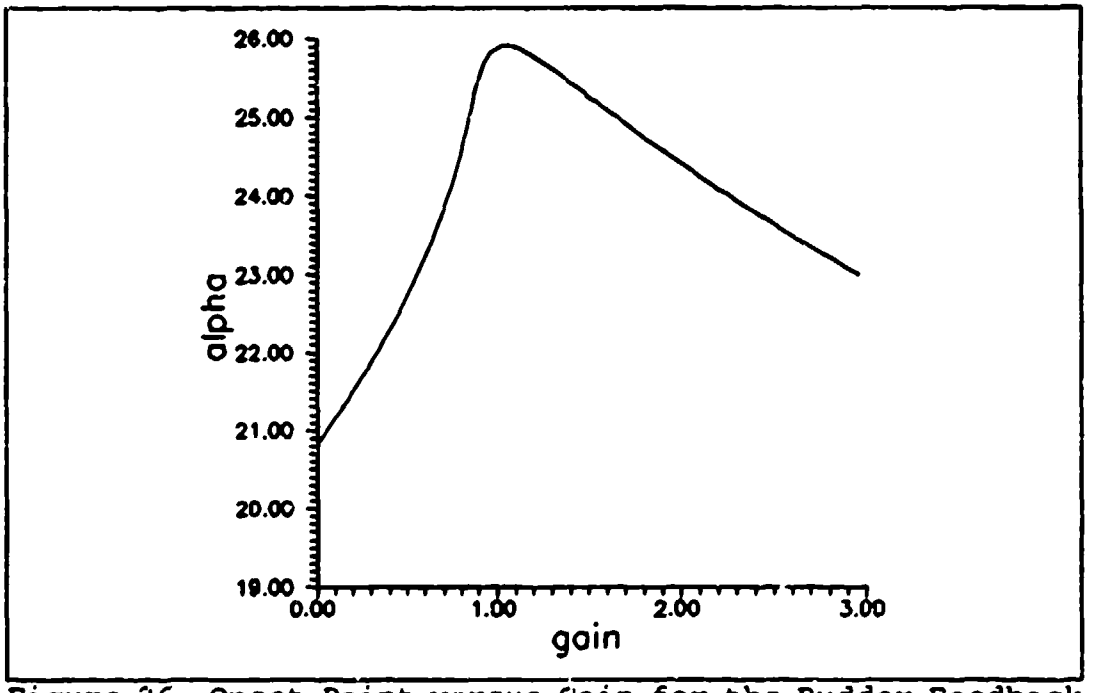


Figure 26. Onset Point versus Gain for the Rudder Feedback case

point and damping the wing rock motion, and like the other two strategies, it requires a series of washout circuitry

to prevent the flight control system from entering any departure inducing controls.

35 State Model

In an effort to model the dynamics of the F-15 control system, models were developed (13) that included the effects of the F-15 control system on the airplane dynamics. Three additional aircraft states, forward acceleration, normal load factor, and lateral load factor were added, as well states for the longitudinal stick dynamics, the lateral stick dynamics, rudder pedal dynamics, aileron-rudder interconnect, and dynamics for the aircraft control system. Originally, these models included all of the servo and high frequency filters that were incorporated in the F-15 control system, rasing the number of states of the model to 50. Since most of the high frequency effects had little effect on the aircraft dynamics, they were eliminated, which reduced the aircraft model to 35 states. Thus, a workable model of the F-15 flight control system was developed, and this model was used to study the effects of the flight control system on the aircraft dynamics.

In developing the model of the control augmentation system, one of the assumptions made was to remove all the limiters from the flight control system. This was done because in limiting the continuation, important, physically

realizable solutions may exist in a different area of the bifurcation diagram and attached by unstable solutions that exist outside the physical limits of the airplane. For example, if the continuation of an elevator sweep stopped at the physical limit of elevator travel, -29 degrees, the stable spin regions which exist at extremely high AOA, (and are physically realizable) would be missed. This would severely limit the usefulness of the bifurcation analysis.

Some of the limiters, however, have an important effect on the aircraft dynamics. One of the limiters removed in both the 50 and 35 state models developed by Beck was the roll damper washout. While this limiter has little effect on the equilibrium solutions, (17:6) it has a profound effect on the periodic solutions. When this limiter is removed, the flight control system provides excellent damping of the wing rock, and possible improvement in the onset point. Unfortunately, this is not realistic, for as recommended in (7), the roll damper is scheduled out by the onset of wing rock.

Figure 27 shows the washout schedule for the roll damper in the F-15 and in the computer model. To modify the 35 state model, this limiter was fit to a fourth order polynomial for smoothness considerations, and placed in the model, to wash out the gain as angle of attack is increased. After an angle of attack of 20.2 degrees, the

gain is set to zero, identical to the schedule found in the F-15.

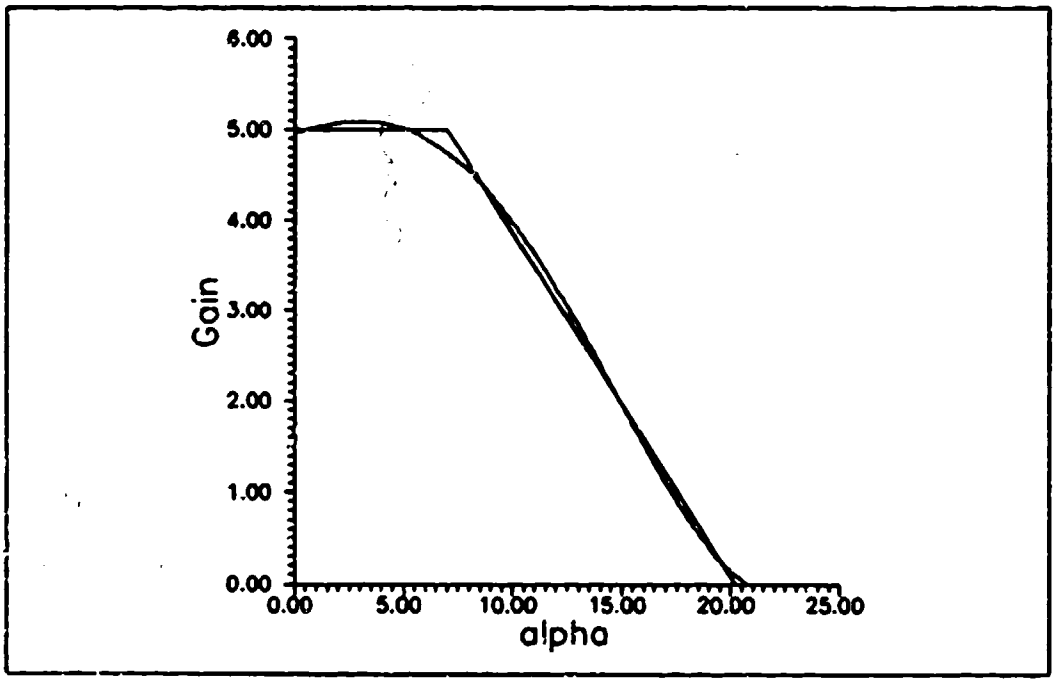


Figure 27. Washout Schedule for F-15 Roll Damper

Figure 28 shows the results of the 35 state model, with and without the limiter. The results are a bit truncated, due to difficulty with the model, but there is enough to show the trends of the analysis. For a more complete run of the 35 state model with the limiter disengaged, the reader is referred to (17). The results from the previous analysis of the simple feedback structures become helpful here. Similar to those cases, when feedback is present, the onset point is increased, and the maximum amplitude AOA excursions are greatly reduced for the same longitudinal stick force. With the limiter, the periodic branch greatly resembles the no feedback case,

with the amplitude staying initially flat and then greatly increasing. Also, wing rock occurs at a lesser stick force, and onset occurs at a slightly lower angle of attack. The improvement in the onset point is to be expected, as in the simple feedback cases. The difference in shape and onset of the periodic branch with the limiter is due to additional control system dynamics in the model.

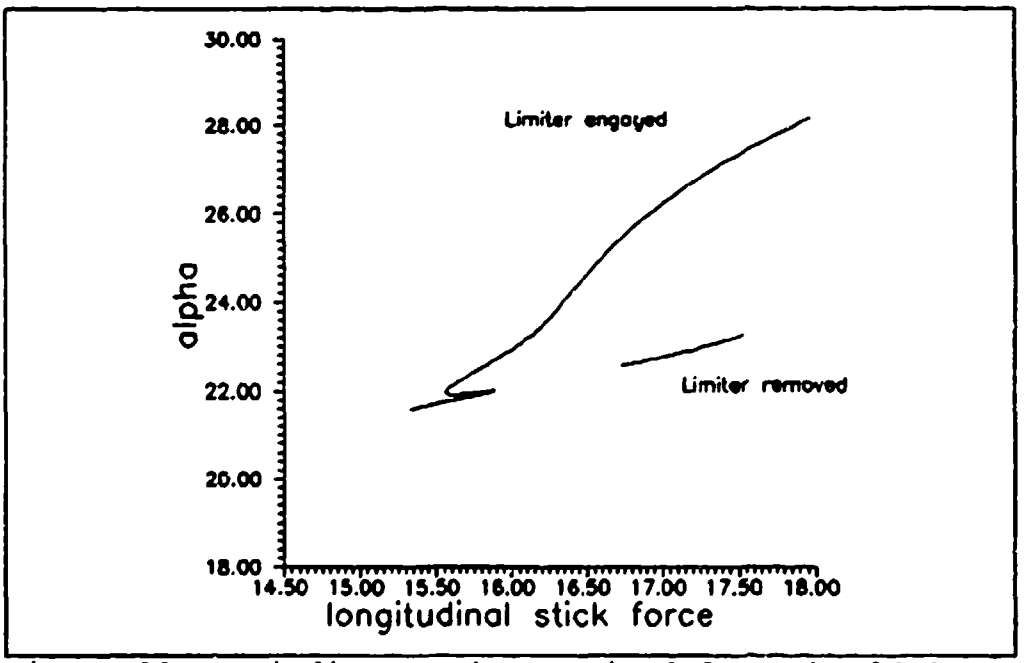


Figure 28. Periodic Branches Derived from the 35 State Model

Conclusions

As seen by the three simple feedback cases, a fairly simple feedback structure can expand the angle of attack range of the F-15. In all three cases explored, an optimum gain was found that raised the onset of wing rock from 20 degrees AOA to 26 degrees AOA. Increasing gain was also shown to damp the wing rock when the oscillations do occur.

The most profitable feedback structures involve augmenting the roll damping derivative. Feedback strategies involving augmenting the roll damping by feeding back roll rate to the differential tail have been successfully flight tested on the F-14A (1). And, despite the significantly higher roll damping the F-15B has over the F-14A in the wing rock region, augmenting the roll damping in the F-15B also proves beneficial in delaying and suppressing the wing rock.

Despite the improvements that these simple feedback strategies offer in expanding the angle of attack envelope, a number of washout circuits would have to be employed in order to keep the roll damper from providing departure inducing control inputs at higher angles of attack, and to control the aircraft at these flight conditions. In the current condition, the F-15B has a circuit that washes out the roll damper by the onset of wing rock to prevent the departure inducing control inputs from the roll damper.

The 35 state model of the flight control system employs a roll damper that is modeled after the roll damper found in the F-15. When this is not washed out, it increases the onset point of the wing rock. When the washout circuit is engaged, the wing rock solution moves towards the unaugmented solution.

There is good reason for washing out the roll damper, however, and the bifurcation diagrams of the simple feedback structures bear this out. As the gain is increased from the no feedback case, the stable periodic solution branch length is greatly decreased. This lends mathematical support to the hypothesis that high gain roll dampers often aggravate divergence. Thus, despite the advantages that roll dampers give, care must be taken that the feedback strategy employed to suppress the wing rock does not aggravate the other non-linear phenomena that occur in this flight regime.

# VII. Conclusions and Recommendations

Both the flight test analysis and computer model revealed that wing rock in the F-15 is primarily a rolling motion. The aircraft's high dihedral effect, combined a high yaw to roll inertia ratio and a loss of directional stability at wing rock onset make the resultant motion primarily roll.

Flight test correlated well with the computer model of the symmetric pullup, with onset occurring at 30 units AOA in both cases. However, in all other maneuvers modeled using bifurcation, the onset point differed by 4 units AOA from the flight test results. This puts into question the assumption that the aerodynamics modeled at M=0.6, 20,000 ft PA is valid for all mach numbers below M=0.6. Furthermore, prior research and the computer generated wing rock limit cycles showed symmetric, periodic behavior, none of which was observed in flight test. Wing rock was characterized by non-symmetric, almost random behavior, with constantly changing bank angle oscillations and equilibrium bank angles.

Computer modeling and analysis showed that a loss of roll damping did not necessarily correspond to the onset of wing rock, as the F-15B still had significant roll damping when onset occurred in the computer model.

Also examined was the effects of a flight control system on the suppression of wing rock. It was seen in the three simple feedback cases studied that an feedback of roll rate was highly beneficial in delaying the onset of wing rock, as well as damping out the resultant wing rock oscillations. However, the resultant stability of each wing rock branch is greatly reduced, increasing the aircraft's departure susceptibility. In order to be implemented, any feedback strategy studied must employ a complex series of washout circuits to reduce this departure susceptibility. A reduced order model of the F-15 flight control system was also studied, with and without the roll damper washout circuit. The 35 state model's performance was comparable with the unaugmented model with the roll damper engaged. With the roll damper washout disengaged the performance of the system is greatly improved.

Despite the failure of the analysis to accurately predict wing rock onset in the majority of cases, and that the computer model and the flight test occurred at different points in the envelope, making any results difficult to compare, bifurcation does hold the power to predict non-linear phenomena such as wing rock, and show the regions where non linear behavior occurs in the aircraft flight envelope. With the following recommendations, it would be possible to predict the onset of wing rock and the developed limit cycle as done in this

research, but more importantly, it will be possible to verify the model at more than one point through flight test.

Recommendations

1. Determine why there is a 4 degree difference in onset point between the flight test results and the bifurcation model for the 1 g stall and the constant bank turns.

2. Examine more closely the effects of various parameters on wing rock, such as pitch rate, g and mach number to get an idea as to what parameters are important in the developed wing rock limit cycle.

3. Determine why the wing rock motion in both the T-38A and F-15D is so random.

4. Examine the developed wing rock limit cycle, and determine if the change in equilibrium bank angle during wing rock has any effect on the resultant motion.

5. Rebuild the model with the Pitch CAS on, to reflect the actual flight condition. The AOA achieved in this study required the pitch CAS to be on in flight, which was not reflected in the 12 state model. For a more accurate, realistic model, the effects of the pitch CAS should be modeled.

# APPENDIX A

# TEST ITEM DESCRIPTION

The F-15B/D aircraft was a two-place, supersonic air superiority fighter. The aircraft was powered by two Pratt and Whitney F100-PW-100 turbofan engines rated at 14,670 lb thrust military and 23,830 lbs thrust in afterburner. The F-15B/D flight control system incorporated irreversible, hydraulically powered ailerons, horizontal stabilizers, and rudders. The horizontal stabilizers could also be moved differentially, to aid in rolling the aircraft. Spring cartridges provided simulated aerodynamic feel to the pilot. All inputs to the actuators were provided by the CAS which augmented the basic stability of the airframe in all three axes. This CAS system also included an aileron-rudder interconnect which served to coordinate the ailerons and rudder. The test F-15D flown was not equipped with any special instrumentation and was outfitted with standard production avionics. A full description of the aircraft is contained in the F-15 A/B/C/D Flight Manual (22).

## Physical Dimensions

The physical dimensions and weight and balance data for the F-15B/D is listed below. This data was obtained from Beck (13) and (23).

Physical Characteristics of the F-15B/D

Wing

| | |
|---|---|
| Area (Theoretical) | 608 sq ft |
| Aspect Ratio | 3.01 |
| Airfoil | |
| Root | NACA64006.6 |
| Xw 155 | NACA64A(x)046 (a=0.8 Mod) |
| Tip | NACA64A203 (a=0.8 Mod) |
| Span | 42.8 ft |
| Taper Ratio | 0.25 |
| Root Chord (Theoretical) | 273.3 in |
| Tip Chord | 68.3 in |
| Mean Aerodynamic Chord | 191.3 |
| Leading Edge Sweep Angle | 45 degrees |
| 25% Chord Sweep Angle | 38.6 degrees |
| Dihedral | 1 degree |
| Incidence | None |
| Twist at Tip | None |
| Aileron Area | 26.5 sq ft |
| Flap Area | 35.8 sq ft |
| Speed Brake - Area | 31.5 sq ft |
| Control Surface Movement | |
| Aileron | +/- 20 degrees |
| Speedbrake | 45 degrees up |
| Flap | 30 degrees down |
| Horizontal Tail | 29 degrees down, 15 degrees up |
| Rudder | +/- 30 degrees |

Vertical Tail

| | |
|---|---|
| Area (Theoretical Each) | 62.6 sq ft |
| Rudder Area (Each) | 10.0 sq ft |
| Span | 10.3 ft |
| Aspect Ratio | 1.70 |
| Root Chord | 115.0 in |
| Tip Chord | 30.6 in |
| Airfoil - Root | NACA0005-64 |
| - Tip | NACA0003.5-64 |
| Taper Ratio | 0.27 |
| Leading Edge Sweep Angle | 36.6 degrees |

| | |
|---|---|
| 25% Chord Sweep Angle | 29.7 degrees |
| Mean Aerodynamic Chord | 81.0 in |
| Cant | 2 degrees out |
| Length (.25$c_w$ to .25$c_h$) | 241.0 in |

| Wetted Area | |
|---|---|
| Fuselage | 1405 sq ft |
| Nozzles | 53 sq ft |
| Horizontal Tail | 216 sq ft |
| Vertical Tail | 257 sq ft |
| Wing | 698 sq ft |
| Total Area | 2629 sq ft |

| Engine Data (each) | |
|---|---|
| Non Afterburning Thrust | 14,871 lb |
| Afterburning Thrust | 25,810 lb |
| Y Direction C.G. Offset | +/- 25.5 in |
| Z Direction C.G. Offset | 0.25 in |
| Nozzle Pivot C.G. Offset | -20.219 ft |

| Miscellaneous Data | | |
|---|---|---|
| Aircraft Length | 63.8 ft | |
| Aircraft Height | 18.6 in | |
| Aircraft Volume | 1996 cu ft | |
| Aircraft Gross Weight (Takeoff) | | 38400 lbs |
| C.G. Station X Direction | 557.173 | |
| Y Direction | 0.0 | |
| Z Direction | 116.173 | |

| Inertial Data | |
|---|---|
| $I_x$ | 25480 slug-ft$^2$ |
| $I_y$ | 166620 slug-ft$^2$ |
| $I_z$ | 186930 slug-ft$^2$ |
| $I_{xz}$ | -1000 slug-ft$^2$ |

The inertia values are for a basic, clean F-15B with ammo, 50% fuel and gear up.

<u>Differences Between F-15B and F-15D</u>

| | F-15B | F-15D |
|---|---|---|
| Engines | PW F100-PW-100 | PW F100-PW-200 |
| Internal Fuel | 11,500 lbs | 13,455 lbs |

# APPENDIX B

# BIFURCATION DRIVER PROGRAM

```
C     PROGRAM STATE12
C     LAST EDITED ON 22 July 1990

C*****************************************************************C
C
C Revised 22 July 1990 -(M.Davison) This is a revision of Capt.
C  Jeff Beck's Model 5 which consisted of the eight aircraft
C  dynamic states plus three additional states for the
C  stabilator,rudder, and aileron control surfaces. It also
C  consisted of 3 parameters for commanded control surface
C  deflections. Furthermore, Model 5 accounted for the
C  differential tail deflection, and this was the final state in
C  the 12 state model. The main diffrence between this program an
C  the Beck model 5 is the introduction of the improved
C  aerodynamic model devloped by Capt. Dan Baumann
C  in 1989. This model is a further refinement of the
C  aerodynamics in the original aircraft model, and allows for a
C  more accurate simulation at high angles of attack. Finally,
C  like the original model, it does not consider the Control
C  Augumentation System (CAS), the Aileron-Rudder Interconnect
C  (ARI), or the stick dynamics.
C
*****************************************************************


      IMPLICIT DOUBLE PRECISION(A-H,O-Z)
      DIMENSION W(150000), IW(100)


C   THIS WAS ADDED SO THAT AUTO CAN READ FROM UNIT
C   3 ON A RESTART

      OPEN(UNIT=3,FILE='fort.3')
      OPEN(UNIT=4,FILE='fort.4')
      OPEN(UNIT=7,FILE='fort.7')
      OPEN(UNIT=8,FILE='fort.8')
      OPEN(UNIT=9,FILE='fort.9')

      REWIND 7
      REWIND 8
      REWIND 9
      REWIND 3
      REWIND 4
      CALL AUTO(W,IW)
      CLOSE(3)
      CLOSE(4)
      CLOSE(7)
      CLOSE(8)
      CLOSE(9)
      STOP
      END
```

```
      SUBROUTINE FUNC(NDIM,NPAR,U,ICP,PAR,IJAC,F,DFDU,DFDP)
C     --------- ----------------------------------------

C   Revised 13 Aug 89 - Moved all calls to subroutine COEFF to
C   the start of subroutine FUNX.  Deleted COMMON block SEIZE.

      IMPLICIT DOUBLE PRECISION (A-H,O-Z)
      COMMON /KS/ K1,K5,K7,K8,K9,K10,K12,K13,K14,K15,K16,K17
      COMMON /ACDATA/ BWING,CWING,SREF,RHO,RMASS,THRUST
      DOUBLE PRECISION K1,K5,K7,K8,K9,K10,K12,K13,K14,K15,K16,K17
C     DOUBLE PRECISION K2,K3,K4,K6,K11,IX,IY,IZ,IXZ


C  Revised 13 Aug 89 to dimension DELF1, DELF2, and DX to 15 (was
   8).
C  Revised 5 Sep 89 - Changed dimension DELF1, DELF2, and DX to
   50 (was 15).

      DIMENSION DFDU(NDIM,NDIM),DFDP(NDIM,NPAR),DELF1(50),
     +          DELF2(50),U(NDIM),PAR(10),F(NDIM),DX(50)

C      WRITE(6,*) 'ENTERED FUNC'


C     INITIALIZE SOME CONSTANTS THAT ARE PASSED THROUGH
C     THE COMMON BLOCK ACDATA

C     DATA IS FROM MCAIR REPORT# A4172 AND AFFTC-TR-75-32
C     F-15A APPROACH-TO-STALL/STALL/POST-STALL EVALUATION

C     BWING  - A/C WINGSPAN, FT
C     CWING  - A/C MEAN AERODYNAMIC CHORD, FT
C     SREF   - A/C WING REFERENCE AREA, SQ FT
C     RHO    - AIR DENSITY AT 20000 FT ALTITUDE, SLUG/FT^3
C     RMASS  - A/C MASS, SLUGS
C     THRUST - TOTAL A/C THRUST, LBS

      BWING=42.8
      CWING=15.94
      SREF=608.
      RHO=.0012673
      RMASS=37000./32.174
      THRUST=8300.


C      DETERMINE CONSTANTS K1 THROUGH K17.  SOME ARE MADE COMMON
AND
C      PASSED TO SUBROUTINE FUNX AND USED IN THE EQUATIONS
C      OF MOTION THERE
C
```

```
C       INERTIAS HAVE UNITS OF SLUG-FT^2
C
C       K1 HAS UNITS OF 1/FT
C
C       K6, K8, K11, K14, AND K17 HAVE UNITS OF 1/FT^2
C
C
C       IX=  25480.
C       IY= 166620.
C       IZ= 186930.
C       IXZ= -1000.
C       K1=.5*RHO*SREF/RMASS
C       K2=(IZ-IY)/IX
C       K3=IXZ*IXZ/(IX*IZ)
C       K4=(IY-IX)/IZ
C       K5=IXZ/IX
C       K6=.5*RHO*BWING*SREF/IX
C       K7=IXZ/IZ
C       K8=.5*RHO*SREF*CWING/IY
C       K9=(IZ-IX)/IY
C       K10=IXZ/IY
C       K11=.5*RHO*SREF*BWING/IZ
C       K12=(K2+K3)/(1.-K3)
C       K13=(1.-K4)*K5/(1.-K3)
C       K14=K6/(1.-K3)
C       K15=(K3-K4)/(1.-K3)
C       K16=(1.+K2)*K7/(1.-K3)
C       K17=K11/(1.-K3)
C
C
        K1   = 3.350088890D-04
        K5   =-3.924646781D-02
        K7   =-5.349596105D-03
        K8   = 3.685650971D-05
        K9   = .96897131196
        K10  =-6.001680471D-03
        K12  = .79747314581
        K13  =-9.615755341D-03
        K14  = 6.472745847D-04
        K15  =-.754990553922
        K16  =  K13
        K17  = 8.822851558D-05


C       FIND THE VALUES OF F(1) THROUGH F(NDIM).  SUBROUTINES
C       COEFF AND FUNX ARE CALLED ONCE.


C       TEST ALPHA AND BETA FOR OUT OF BOUNDS CONDITION.
C       -8 .GE. ALPHA .LE. 50 DEGREES AND -30 .GE. BETA .LE. 30
C       DEGREES.  IF A VARIABLE PASSES OUTSIDE A BOUNDARY, SET THAT
```

```
C     VARIABLE EQUAL TO THAT LIMIT AND ISSUE A MESSAGE TO THE
C     SCREEN AND CONTINUE TO EXECUTE.

C      IF(U(1) .GT. 50.) WRITE(6,*) 'ALPHA > 50 DEGREES, CONTINUE
      TO RUN'
      IF(U(1) .LT. -8.) WRITE(6,*) 'ALPHA < -8 DEGREES, CONTINUE
      TO RUN'
      IF(U(2) .GT. 30.) WRITE(6,*) 'BETA > 30 DEGREES, CONTINUE
TO RUN'
      IF(U(2) .LT. -30.) WRITE(6,*)'BETA < -30 DEGREES, CONTINUE
      TO RUN'


C      WRITE(6,*)'ALPHA,BETA,P,Q=',U(1),U(2),U(3),U(4)
C      WRITE(6,*)'R,THETA,PHI,VELOCITY=',U(5),U(6),U(7),U(8)

      CALL FUNX(NDIM,U,PAR,F)

C      WRITE(6,*) 'F1,F2= ',F(1),F(2)
C      WRITE(11,*) 'F1,F2= ',F(1),F(2)
C      WRITE(6,*) 'F3,F4= ',F(3),F(4)
C      WRITE(11,*) 'F3,F4= ',F(3),F(4)
C      WRITE(6,*) 'F5,F6= ',F(5),F(6)
C      WRITE(11,*) 'F5,F6= ',F(5),F(6)
C      WRITE(6,*) 'F7,F8= ',F(7),F(8)
C      WRITE(11,*) 'F7,F8= ',F(7),F(8)

      IF(IJAC.EQ.0) RETURN

C   SET THE VALUES OF DX
C   MODIFIED TO SCALE DX ACCORDING TO VARIABLE
C   13 JUN 88

C  Revised 13 Aug 89 - Added DX(9) to DX(11) for the control
C  surface states.  Used DX0*50. since this was already being
C  used for DPAR when these were parameters rather than states.
C  Revised 5 Sep 89 - Added DX(12) for differential tail.
      DX0=1.0D-9
      DX(1)=DX0*50.
      DX(2)=DX0*10.
      DX(3)=DX0*.5
      DX(4)=DX0*.25
      DX(5)=DX0*.5
      DX(6)=DX0*50.
      DX(7)=DX0*50.
      DX(8)=DX0*.5
      DX(9)=DX0*50.
      DX(10)=DX0*50.
      DX(11)=DX0*50.
      DX(12)=DX0*50.

C     NEXT THE PARTIAL OF F W.R.T. A GIVEN PARAMETER ARE FINITE
```

```
C     DIFFERENCED

      PTEMP=PAR(ICP)
      PAR(ICP)=PTEMP+DX(1)
      CALL FUNX(NDIM,U,PAR,DELF1)

      PAR(ICP)=PTEMP-DX(1)
      CALL FUNX(NDIM,U,PAR,DELF2)

        DO 13 I=1,NDIM
           DFDP(I,ICP)=(DELF1(I)-DELF2(I))/(2.*DX(1))
 13     CONTINUE
      PAR(ICP)=PTEMP

C     THE NEXT DO LOOP CALCULATES THE PARTIAL DERIVATIVE OF F
C     W.R.T.TO U USING FINITE DIFFERENCES.

C     SET U(J) EQUAL TO U+DU, THEN CALL COEFF WITH THIS UPDATED
C     STATE VECTOR.  THIS IS DONE SIMILARLY WITH U-DU

      DO 20 J=1,NDIM

         UTEMP=U(J)

         U(J)=UTEMP+DX(J)
         CALL FUNX(NDIM,U,PAR,DELF1)
         U(J)=UTEMP-DX(J)
         CALL FUNX(NDIM,U,PAR,DELF2)
         DO 16 I=1,NDIM
            DFDU(I,J)=(DELF1(I)-DELF2(I))/(2.*DX(J))
 16         CONTINUE

         U(J)=UTEMP

 20   CONTINUE


C      WRITE(6,30) ((DFDU(I,J),J=1,NDIM),I=1,NDIM)
C 30   FORMAT(8(1X,E8.2)/)
C      WRITE(6,*) 'LEAVING FUNC'

      RETURN
      END

      SUBROUTINE FUNX(NDIM,U,PAR,F)
C     ---------- ---------

C     SUBROUTINE FUNX EVALUATES THE NDIM EQUATIONS GIVEN THE
C     STATE VECTOR U.

C     Revised 13 Aug 89 - Added PAR to the argument list
C     for FUNX.  Moved the call for subroutine COEFF from several
```

```
C     places in FUNC to the start of FUNX.  Added PAR to DIMENSION
C     statement.

C     NDIM- THE DIMENSION OF THE PROBLEM
C     U    - THE VECTOR OF STATES ALPHA, BETA, ... (INPUT)
C     PAR - THE VECTOR OF PARAMETERS
C     F    - THE VECTOR RESULT OF FUNCTION EVALUATIONS (OUTPUT)

      IMPLICIT DOUBLE PRECISION (A-H,O-Z)
      COMMON /SEIZE/ CX,CY,CZ,CLM,CMM,CNM
      COMMON /KS/ K1,K5,K7,K8,K9,K10,K12,K13,K14,K15,K16,K17
      DOUBLE PRECISION K1,K5,K7,K8,K9,K10,K12,K13,K14,K15,K16,K17
      DIMENSION U(NDIM),F(NDIM),PAR(10)

C     CALL SUBROUTINE COEFF TO SET VALUES.

      CALL COEFF(U,NDIM)

C     SET TRIGONOMETRIC RELATIONSHIPS OF THE STATES ALPHA, BETA,
C     THETA, AND PHI AND THEN SET P, Q, R, AND VTRFPS

C      WRITE(6,*) 'ENTERED FUNX'
      IWRITE=1
C
C     IF(IWRITE.EQ.1)WRITE(6,*)'K1,5,7,8,9,10,12-17=',K1,K5,K7,K8,
C     +                              K9,K10,K12,K13,K14,K15,K16,K17
C      IF(IWRITE.EQ.1)WRITE(6,*)'FUNX U(1)-U(8)=',U(1),U(2),U(3),
C     +    U(4),U(5),U(6),U(7),U(8)

      DEGRAD=57.29577951

      CA=COS(U(1)/DEGRAD)
      SA=SIN(U(1)/DEGRAD)
      CB=COS(U(2)/DEGRAD)
      SB=SIN(U(2)/DEGRAD)
      CTHE=COS(U(6)/DEGRAD)
      STHE=SIN(U(6)/DEGRAD)
      CPHI=COS(U(7)/DEGRAD)
      SPHI=SIN(U(7)/DEGRAD)

      P=U(3)
      Q=U(4)
      R=U(5)
      VTRFPS=1000.*U(8)

C     Revised 13 Aug 89 - Added 3 new states for the control
      surfaces.
C     Deflections are in degrees.  Also added variables for
      commanded
C     control surface deflections in degrees.
C     Revised 5 Sep 89 - Added new state for differential tail
      control
```

```
C     surface deflection.

      DSTBD=U(9)
      DRUDD=U(10)
      DAILD=U(11)
      DDTD=U(12)


      CDSTBD=PAR(1)
      CDRUDD=PAR(2)
      CDAILD=PAR(3)

C     SET THE GRAVITATIONAL CONSTANT, FT/SEC

      G=32.174

C     THE FOLLOWING SYSTEM OF NONLINEAR DIFFERENTIAL EQUATIONS
C     GOVERN AIRCRAFT MOTION

C     UPDATED FOR PROPER DEGREE-RADIAN UNITS AND PROPERLY
C     SCALED VELOCITY EQUATION:  7 JUN 88

C    F(1)=ALPHA-DOT

  1    F(1)=Q+(-(K1*VTRFPS*CX-G*STHE/VTRFPS+R*SB)*SA+(K1*VTRFPS
     +           *CZ+(G*CTHE*CPHI/VTRFPS)-P*SB)*CA)/CB
       F(1)=F(1)*DEGRAD


C    F(2)=BETA-DOT

  2    F(2)=-((K1*VTRFPS*CX-G*STHE/VTRFPS)*SB+R)*CA+(K1*VTRFPS*CY
     +   +G*CTHE*SPHI/VTRFPS)*CB-((K1*VTRFPS*CZ+G*CTHE*CPHI/VTRFPS)
     +    *SB-P)*SA
       F(2)=F(2)*DEGRAD

C
WRITE(6,*)'K1,CX,CY,CZ,F(2),G,SB,CB,CA,SA,SPHI,CPHI,CTHE,STHE',
C                                +
K1,CX,CY,CZ,F(2),G,SB,CB,CA,SA,SPHI,CPHI,CTHE,STHE

C    F(3)=P-DOT

  3    F(3)=-K12*Q*R+K13*P*Q+K14*(CLM+K7*CNM)*VTRFPS*VTRFPS


C    F(4)=Q-DOT

  4    F(4)=K8*VTRFPS*VTRFPS*CMM+K9*P*R+K10*(R*R-P*P)


C    F(5)=R-DOT
```

```
  5   F(5)=K15*P*Q-K16*Q*R+K17*VTRFPS*VTRFPS*(K5*CLM+CNM)

C     F(6)=THETA-DOT

  6   F(6)=Q*CPHI-R*SPHI
      F(6)=F(6)*DEGRAD

C     F(7)=PHI-DOT

  7   F(7)=P+Q*(STHE/CTHE)*SPHI+R*(STHE/CTHE)*CPHI
      F(7)=F(7)*DEGRAD

C     F(8)=VTRFPS-DOT  (SCALED BY A FACTOR OF 1000)

  8   F(8)=U(8)*((K1*VTRFPS*CX-G*STHE/VTRFPS)*CA*CB+(K1*VTRFPS*CY
                                                              +
+G*CTHE*SPHI/VTRFPS)*SB+(K1*VTRFPS*CZ+G*CTHE*CPHI/VTRFPS)*SA*CB)

C     Revised 13 Aug 89 - Added differential equations governing
      control surfaces.  Equations assume CAS off and
      Aileron-Rudder Interconnect off.  Deflections are in degrees.

C     F(9)=DSTBD-DOT

  9   F(9)=20.*(CDSTBD-DSTBD)

C     F(10)=DRUDD-DOT

  10  F(10)=28.*(CDRUDD-DRUDD)

C     F(11)=DAILD-DOT

  11  F(11)=20.*(CDAILD-DAILD)

C     F(12)=DDTD-DOT

C     Revised 5 Sep 89 - Added new state for differential tail
C     deflection.  Neglecting CAS inputs, the differential tail
C     deflection is 6/20 of the commanded aileron deflection,
C     acting through the stabilator actuators.

  12  F(12)=20.*(.3*CDAILD-DDTD)
```

```
C      WRITE(6,*) 'LEAVING FUNX'
C                        W R I T E ( 6 , * ) ' l v    f u n x
F=',F(1),F(2),F(3),F(4),F(5),F(6),F(7),F(8)
      RETURN
      END

      SUBROUTINE STPNT(NDIM,U,NPAR,ICP,PAR)
C     ---------- ------------------------

C     THIS SUBROUTINE SETS THE VALUES OF THE STATES AND
C     PARAMETERS AT THE START OF THE ANALYSIS.  THE STATES AND
C     CONTROL SURFACE SETTINGS REPRESENT AN EQUILIBRIUM STATE OF
C     THE AIRCRAFT

C   Revised 13 Aug 89 - Changed to incorporate control surface
C   deflections as states and commanded control surface
C   deflections as parameters.  Changed READ statements to DO
C   loop format.
C   Revised 5 Sep 89 - Added new state for differential tail
C   control surface deflection.

      IMPLICIT DOUBLE PRECISION (A-H,O-Z)

      DIMENSION U(NDIM),PAR(10)

C      WRITE(6,*) 'ENTERED STPNT'

C     U(1) - ALPHA, DEG
C     U(2) - BETA, DEG
C     U(3) - P, RAD/SEC
C     U(4) - Q, RAD/SEC
C     U(5) - R, RAD/SEC
C     U(6) - THETA, DEG
C     U(7) - PHI, DEG
C     U(8) - TRUE VELOCITY, IN THOUSANDS OF FT/SEC
C     U(9) - DSTBD, STABILATOR DEFLECTION, DEG
C     U(10) - DRUDD, RUDDER DEFLECTION, DEG
C     U(11) - DAILD, AILERON DEFLECTION, DEG
C     U(12) - DDTD, DIFFERENTIAL TAIL DEFLECTION, DEG

C     THE STARTING POINT (VECTOR) IS READ IN THIS WAY
C     SO THAT THE DATA FILE (UNIT 15) HAS A COLUMN OF
C     NUMBERS.  I BELIEVE THAT USING A COLUMN WILL MAKE IT
C     EASIER TO GET THE NUMBERS RIGHT THE FIRST TIME.

      OPEN(UNIT=15,FILE='fort.15')
      REWIND (15)

      DO 10 I=1,NDIM
         READ(15,*) U(I)
   10 CONTINUE
      U(8)=U(8)/1000.
```

```
C     PAR(1)=CDSTBD
C     PAR(2)=CDRUDD     THE PARAMETERS, IN DEGREES
C     PAR(3)=CDAILD

      DO 20 I=1,3
         READ(15,*) PAR(I)
   20 CONTINUE


      RETURN
      END


      SUBROUTINE INIT
C     ---------- ----

      IMPLICIT DOUBLE PRECISION(A-H,O-Z)

      COMMON /BLCSS/ NDIM,ITMX,NPAR,ICP,IID,NMX,IPS,IRS
      COMMON /BLCPS/ NTST,NCOL,IANCH,NMXPS,IAD,NPR,NWTN,ISP,ISW1
      COMMON /BLDLS/ DS,DSMIN,DSMAX,IADS
      COMMON /BLLIM/ RL0,RL1,A0,A1,PAR(10)
      COMMON /BLOPT/ ITNW,MXBF,IPLT,ICP2,ILP
      COMMON /BLEPS/ EPSU,EPSL,EPSS,EPSR


C IN THIS SUBROUTINE THE USER SHOULD SET THOSE CONSTANTS THAT
  REQUIRE VALUES DIFFERENT FROM THE DEFAULT VALUES ASSIGNED IN
  THE LIBRARY SUBROUTINE DFINIT. FOR A DESCRIPTION OF THESE
  CONSTANTS SEE THE DOCUMENTATION CONTAINED IN THE LIBRARY.
  COMMON BLOCKS CORRESPONDING TO CONSTANTS THAT THE USER WANTS TO
  CHANGE MUST BE INSERTED ABOVE.  THESE COMMON BLOCKS SHOULD OF
  COURSE BE IDENTICAL TO THOSE IN DFINIT.


      DSMAX = 10.
      DSMIN = .0000001
      EPSU  = 1.0D-07
      EPSL  = 1.0D-07
      EPSS  = 1.0D-05
      EPSR  = 1.0D-07
      IAD   = 1
      ILP   = 1
      ITMX  = 10
      ITNW  = 5
      MXBF  = 5
C   Revised 13 Aug 89 - Changed NDIM from 8 to 11.
C   Revised 5 Sep 89 - Changed NDIM from 11 to 12.
      NDIM  = 12
      NPAR  = 3
```

```
      OPEN(UNIT=25,FILE='fort.25')
      REWIND (25)

      READ(25,*) RL0,RL1
      READ(25,*) A0,A1
      READ(25,*) DS
      READ(25,*) NMX
      READ(25,*) NTST,NCOL,NMXPS,NPR
      READ(25,*) ISP,IRS,ICP,ICP2,IPLT,IPS
      READ(25,*) ISW1

C      WRITE(6,*) 'LEAVING INIT'

      RETURN
      END
      SUBROUTINE BCND
C     ---------- ----

      RETURN
      END

      SUBROUTINE ICND
C     ---------- ----

      RETURN
      END



**********************************************************************
*******
      SUBROUTINE COEFF(U,NDIM)
**********************************************************************C
Last Edited:  30 May 90 by J.Beck

C  This subroutine computes the aerodynamic force and moment
C  coefficients to be used in subroutine FUNX.  It was taken
C  directly from Dan Baumann's program D2ICC.  The only changes
C  made were to incorporate the CONSTANT common block, to change
C  the control surface deflections from parameters to states
C  (i.e., DSTBD=U(13) rather than DSTBD=PAR(1)), to remove PAR
C  from the argument list, to use the 1988 data base control
C  surface deflection names (DSTBD, DAILD, DTALD, and
C  DRUDD), and to use the differential tail deflection state
C  rather than .3*DAILD.
C=====================================================================
      IMPLICIT DOUBLE PRECISION (A-H,O-Z)
      DIMENSION U(NDIM)
      COMMON /ACDATA/ BWING,CWING,SREF,RHO,RMASS,THRUST
      COMMON /SEIZE/ CX,CY,CZ,CLM,CMM,CNM
```

```
C   THE PRIMARY SOURCE OF THESE COEFFICIENT EQUATIONS IS
C   SUBROUTINE ARO10 FROM MCAIR CODE USED IN THE F15 BASELINE
C   SIMULATOR. MOST OF THE COEFFICIENTS USED IN THE EQUATIONS
C   WERE COMPUTED USING SAS WITH RAW DATA FROM THE F15 SIMULATOR
C   DATA TABLES. THIS SUBROUTINE IS CALLED BY THE DRIVER PROGRAM
C   FOR THE AUTO SOFTWARE.  IT MERELY TAKES INPUTS ON THE A/C
C   STATE AND CONTROL SURFACE POSITIONS AND RETURNS THE
C   APPROPRIATE AERO COEFFICIENTS CX, CY, CZ, CL, CM, AND CM.

C    22 July 1990- Due to the fact that this is a merger of a
C    later subroutine to an earlier version, some of the
C    complexity of the later version has to be taken out. In
C    this case it involves restating certian constants.

C     GRAVITATIONAL CONSTANT
      G=32.174

C     DEGREE TO RADIAN CONVERSION
      DEGRAD=57.2957795131

C     PI
      PI=3.1415926536

C   INPUTS TO THIS SUBROUTINE

C   AL       - ANGLE OF ATTACK, DEG
C   BETA     - SIDESLIP ANGLE, DEG
C   DDA      - AILERON DEFLECTION ANGLE, DEG
C   DELEDD   - DIFFERENTIAL TAIL DEFLECTION ANGLE, DEG
C   DELESD   - SYMMETRICAL TAIL DEFLECTION ANGLE, DEG
C   DRUDD    - RUDDER DEFLECTION, POSITIVE TRAILING EDGE LEFT, DEG

C   P        - ROLL RATE, RAD/SEC
C   Q        - PITCH RATE, RAD/SEC
C   R        - YAW RATE, RAD/SEC
C   THRUST   - TOTAL ENGINE THRUST, POUNDS
C   VTRFPS   - TRUE AIRSPEED, FT/SEC

C   INTERMEDIATE VARIABLES USED IN THIS SUBROUTINE

C   ABET     - ABSOLUTE VALUE OF BETA, DEG
C   ARUD     - ABSOLUTE VALUE OF RUDDER DEFLECTION, DEG
C   BWING    - WING SPAN, FEET
C   CA       - COSINE RAL (RAL IN RADIANS)
C   CD       - COEFFICIENT OF DRAG
C   CL       - BASIC LIFT COEFFICIENT
C   CWING    - MEAN AERODYNAMIC CHORD, FEET
C   DAHD     - DIFFERENTIAL ELEVATOR DEFLECTION, DEG
C   DAHLD    - LEFT AILERON DEFLECTION, DEG
C   DAHRD    - RIGHT AILERON DELFECTION, DEG
C   DELEDR   - DIFFERENTIAL TAIL DEFLECTION ANGLE, RAD
C   DELESR   - SYMMETRIC TAIL DEFLECTION ANGLE, RAD
```

```
C   QBARS    - DYNAMIC PRESSURE TIMES WING REFERENCE AREA, LBF
C   RABET    - ABSOLUTE VALUE OF BETA, RADIANS
C   RAL      - ABSOLUTE VALUE OF ALPHA, RADIANS
C   RARUD    - ABSOLUTE VALUE OF RUDDER, RADIANS
C   SA       - SINE RAL (RAL IN RADIANS)

C   OUTPUTS FROM THIS SUBROUTINE

C   CX  - BASIC AXIAL FORCE COEFFICIENT, BODY AXIS, + FORWARD
C   CY  - BASIC SIDE FORCE COEFFICIENT, BODY AXIS, + RIGHT
C   CZ  - BASIC NORMAL FORCE COEFFICIENT, BODY AXIS, + DOWN
C   CLM - BASIC ROLLING MOMENT COEFFICIENT, BODY AXIS, + R WING
C         DOWN
C   CMM - BASIC PITCHING MOMENT COEFFICIENT, BODY AXIS, + NOSE UP
C   CNM - BASIC YAWING MOMENT COEFFICIENT, BODY AXIS, + NOSE
C         RIGHT
C    ANGLES USED IN CALCULATING CL, CLLDB, ..., ARE IN RADIANS.
C    THIS IS BECAUSE RADIANS WERE USED IN THE CURVE FITTING
C     PROGRAM TO OBTAIN THE COEFFICIENTS OF THE ALPHA, BETA, ...,
C    TERMS IN THE FOLLOWING EQUATIONS.

C   MOMENT REFERENCE CENTER WAS SET IN ARO10 PROGRAM AS:

C     DATA CMCGR /.2565/, CNCGR /.2565/

C   THE AERO STABILITY DATA WAS TAKEN REFERENCED TO THESE CG
C   LOCATIONS.  THE MOMENTS OF INERTIA AND OTHER AIRCRAFT DATA
C   ARE FOR A CLEAN CONFIGURATION TEST AIRCRAFT WITH A CG AT
C   THE SAME CG.  AS A RESULT, THERE IS NO 'CG OFFSET' TO BE
C   COMPUTED.

      AL=U(1)
      BETA=U(2)
      P=U(3)
      Q=U(4)
      R=U(5)
      THETA=U(6)
      PHI=U(7)
      VTRFPS=U(8)*1000.
      DSTBD=U(9)
      DAILD=U(10)
      DTALD=U(11)
      DRUDD=U(12)

      QBARS=.5*RHO*VTRFPS*VTRFPS*SREF
      CO2V=CWING/(2.*VTRFPS)
      BO2V=BWING/(2.*VTRFPS)
      QSB=BWING*QBARS
      ARUD=ABS(DRUDD)
      RARUD=ARUD/DEGRAD
      RAL=AL/DEGRAD
      ABET=ABS(BETA)
```

```
      RABET=ABET/DEGRAD
      RBETA=BETA/DEGRAD
      DAILA=ABS(DAILD)
      DSTBR=DSTBD/DEGRAD

C*****************************************************************C
C
C
C     NEW SECTION OF CODE - 1) ALL THE AERODYNAMIC COEFFICIENTS
                            IN THIS VERSION OF THE DRIVER
                          PROGRAM ARE TAKEN DIRECTLY FROM
                     THE 1988 F15 AEROBASE (0.6 MACH,
               20000 FEET)
C
C                               2) THIS SECTION SUMMARIZES THE
C                                  AERODYNAMIC COEFFICIENTS AS TO
                              WHAT THEY ARE AND HOW THEY ARE
                         USED. THE FIRST ACCRONYM IS THE
                    JOVIAL NAME OF THE AERODYNAMIC
               COEFFICIENT (CFX1, ETC), THE
          SECOND ACCRONYM IS THE  F15
AEROBASE CODE OR CTAB NAME
C                                  (ATAB15, ETC).  A BRIEF DEFINITION
C                                   OF THE AERODYNAMIC COEFFICIENT IS
                                   ALSO PROVIDED.
C
C                               3) THERE IS ALSO A SECTION THAT
                              PROVIDES A TABLE OF CONVERSIONS
                         BETWEEN WHAT THE VARIABLE IS
                    CALLED IN THE ORIGINAL SECTION OF
                    THIS PROGRAM AND ITS NAME IN THE
               1988 F15 AEROBASE.
C                                  FOR THE SAKE OF CONTINUITY THE
C                                  ORIGINAL PROGRAM NAME IS USED AND
C                                  THE 1988 F15 AEROBASE NAME
C                                  IS PROVIDED AS BOOK KEEPING
C                                  INFORMATION.
C
C
C*****************************************************************
C
C
C
C  CFX = FORCE IN STABILITY AXIS X DIRECTION (CD IN BODY AXIS)
C        (FUNCTION OF CL OR CFZ1)
C  CFX = CFX1 + CXRB + STORE INCREMENTS + CXDSPD + DCXLG + DCD
C
C  CFX1 = ATAB15 = PERFORMANCE DRAG COEFFICIENT - CD
C  CXRB = ATAB22 = DELTA CD DUE TO CG (=0.0)
C  CXDSPD = ATAB27 = DELTA CD DUE TO SPEEDBRAKE (NORMALLY =
                0.0436)
C                    SET TO 0 SINCE THIS STUDY IS CONCERNED
```

```
C                    WITH HIGH ANGLES
C                          OF ATTACK PHENOMENON (>40 DEGREES)
C                    AND BECAUSE THE SPEEDBRAKE WILL NOT DEPLOY
C                    AT ANGLES OF ATTACK GREATER THAN 15 DEGREES.
C
C   DCXLG = ATAB19 = DELTA CD DUE TO REYNOLD'S NUMBER  (=-0.0005)
C   DCD = BTAB03 = DELTA CD DUE TO 2-PLACE CANOPY (F15B) (=0.0005)
C          ******* NOTE THAT DCXLG AND DCD CANCEL EACH OTHER
C
C
C*****************************************************************C
C
C
C   CFY = FORCE IN BODY AXIS Y DIRECTION
C   CFY = CFY1*EPA02 + CYDAD*DAILD + [CYDRD*DRUDD*DRFLX5]*EPA43
C         +[CYDTD*DTFLX5 + DTFLX6]*DTALD + CFYP*PB + CFYR*RB
C         +CYRB + STORE INCREMENTS + DCYB*BETA
C
C   CFY1   = ATAB16 = BASIC SIDE FORCE COEFFICIENT - CY(BETA)
C   EPA02 = ATAB21 = BETA MULTIPLIER TABLE
C    CYDAD  =  ATAB75  =  SIDE  FORCE  COEFFICIENT  DUE  TO  AILERON
C                    DEFLECTION
C   DAILD           = AILERON DEFLECTION (DEG)
C    CYDRD  =  ATAB69  =  SIDE  FORCE  COEFFICIENT  DUE  TO  RUDDER
C                    DEFLECTION
C   DRUDD           = RUDDER DEFLECTION  (DEG)
C   DRFLX5 = ATAB88 = FLEX MULTIPLIER ON CYDRD (=0.89)
C    EPA43  =  ATAB30  =  MULTIPLIER  ON  CNDR,  CLDR,  CYDR  DUE  TO
C                    SPEEDBRAKE
C                    (=1.0)
C   CYDTD = ATAB72 = SIDE FORCE COEFFICIENT DUE TO DIFFERENTIAL C
                TAIL
C                    DEFLECTION - CYDDT
C   DTFLX5 = ATAB10 = FLEX MULTIPLIER ON CYDTD (=0.975)
C   DTFLX6 = ATAB77 = FLEX INCREMENT TO CYDTD (=0.0)
C   DTALD           = DIFFERENTIAL TAIL DEFLECTION (DEG) WHICH IS
C                       DIRECTLY PROPORTIONAL TO AILERON DEFLECTION
                    AND IS PRIMARILY USED TO ASSIST IN ROLLING
                THE F-15B (DTALD=0.3*DAILD)
C   CFYP = ATAB13 = SIDE FORCE COEFFICIENT DUE TO ROLL RATE (CYP)
C   PB              = (PEOBB*SPAN)/(2*VILWF)
C                    PEOBB = ROLL RATE IN RAD/SEC = P
C                    SPAN = WING SPAN = 42.8 FEET = BWING
C                    VILWF = VELOCITY IN FT/SEC = VTRFPS
C   CFYR = ATAB07 = SIDE FORCE COEFFICIENT DUE TO YAW RATE (CYR)
C   RB              = (REOBB*SPAN)/(2*VILWF)
C                    REOBB = YAW RATE IN RAD/SEC = R
C   CYRB = ATAB93 = ASSYMETRIC CY AT HIGH ALPHA (ANGLE OF ATTACK)

C   DCYB     = 0.0  THERE IS NO INCREMENT DELTA CYB (SIDE FORCE)
C              DUE TO A 2-PLACE CANOPY ON THE F15B.  THIS IS
C              BECAUSE THE SAME CANOPY IS USED ON BOTH THE
```

```
C            BASELINE F15A AND THE F15B.  THE SIDEFORCE IS THE
C            SAME FOR BOTH VERSIONS OF THE F15 AND ALREADY
C            INCLUDED IN THE BASIC SIDE FORCE (CFY1).  THE TWO
C            PLACE CANOPY IS MOUNTED DIFFERENTLY HOWEVER, SO
C            THERE IS A DIFFERENCE IN YAWING AND ROLLING MOMENT.
C            (SEE DCNB AND DCLB)
C
C
C*****************************************************************
C
C
C
C  CFZ = FORCE IN STABILITY AXIS Z DIRECTION (CL IN BODY AXIS)
C  CFZ = CFZ1 + CZDSPD + STORE INCREMENTS + DCL*BETA
C
C
C  CFZ1 = ATAB17 = BASIC LIFT COEFFICIENT - CL
C  CZDSPD = ATAB26 = DELTA CL DUE TO SPEEDBRAKE
C               SET TO 0 DUE TO THE REASONS GIVEN ABOVE IN CXDSPD
C  DCL = BTAB01 = DELTA CL DUE TO 2-PLACE CANOPY (F15B) (=0.0)
C
C
C*****************************************************************
C
C
C
C  CML = TOTAL ROLLING MOMENT COEFFICIENT IN BODY AXIS
C  CML = CML1*EPA02 + CLDAD*DAILD + [CLDRD*DRUDD*DRFLX1]*EPA43 +
C        [CLDTD*DTFLX1 + DTFLX2]*DTALD + CMLP*PB + CMLR*RB +
C        STORE INCREMENTS + CLDSPD + DCLB*BETA
C
C
C  CML1 = ATAB01 = BASIC ROLLING MOMENT COEFFICIENT - CL(BETA)
C  EPA02 = ATAB21 = BETA MULTIPLIER TABLE
C  CLDAD = ATAB73 = ROLL MOMENT COEFFICIENT DUE TO AILERON C
C                DEFLECTION
C                     -(CLDA)
C  DAILD           = AILERON DEFLECTION (DEG)
C  CLDRD = ATAB67 = ROLLING MOMENT COEFFICIENT DUE TO RUDDER
C                     DEFLECTION  -(CLD)
C  DRUDD           = RUDDER DEFLECTION (DEG)
C  DRFLX1 = ATAB80 = FLEX MULTIPLIER ON CLDRD (=0.85)
C   EPA43  =  ATAB30  =  MULTIPLIER  ON  CNDR,  CLDR,  CYDR  DUE  TO
C                     SPEEDBRAKE
C                     (=1.0)
C  CLDTD = ATAB70 = ROLL MOMENT COEFFICIENT DUE TO DIFFERENTIAL
C                     TAIL
C                     DEFLECTION - CLDD
C  DTFLX1 = ATAB04 = FLEX MULTIPLIER ON CLDTD (=0.975)
C  DTFLX2 = ATAB84 = FLEX INCREMENT TO CLDTD (=0.0)
C  DTALD           = DIFFERENTIAL TAIL DEFLECTION (DEG) WHICH IS
```

```
C                      DIRECTLY PROPORTIONAL TO AILERON DEFLECTION
C                     AND IS PRIMARILY USED TO ASSIST IN ROLLING
C                     THE F-15B (DTALD = 0.3*DAILD)
C  CMLP = ATAB02 = ROLL DAMPING DERIVATIVE -CLP
C  PB            = (PEOBB*SPAN)/(2*VILWF)
C                    PEOBB = ROLL RATE IN RAD/SEC = P
C                    SPAN = WING SPAN = 42.8 FEET = BWING
C                    VILWF = VELOCITY IN FT/SEC = VTRFPS
C  CMLR = ATAB11 = ROLLING MOMENT COEFFICIENT DUE TO YAW RATE -
C                    CLR
C  RB            = (REOBB*SPAN)/(2*VILWF)
C                   REOBB = YAW RATE IN RAD/SEC = R
C  CLDSPD = ATAB29 = DELTA CL DUE TO SPEEDBRAKE
C                     SET TO 0 DUE TO THE REASONS GIVEN ABOVE IN
C                    CXDSPD
C  DCLB = BTAB04 = INCREMENT DELTA CLB (ROLLING MOMENT) DUE TO C
            2-PLACE CANOPY FROM PSWT 499
C
C
C*****************************************************************C
C
C
C  CMM = TOTAL PITCHING MOMENT COEFFICIENT IN STABILITY AXIS
C        (BODY AXIS - AS WELL)
C  CMM = CMM1 + CMMQ*QB + STORE INCREMENTS + CMDSPD + DCM
C
C  CMM1 = ATAB03 = BASIC PITCHING MOMENT COEFFICIENT - CM
C  CMMQ = ATAB05 = PITCH DAMPING DERIVATIVE - CMQ
C  QB            = (QEOBB*MAC)/(2*VILWF)
C                  QEOBB = PITCH RATE IN RAD/SEC = Q
C                  MAC = MEAN AERODYNAMIC CHORD = 15.94 FEET = C
C                   CWING
C                  VILWF = VELOCITY IN FT/SEC = VTRFPS
C  CMDSPD = ATAB25 = DELTA CM DUE TO SPEEDBRAKE
C                    SET TO 0 DUE THE REASONS GIVEN ABOVE IN C
               CXDSPD
C  DCM = BTAB02 = DELTA CM DUE TO 2-PLACE CANOPY (F15B) (=0.0)
C
C
C*****************************************************************C
C
C
C  CMN = TOTAL YAWING MOMENT COEFFICIENT IN BODY AXIS
C  CMN = CMN1*EPA02 + CNDAD*DAILD + [CNDRD*DRUDD*DRFLX3]*EPA43
C        +[CNDTD*DTLX3 + DTFLX4]*DTALD + CMNP*PB + CMNR*RB + CNRB
C        +DCNB2*EPA36 + STORE INCREMENTS + CNDSPD + DCNB*BETA
C
C
C  CMN1 = ATAB12 = BASIC YAWING MOMENT COEFFICIENT  - CN (BETA)
C  EPA02 = ATAB21 = BETA MULTIPLIER TABLE
C  CNDAD = ATAB74 = YAW MOMENT COEFFICIENT DUE TO AILERON
C                   DEFLECTION -CNDA
```

```
C  DAILD =          = AILERON DEFLECTION (DEG)
C  CNDRD = ATAB68 = YAWING MOMENT COEFFICIENT DUE TO RUDDER
C                    DEFLECTION -CNDR
C  DRUDD           = RUDDER DEFLECTION (DEG)
C  DRFLX3 = ATAB85 = FLEX MULTIPLIER ON CNDRD
C  EPA43 = ATAB30 =  MULTIPLIER ON CNDR, CLDR, CYDR DUE TO C
               SPEEDBRAKE
C  CNDTD = ATAB71 = YAWING MOMENT COEFFICIENT DUE TO DIFFERENTIAL
C                    TAIL
C                    DEFLECTION - CNDDT
C  DTFLX3 = ATAB08 = FLEX MULTIPLIER ON CNDTD
C  DTFLX4 = ATAB09 = FLEX INCREMENT ON CNDTD  (=0.0)
C  DTALD =         = DIFFERENTIAL TAIL DEFLECTION (DEG) WHICH IS
C                    DIRECTLY PROPORTIONAL TO AILERON DEFLECTION
C                    AND IS PRIMARILY USED TO ASSIST IN ROLLING
C                    THE F-15B (DTALD = 0.3*DAILD)
C  CMNP = ATAB06 = YAWING MOMENT COEFFICIENT DUE TO ROLL RATE -
C                  CNP
C  PB            = (PEOBB*SPAN)/(2*VILWF)
C                  PEOBB=ROLL RATE IN RAD/SEC = P
C                  SPAN = WING SPAN = 42.8 FT = BWING
C                  VILWF = VELOCITY IN FT/SEC = VTRFPS
C  CMNR = ATAB14 = YAW DAMPING DERIVATIVE - CNR
C  RB            = (REOBB*SPAN)/(2*VILWF)
C                  REOBB = YAW RATE IN RAD/SEC = R
C  CNRB = ATAB86 = ASSYMETRIC CN AT HIGH ALPHA
C  DCNB2 = ATAB44 = DELTA CNB WITH STABILATOR EFFECT - DELCNB C
            (=0.0)
C  EPA36 = ATAB94 = MULTIPLIER ON DCNB2  (=BETA)
C  CNDSPD = ATAB28 = DELTA CN DUE TO SPEEDBRAKE
C                    SET TO 0 DUE TO THE REASONS GIVEN ABOVE IN
C                  CXDSPD
C  DCNB = BTAB05 = INCREMENT DELTA CNB (YAWING MOMENT) DUE TO
C                  2-PLACE CANOPY (F15B)
C
C
C*****************************************************************C
C
C
C  MISCELLANEOUS COEFFICIENTS AND NAME CONVERSION TABLE
C
C
C       1988 F15                ORIGINAL
C       AEROBASE NAME           PROGRAM NAME          DEFINITION
C       *************           ************          **********
C
C       AL77D                   AL                ANGLE OF ATTACK
C                                                       (DEG)
C       BE77D                   BETA              SIDESLIP ANGLE
C                                                       (DEG)
C       BE77D                   RBETA             SIDESLIP ANGLE
C                                                       (RAD)
```

```
C       BO77D                   ABET            ABSOLUTE VALUE OF
C                                                SIDESLIP ANGLE
C                                                    (DEG)
C       DAILA                   DAILA           ABSOLUTE VALUE OF
C                                                AILERON DEFLEC-
C                                                TION (DEG)
C       DAILD                    DDA             AILERON DEFLEC-
C                                                 TION (DEG)
C       DRUABS                  ARUD            ABSOLUTE VALUE OF
C                                                RUDDER DEFLEC-
C                                                 TION (DEG)
C       DRUABS                  RARUD           ABSOLUTE VALUE OF
C                                                RUDDER DEFLEC-
C                                                TION (RAD)
C       DRUDD                   DRUDD           RUDDER DEFLECTION
C                                                    (DEG)
C       DST3D                   DELESD(R)       AVERAGE
C                                                STABILATOR
C                                                DEFLECTION
C                                                DEG (RAD)
C       DTALD                   DELEDD(R)       DIFFERENTIAL TAIL
C                                                DEFLECTION
C                                                DEG (RAD)
C
C
C
C
C
C
C
        PB=(P*BWING)/(2*VTRFPS)
        QB=(Q*CWING)/(2*VTRFPS)
        RB=(R*BWING)/(2*VTRFPS)
C
C     THE F-15B AERO DATA TABLES DO NOT CONTAIN STABILITY
      COEFFICIENT
C       DATA FOR BETA AND RUDDER DEFLECTION ,DRUDD, LESS THAN 0

C       DEGREES.  THE ABSOLUTE VALUE OF BETA, ABET, AND THE ABSOLUTE

C       VALUE OF RUDDER DEFLECTION, ARUDD, ARE USED IN THE FOLLOWING

C       EQUATIONS.  IN RADIANS THESE PARAMETERS ARE RABET AND RARUD,

C     RESPECTIVELY.  IN SOME CASES THE COEFFICIENT IS MULTIPLIED BY
      A
C       -1 FOR PARAMETER VALUES LESS THAN ZERO.
C
C     EPA02 IS A MULTIPLIER THAT ADJUSTS THE PARTICULAR COEFFICIENT

C     IT IS WORKING ON (CFY1,CML1,CMN1) BY CHANGING THAT PARTICULAR
C     COEFFICIENTS SIGN (POSITIVE OR NEGATIVE) DEPENDENT ON THE SIGN
C       OF THE SIDESLIP ANGLE (BETA).  IF BETA IS NEGATIVE THEN
```

```
C      EPA02=-1.0.  IF BETA IS POSITIVE THEN EPA02=1.0.  SINCE THIS

C      FUNCTION IS DISCONTINUOUS AT THE ORIGIN A CUBIC SPLINE HAS
C      BEEN EMPLOYED TO REPRESENT THIS FUNCTION IN ORDER THAT
C      AUTO CAN RUN.
C
C     Revised 15 Jun 90 - Combined three IF statements into
      IF-THEN-ELSE.
        IF(BETA.LE.-1.0)THEN
          EPA02S=-1.00
        ELSEIF(BETA.GE.1.0)THEN
          EPA02S=1.00
        ELSE
          EPA02S=-1.00+(1.5*((BETA+1.0)**2))-(0.5*((BETA+1.0)**3))
        ENDIF
C
C     Revised 15 Jun 90 - Combined three IF statements into
      IF-THEN-ELSE.
        IF(BETA.LE.-5.0)THEN
          EPA02L=-1.00
        ELSEIF(BETA.GE.5.0)THEN
          EPA02L=1.00
        ELSE

EPA02L=-1.00+(0.06*((BETA+5.0)**2))-(0.004*((BETA+5.0)**3))
        ENDIF
C
C
C
C
C
C
C**************************************************************C
C
C
C

CFZ1=-0.00369376+(3.78028702*RAL)+(0.6921459*RAL*RAL)-(5.0005867

+*(RAL**3))+(1.94478199*(RAL**4))+(0.40781955*DSTBR)+(0.10114579
     +*(DSTBR*DSTBR))
C
       CFZ=CFZ1
C
C
C**************************************************************C
C
C
C
C
C
       CL=CFZ1/57.29578
C
```

```
C      THIS CONVERSION OF CFZ1 TO CL IS AN ARTIFACT FROM THE
C      CURVE FITTING PROCESS WHERE ALL THE INDEPENDENT VARIABLES
C      WERE ANGLES THAT WERE CONVERTED FROM DEGREES TO RADIANS.
C      IT JUST SO HAPPENED THAT FOR CFX1 ONE OF THE VARIABLES
C      WAS NOT AN ANGLE BUT A DIMENSIONLESS COEFFICIENT.
C
C
       CFX1=0.01806821+(0.01556573*CL)+(498.96208868*CL*CL)
      +-(14451.56518396*(CL**3))+(2132344.6184755*(CL**4))
C
C      TRANSITIONING FROM LOW AOA DRAG TABLE TO HIGH AOA DRAG TABLE
C
       CFX2=0.0267297-(0.10646919*RAL)+(5.39836337*RAL*RAL)
      +-(5.0086893*(RAL**3))+(1.34148193*(RAL**4))+
      +(0.20978902*DSTBR)+(0.30604211*(DSTBR**2))+0.09833617
C
       A1=20.0/DEGRAD
       A2=30.0/DEGRAD
       A12=A1+A2
       BA=2.0/(-A1**3+3.*A1*A2*(A1-A2)+A2**3)
       BB=-3.*BA*(A1+A2)/2.
       BC=3.*BA*A1*A2
       BD=BA*A2**2*(A2-3.*A1)/2.
       F1=BA*RAL**3+BB*RAL**2+BC*RAL+BD
       F2=-BA*RAL**3+(3.*A12*BA+BB)*RAL**2-
      +    (BC+2.*A12*BB+3.*A12**2*BA)*RAL+
      +    BD+A12*BC+A12**2*BB+A12**3*BA
C
       IF (RAL .LT. A1) THEN
C
         CFX=CFX1
C
       ELSEIF (RAL .GT. A2) THEN
C
         CFX=CFX2
C
       ELSE
C
         CFX=CFX1*F1+CFX2*F2
C
       ENDIF
C
C
C*****************************************************************C

C
       DTFLX5=0.975
       DRFLX5=0.89
C
       CFY1=-0.05060386-(0.12342073*RAL)+(1.04501136*RAL*RAL)
      +-(0.17239516*(RAL**3))-(2.90979277*(RAL**4))
      ++(3.06782935*(RAL**5))-(0.88422116*(RAL**6))
```

```
     +-(0.06578812*RAL*RABET)-(0.71521988*RABET)-(0.00000475273
     +*(RABET**2))-(0.04856168*RAL*DSTBR)-(0.05943607*RABET*DSTBR)+
     +(0.02018534*DSTBR)
C
      IF (RAL .LT. .52359998) THEN
C
      CFYP=0.014606188+(2.52405055*RAL)-(5.02687473*(RAL**2))
     +-(106.43222962*(RAL**3))+(256.80215423*(RAL**4))
     ++(1256.39636248*(RAL**5))
     +-(3887.92878173*(RAL**6))-(2863.16083460*(RAL**7))+
     +(17382.72226362*(RAL**8))-(13731.65408408*(RAL**9))
      ENDIF
C
      IF ((RAL .GE. .52359998) .AND. (RAL .LE. .610865)) THEN
C
CFYP=0.00236511+(0.52044678*(RAL-0.52359998))-(12.8597002*(RAL-
     +0.52359998)**2)+(75.46138*(RAL-0.52359998)**3)
      ENDIF
C
      IF (RAL .GT. 0.610865) THEN
C
      CFYP=0.0
      ENDIF
C
      IF (RAL .LT. -0.06981) THEN
C
      CFYR=0.35
      ENDIF
C
      IF ((RAL .GE. -0.06981) .AND. (RAL .LT. 0.0)) THEN
C
      CFYR=0.34999999+(35.40124113*(RAL+0.06981)**2)-(493.33441162*
     +(RAL+0.06981)**3)
      ENDIF
C
      IF ((RAL .GE. 0.0) .AND. (RAL .LE. 0.523599)) THEN
C
      CFYR=0.35468605-(2.26998141*RAL)+(51.82178387*RAL*RAL)
     +-(718.55069823*(RAL**3))
     ++(4570.00492172*(RAL**4))-(14471.88028351*(RAL**5))+
     +(22026.58930662*(RAL**6))-(12795.99029404*(RAL**7))
      ENDIF
C
      IF ((RAL .GT. 0.523599) .AND. (RAL .LE. 0.61087)) THEN

C

CFYR=0.00193787+(1.78332496*(RAL-0.52359903))-(41.63198853*(RAL-
     +0.52359903)**2)+(239.97909546*(RAL-0.52359903)**3)
      ENDIF
C
```

```
      IF (RAL .GT. 0.61087) THEN
C
      CFYR=0.0
      ENDIF
C
      IF (RAL .LT. 0.55851) THEN
C
      CYDAD=-0.00020812+(0.00062122*RAL)+(0.00260729*RAL*RAL)
     ++(0.00745739*(RAL**3))-(0.0365611*(RAL**4))
     +-(0.04532683*(RAL**5))+(0.20674845*(RAL**6))
     +-(0.13264434*(RAL**7))-(0.00193383*(RAL**8))
      ENDIF
C
      IF ((RAL .GE. 0.55851) .AND. (RAL .LT. 0.61087)) THEN
C
      CYDAD=0.00023894+(0.00195121*(RAL-0.55851001))+(0.02459273
     +*(RAL-0.55851001)**2)-(0.1202244*((RAL-0.55851001)**3))
      ENDIF
C
      IF (RAL .GE. 0.61087) THEN
C
      CYDAD=0.27681285-(2.02305395*RAL)+(6.01180715*RAL*RAL)
     +-(9.24292188*(RAL**3))+(7.59857819*(RAL**4))
     +-(2.8565527*(RAL**5))+(0.25460503*(RAL**7))
     +-(0.01819815*(RAL**9))
      ENDIF
C
C
C     IF (RAL .LE. 0 (  THEN
C     EPA43=1.0
C     ENDIF
C     IF (RAL .GT. 0.0 AND .LE. 0.6283185) THEN
C     0.6283185 RADIANS = 36 DEGREES
C     EPA43=0.9584809+(4.13369452*RAL)-(18.31288396*RAL*RAL)+
C    +(19.5511466*(RAL**3))-(1.09295946*RAL*DSPBD)+(0.17441033*
C    +DSPBD*DSPBD)
C     ENDIF
C     IF (RAL .GT. 0.6283185) THEN
      EPA43=1.0
C     ENDIF
C
*****************************************************************
C          *  NOTE - THE PARAMETER EPA43 IS A MULTIPLIER ON RUDDER
*
C          *  EFFECTIVENESS DUE TO SPEEDBRAKE.  THIS TABLE IS ALSO
*
C          *  LIMITED TO 36 DEG AOA.  HOWEVER, THERE IS NO AERODY
*
C          *  NAMIC EFFECT FOR ANGLES OF ATTACK LESS THAN 16 DEG,
*
C          *  AND THE SPEEDBRAKE IS AUTOMATICALLY RETRACTED AT AOA
*
```

```
C           *  GREATER THAN 15 DEG.  THEREFORE, THIS TABLE SHOULD
C           *
C           *  NOT BE NECESSARY FOR THE ORDINARY OPERATION OF THE
C           *
C           *  AIRCRAFT
C           *
C
C*************************************************************
C
      CYDRD=0.00310199+(0.00119963*RAL)+(0.02806933*RAL*RAL)
     +-(0.12408447*(RAL**3))-(0.12032121*(RAL**4))
     ++(0.79150279*(RAL**5))-(0.86544347*(RAL**6))
     ++(0.27845115*(RAL**7))+(0.00122999*RAL*RARUD)+(0.00145943
     +*RARUD)-(0.01211427*RARUD*RARUD)+(0.00977937*(RARUD**3))
C
      CYDTD=-0.00157745-(0.0020881*RAL)+(0.00557239*RAL*RAL)
     +-(0.00139886*(RAL**3))+(0.04956247*(RAL**4))
     +-(0.0135353*(RAL**5))-(0.11552397*(RAL**6))
     ++(0.11443452*(RAL**7))-(0.03072189*(RAL**8))-(0.01061113*
     +(RAL**3)*DSTBR)-(0.00010529*RAL*RAL*DSTBR*DSTBR)
     +-(0.00572463*RAL*DSTBR*DSTBR)
     ++(0.01885361*RAL*RAL*DSTBR)-(0.01412258*RAL*(DSTBR**3))
     +-(0.00081776*DSTBR)+(0.00404354*(DSTBR**2))-
     +(0.00212189*(DSTBR**3))+(0.00655063*(DSTBR**4))
     ++(0.03341584*(DSTBR**5))
C
      RALY1=0.6108652
      RALY2=90.0/DEGRAD
      RBETY1=-0.0872665
      RBETY2=0.1745329
C
      AY=0.164
      ASTARY=0.95993
      BSTARY=0.087266
C
      ZETAY=(2.0D0*ASTARY-(RALY1+RALY2))/(RALY2-RALY1)
      ETAY=(2.0D0*BSTARY-(RBETY1+RBETY2))/(RBETY2-RBETY1)
C
      X=(2.0D0*RAL-(RALY1+RALY2))/(RALY2-RALY1)
      Y=(2.0D0*RBETA-(RBETY1+RBETY2))/(RBETY2-RBETY1)
C

      FY=((5.0D0*(ZETAY**2))-(4.0D0*ZETAY*X)-1.0D0)*(((X**2)-1.0D0)
     +**2)*(1.0D0/(((ZETAY**2)-1.0D0)**3))
C

GY=((5.0D0*(ETAY**2))-(4.0D0*ETAY*Y)-1.0D0)*(((Y**2)-1.0D0)**2)
     +*(1.0DC/(((ETAY**2)-1.0D0)**3))
C
      CYRB=AY*FY*GY
C
      IF (RAL .LT. 0.6108652) THEN
```

```
C
      CYRB=0.0
      GOTO 500
      ENDIF
C
      IF ((RBETA .LT. -0.0872665) .OR. (RBETA .GT. 0.1745329)) THEN
C
      CYRB=0.0
      GOTO 500
      ENDIF
C
 500  CFY=(CFY1*EPA02L)+(CYDAD*DAILD)+(CYDRD*DRUDD*DRFLX5*EPA43)+
     +((CYDTD*DTFLX5)*DTALD)+(CFY*PB)+(CFYR*RB)
     ++CYRB
C
C
C*****************************************************************
*****
C
C
C
      DTFLX1=0.975
      DRFLX1=0.85
C
      CML1=-0.00238235-(0.04616235*RAL)+(0.10553168*RAL*RAL)
     ++(0.10541585*(RAL**3))-(0.40254765*(RAL**4))
     ++(0.32530491*(RAL**5))-(0.08496121*(RAL**6))
     ++(0.00112288*(RAL**7))-(0.05940477*RABET*RAL)-
     +(0.07356236*RABET)-(0.00550119*RABET*RABET)+(0.00326191
     +*(RABET**3))
C
      IF (RAL .LT. 0.29671) THEN
C
      CMLP=-0.24963201-(0.03106297*RAL)+(0.12430631*RAL*RAL)
     +-(8.95274618*(RAL**3))+(100.33109929*(RAL**4))
     ++(275.70069578*(RAL**5))-(1178.83425699*(RAL**6))
     +-(2102.66811522*(RAL**7))+(2274.89785551*(RAL**8))
      ENDIF
C
      IF ((RAL .GE. 0.29671) .AND. (RAL .LT. 0.34907)) THEN
C
      CMLP=-0.1635261-(3.77847099*(RAL-0.29671001))+(147.47639465
     +*(RAL-0.29671001)**2)-(1295.94799805*(RAL-0.29671001)**3)
      ENDIF
C
      IF (RAL .GE. 0.34907) THEN
C
      CMLP=-1.37120291+(7.06112181*RAL)-(13.57010422*RAL*RAL)
     ++(11.21323850*(RAL**3))
     +-(4.26789425*(RAL**4))+(0.6237381*(RAL**5))
      ENDIF
```

```
C
      IF (RAL .LT. 0.7854) THEN
C
      CMLR=0.03515391+(0.59296381*RAL)+(2.27456302*RAL*RAL)
     +-(3.8097803*(RAL**3))
     +-(45.83162842*(RAL**4))+(55.31669213*(RAL**5))+

+(194.29237485*(RAL**6))-(393.22969953*(RAL**7))+(192.20860739*
     +(RAL**8))
      ENDIF
C
      IF ((RAL .GE. 0.7854) .AND. (RAL .LE. 0.87266)) THEN
C
      CMLR=0.0925579071-(0.6000000238*(RAL-0.7853999734))
     ++(1.3515939713*((RAL-0.7853999734)**2))
     ++(29.0733299255*((RAL-0.7853999734)**3))
      ENDIF
C
      IF (RAL .GT. 0.87266) THEN
C
      CMLR=-311.126041+(1457.23391042*RAL)-(2680.19461944*RAL*RAL)+

+(2361.44914738*(RAL**3))-(893.83567263*(RAL**4))+(68.23501924*
     +(RAL**6))-(1.72572994*(RAL**9))
      ENDIF
C
      CLDAD=0.00057626+(0.00038479*RAL)-(0.00502091*RAL*RAL)
     ++(0.00161407*(RAL**3))+(0.02268829*(RAL**4))
     +-(0.03935269*(RAL**5))+(0.02472827*(RAL**6))
     +-(0.00543345*(RAL**7))+(0.0000007520348*DSTBR*RAL)+
     +(0.000000390773*DSTBR)
C
      CLDRD=0.00013713-(0.00035439*RAL)-(0.00227912*RAL*RAL)
     ++(0.00742636*(RAL**3))+(0.00991839*(RAL**4))
     +-(0.04711846*(RAL**5))+(0.046124*(RAL**6))
     +-(0.01379021*(RAL**7))+(0.00003678685*RARUD*RAL)+
     +(0.00001043751*RARUD)-(0.00015866*RARUD*RARUD)+(0.00016133
     +*(RARUD**3))
C
      CLDTD=0.00066663+(0.00074174*RAL)+(0.00285735*RAL*RAL)
     +-(0.02030692*(RAL**3))-(0.00352997*(RAL**4))
     ++(0.0997962*(RAL**5))-(0.14591227*
     +(RAL**6))+(0.08282004*(RAL**7))
     +-(0.0168667*(RAL**8))+(0.00306142*(RAL**3)*DSTBR)
     +-(0.00110266*RAL*RAL*(DSTBR**2))+(0.00088031*RAL*
     +(DSTBR**2))-(0.00432594*RAL*RAL*DSTBR)-
     +(0.00720141*RAL*(DSTBR**3))
     +-(0.00034325*DSTBR)+(0.00033433*(DSTBR**2))+(0.00800183
     +*(DSTBR**3))-(0.00555986*(DSTBR**4))-(0.01841172*(DSTBR**5))
C
      IF (RAL .LT. 0.0) THEN
C
```

```
      DCLB=-0.00006
      ENDIF
C
      IF ((RAL .GE. 0.0) .AND. (RAL .LE. 0.209434)) THEN
C
      DCLB=-0.00006+(0.0041035078*RAL*RAL)-(0.0130618699*(RAL**3))
      ENDIF
C
      IF (RAL .GT. 0.209434) THEN
C
      DCLB=0.0
      ENDIF
C
C
      CML=(CML1*EPA02S)+(CLDAD*DAILD)+(CLDRD*DRUDD*DRFLX1*EPA43)+
     +((CLDTD*DTFLX1)*DTALD)+(CMLP*PB)+(CMLR RB)+(DCLB*BETA)
C
C
C*****************************************************************
*****C
C
C
      CMM1=0.00501496-(0.08004901*RAL)-(1.03486675*RAL*RAL)
     +-(0.68580677*(RAL**3))+(6.46858488*(RAL**4))
     +-(10.15574108*(RAL**5))+
     +(6.44350808*(RAL**6))-(1.46175188*(RAL**7))
     ++(0.24050902*RAL*DSTBR)
     +-(0.42629958*DSTBR)-(0.03337449*DSTBR*DSTBR)
     +-(0.53951733*(DSTBR**3))
C
      IF (RAL .LE. 0.25307) THEN
C
      CMMQ=-3.8386262+(13.54661297*RAL)+(402.53011559*RAL*RAL)
     +-(6660.95327122*(RAL**3))-(62257.89908743*(RAL**4))
     ++(261526.10242329*(RAL**5))
     ++(2177190.33155227*(RAL**6))-(703575.13709062*(RAL**7))-
     +(20725000.34643054*(RAL**8))-(27829700.53333649*(RAL**9))
      ENDIF
C
      IF ((RAL .GT. 0.25307) .AND. (RAL .LT. 0.29671)) THEN
C
      CMMQ=-8.4926528931-(2705.3000488281*(RAL-0.2530699968))
     ++(123801.5*(RAL-0.2530699968)**2)
     +-(1414377*(RAL-0.2530699968)**3)
      ENDIF
C
      IF (RAL .GE. .29671) THEN
C
      CMMQ=47.24676075-(709.60757056*RAL)+(3359.08807193*RAL*RAL)-
     +(7565.32017266*(RAL**3))+(8695.1858091*(RAL**4))
     +-(4891.77183313*(RAL**5))+(1061.55915089*(RAL**6))
```

```
      ENDIF
C
      CMM=CMM1+(CMMQ*QB)
C
C
C*****************************************************************
*****C
C
C
      DTFLX3=0.975
      DRFLX3=0.89
C
C
      CMN1=0.01441512+(0.02242944*RAL)-(0.30472558*(RAL**2))
     ++(0.14475549*(RAL**3))
     ++(0.93140112*(RAL**4))-(1.52168677*(RAL**5))+
     +(0.90743413*(RAL**6))-(0.16510989*(RAL**7))
     +-(0.0461968*(RAL**8))
     ++(0.01754292*(RAL**9))-(0.17553807*RAL*RABET)+
     +(0.15415649*RAL*RABET*DSTBR)
     ++(0.14829547*(RAL**2)*(RABET**2))
     +-(0.11605031*(RAL**2)*RABET*DSTBR)
     +-(0.06290678*(RAL**2)*(DSTBR**2))
     +-(0.01404857*(RAL**2)*(DSTBR**2))
     ++(0.07225609*RABET)-(0.08567087*(RABET**2))
     ++(0.01184674*(RABET**3))
     +-(0.00519152*RAL*DSTBR)+(0.03865177*RABET*DSTBR)
     ++(0.00062918*DSTBR)
C
      CNDRD=-0.00153402+(0.00184982*RAL)-(0.0068693*RAL*RAL)
     ++(0.01772037*(RAL**3))
     ++(0.03263787*(RAL**4))-(0.15157163*(RAL**5))+(0.18562888

+*(RAL**6))-(0.0966163*(RAL**7))+(0.01859168*(RAL**8))+(0.0002587

+*RAL*DSTBR)-(0.00018546*RAL*DSTBR*RBETA)-(0.00000517304*RBETA)

+-(0.00102718*RAL*RBETA)-(0.0000689379*RBETA*DSTBR)-(0.00040536
     +*RBETA*RARUD)-(0.00000480484*DSTBR*RARUD)
     +-(0.00041786*RAL*RARUD)
     ++(0.0000461872*RBETA)+(0.00434094*(RBETA**2))
     +-(0.00490777*(RBETA**3))
     ++(0.000005157867*RARUD)+(0.00225169*RARUD*RARUD)-(0.00208072
     +*(RARUD**3))
C
      IF (RAL .LT. 0.55851) THEN
C
      CMNP=-0.00635409-(1.14153932*RAL)+(2.82119027*(RAL**2))+
     +(54.4739579*(RAL**3))-(140.89527667*(RAL**4))-(676.73746128*

     +(RAL**5))+(2059.18263976*(RAL**6))+(1579.41664748*(RAL**7))
```

```
     +-(8933.08535712*(RAL**8))+(6806.54761267*(RAL**9))
      ENDIF
C
      IF ((RAL .GE. 0.55851001) .AND. (RAL .LE. 0.61087)) THEN
C
      CMNP=-.07023239+(1.085815*(RAL -0.55851))
     ++(8.852651*((RAL-.55851)**2))-(192.6093*((RAL-0.55851)**3))
      ENDIF
C
      IF (RAL .GT. 0.61087) THEN
C
      CMNP=-71.03693533+(491.32506715*RAL)
     +-(1388.11177979*(RAL**2))+
     +(2033.48621905*(RAL**3))
     +-(1590.91322362*(RAL**4))+(567.38432316*(RAL**5))
     +-(44.97702536*(RAL**7))+(2.8140669*(RAL**9))
      ENDIF
C
C
C
      IF (RAL .LE. -.069813) THEN
C
      CMNR= -0.2805
      ENDIF
C
      IF ((RAL .GT. -.069813) .AND. (RAL .LT. 0.0)) THEN
C
      CMNR=-0.2804999948+(35.9903717041*(RAL+.0698129982)**2)
     +-(516.1574707031*(RAL+.0698129982)**3)
      ENDIF
C
      IF ((RAL .GE. 0.0) .AND. (RAL .LE. 0.78539801)) THEN
C
      CMNR=-.28071511-(2.52183924*RAL)+(68.90860031*(RAL**2))
     +-(573.23100511*(RAL**3))+(2009.08725005*(RAL**4))
     +-(3385.15675307*(RAL**5))
     ++(2730.49473149*(RAL**6))-(848.12322034*(RAL**7))
      ENDIF
C
      IF ((RAL .GT. 0.78539801) .AND. (RAL .LT. 0.95993102)) THEN

C

CMNR=-0.1096954+(0.52893072*(RAL-0.78539801))-(6.09109497*(RAL-
     +0.78539801)**2)+(17.47834015*(RAL-0.78539801)**3)
      ENDIF
C
      IF (RAL .GE. 0.95993102) THEN
C
      CMNR=-0.11
      ENDIF
C
```

```
      CNDTD=0.00058286+(0.0007341*RAL)-(0.00746113*RAL*RAL)
     +-(0.00685223*(RAL**3))
     ++(0.03277271*(RAL**4))-(0.02791456*(RAL**5))
     ++(0.00732915*(RAL**6))
     ++(0.00120456*RAL*DSTBR)-(0.00168102*DSTBR)+(0.0006462*
     +DSTBR*DSTBR)
C
      CNDAD=0.00008228887-(0.00014015*RAL)-(0.0013493*RAL*RAL)+
     +(0.00020487*(RAL**3))+(0.00561241*(RAL**4))
     +-(0.00634392*(RAL**5))

++(0.00193323*(RAL** 6))-(2.05815E-17*(RAL*DAILA))+(3.794816E-17*
     +(DAILA**3))
C
      DCNB=-2.500E-4
C
      RALN1=0.69813
      RALN2=90.0/DEGRAD
      RBETN1=-0.174532
      RBETN2=0.34906
C
      AN=0.034
      ASTARN=1.0472
      BSTARN=0.087266
C
      ZETAN=(2.0D0*ASTARN-(RALN1+RALN2))/(RALN2-RALN1)
      ETAN=(2.0D0*BSTARN-(RBETN1+RBETN2))/(RBETN2-RBETN1)
C
      XN=(2.0D0*RAL-(RALN1+RALN2))/(RALN2-RALN1)
      YN=(2.0D0*RBETA-(RBETN1+RBETN2))/(RBETN2-RBETN1)
C
      FN=((5.0D0*(ZETAN**2))-(4.0D0*ZETAN*XN)-1.0D0)*
     +(((XN**2)-1.0D0)**2)/(((ZETAN**2)-1.0D0)**3)
C
      GN=((5.0D0*(ETAN**2))-(4.0D0*ETAN*YN)-1.0D0)*
     +(((YN**2)-1.0D0)**2)/(((ETAN**2)-1.0D0)**3)
C
      CNRB=AN*FN*GN
C
      IF (RAL .LT. 0.69813) THEN
C
      CNRB=0.0
      GOTO 1000
      ENDIF
C
      IF ((RBETA .LT. -0.174532) .OR. (RBETA .GT. 0.34906)) THEN
C
      CNRB=0.0
      GOTO 1000
      ENDIF
C
C
```

```
C
 1000 CMN=(CMN1*EPA02S)+(CNDAD*DAILD)+((CNDRD*DRUDD*DRFLX3)*EPA43)+
     +((CNDTD*DTFLX3)*DTALD)+(CMNP*PB)+(CMNR*RB)+(DCNB*BETA)
     ++CNRB
C
C
C*****************************************************************
*****C
C
C
      CX=CFZ*SIN(RAL)-CFX*COS(RAL)+THRUST/QBARS
      CY=CFY
      CZ=-(CFZ*COS(RAL)+CFX*SIN(RAL))
      CLM=CML
      CMM=CMM+THRUST*(0.25/12.0)/(QBARS*CWING)
C
C     THE (0.25/12.0) IS THE OFFSET OF THE THRUST VECTOR FROM THE
C     CG
C
      CNM=CMN
C
C    RETURN CX, CY, CZ, CLM, CMM, CNM TO CALLING PROGRAM.
C
C
C      IWRITE=0
C      IF(IWRITE.EQ.1) WRITE(6,*)' CX,CY,CZ,CLM,CMM,CNM=',
C     +                           CX,CY,CZ,CLM,CMM,CNM
C
C      WRITE(6,*) ' END OF SUB COEFF U(1,2,3)=',U(1),U(2),U(3)
C      WRITE(6,*)'LEAVING COEFF'
      RETURN
      END
```

# APPENDIX C

# SIMULATOR PROGRAM

```
c
      program integ
c
c     ordinary differential equations propagator
c     using routine 'haming' as supplied by w. wiesel
c
      implicit double precision(a-h,o-z)
      common /ham/ t,x(12,4),f(12,4),errest(12),n,h
      common /bpars/ PAR(10)
      open(15,file='fort.15')
      open(7,file='fort.7')
     write (*,*) 'help me'
c
c     read in max printout, number of
c     steps between printing
c
      n = 8
      npar = 3
      read (15,*) nprint,nstep
     write (*,*) 'I M trapped'
c
c     read timestep
c
      t = 0.D 00
      read (15,*) h
     write (*,*) 'in the body'
     write (*,*) 'h=',h
c
c     read initial conditions and parameter values
c

      read (15,*) (x(i,1),i=1,n)
     write (*,*) 'of an aeronautical engineer'
      read (15,*) (PAR(i),i=1,npar)
     write (*,*) 'I m really'
c
c     initialize haming
c
      nxt = 0
      call haming(nxt)
      if(nxt .ne. 0) go to 50
      write (*,1)
 1    format(2x,' haming did not initialize')
      stop
c
 50   continue
C
C
     write (*,*) 'a wily coyote'
c
c     integrate ode....two nested loops
c
```

```
      do 200 ipr = 1,nprint
c
      do 100 istp = 1,nstep
c
c     each call to haming advances one step...
c
      call haming(nxt)
c
 100  continue
c
c     after nstp integration steps, print current values
c
      write(6,2) t,(x(ii,nxt),ii=1,n)
 2    format(1x,9e14.7)
c
 200  continue
c
c
      stop
      end
c
      subroutine rhs(nxt)
c
c     rhs is the right - hand - side subroutine, customized
c     to the particular set of odes being integrated
c
c
      IMPLICIT DOUBLE PRECISION (A-H,O-Z)
      COMMON /KS/ K1,K5,K7,K8,K9,K10,K12,K13,K14,K15,K16,K17
      COMMON /ACDATA/ BWING,CWING,SREF,RHO,MASS,THRUST
      DOUBLE PRECISION K1,K5,K7,K8,K9,K10,K12,K13,K14,K15,K16,K17
c     DOUBLE PRECISION K2,K3,K4,K6,K11,IX,IY,IZ,IXZ
      COMMON /SEIZE/ CX,CY,CZ,CLM,CMM,CNM
      common /ham/ t,xin(12,4),f(12,4),err(12),n,h
      common /pars/ PAR(10)
C
C
      DIMENSION U(20),FF(20)
C
C      WRITE(6,*) 'ENTERED FUNC'
C
C
C     INITIALIZE SOME CONSTANTS THAT ARE PASSED THROUGH
C     THE COMMON BLOCK ACDATA
C
C     DATA IS FROM MCAIR REPORT# A4172 AND AFFTC-TR-75-32
C     F-15A APPROACH-TO-STALL/STALL/POST-STALL EVALUATION
C
C     BWING   - A/C WINGSPAN, FT
C     CWING   - A/C MEAN AERODYNAMIC CHORD, FT
C     SREF    - A/C WING REFERENCE AREA, SQ FT
C     RHO     - AIR DENSITY AT 20000 FT ALTITUDE, SLUG/FT^3
```

```
C       RMASS  - A/C MASS, SLUGS
C       THRUST - TOTAL A/C THRUST, LBS
C
        BWING=42.8D 00
        CWING=15.94D 00
        SREF=608.D 00
        RHO=.0012673D 00
        RMASS=37000.D 00/32.174D 00
        THRUST=8300.D 00
C
C
C        DETERMINE CONSTANTS K1 THROUGH K17.  SOME ARE MADE COMMON
AND
C       PASSED TO SUBROUTINE FUNC AND USED IN THE EQUATIONS
C       OF MOTION THERE
C
C       INERTIAS HAVE UNITS OF SLUG-FT^2
C
C       K1 HAS UNITS OF 1/FT
C
C       K6, K8, K11, K14, AND K17 HAVE UNITS OF 1/FT^2
C
C
C       IX=  25480.
C       IY= 166620.
C       IZ= 186930.
C       IXZ= -1000.
C       K1=.5*RHO*SREF/RMASS
C       K2=(IZ-IY)/IX
C       K3=IXZ*IXZ/(IX*IZ)
C       K4=(IY-IX)/IZ
C       K5=IXZ/IX
C       K6=.5*RHO*BWING*SREF/IX
C       K7=IXZ/IZ
C       K8=.5*RHO*SREF*CWING/IY
C       K9=(IZ-IX)/IY
C       K10=IXZ/IY
C       K11=.5*RHO*SREF*BWING
C       K12=(K2+K3)/(1.-K3)
C       K13=(1.-K4)*K5/(1.-K3)
C       K14=K6/(1.-K3)
C       K15=(K3-K4)./(1.-K3)
C       K16=(1.+K2)*K7/(1.-K3)
C       K17=K11/(1.-K3)
C
C
        K1  = 3.350088890D-04
        K5  =-3.924646781D-02
        K7  =-5.349596105D-03
        K8  = 3.685650971D-05
        K9  = .96897131196D 00
        K10 =-6.001680471D-03
```

```
      K12 = .79747314581D 00
      K13 =-9.615755341D-03
      K14 = 6.472745847D-04
      K15 =-.754990553922D 00
      K16 =  K13
      K17 = 8.822851558D-05
C
C
C
C     FIND THE VALUES OF F(1) THROUGH F(NDIM).  SUBROUTINES
C     COEFF AND FUNX ARE CALLED ONCE.
C
C     U(1) - ALPHA, DEG
C     U(2) - BETA, DEG
C     U(3) - P, RAD/SEC
C     U(4) - Q, RAD/SEC
C     U(5) - R, RAD/SEC
C     U(6) - THETA, DEG
C     U(7) - PHI, DEG
C     U(8) - TRUE VELOCITY, IN THOUSANDS OF FT/SEC
C
C     PAR(1)=DELESD
C     PAR(2)=DRUDD       THE PARAMETERS, IN DEGREES
C     PAR(3)=DDA
C
C
      do 12 i=1,n
      u(i)=xin(i,nxt)
 12   continue
C
C     TEST ALPHA AND BETA FOR OUT OF BOUNDS CONDITION.
C     -8 .GE. ALPHA .LE. 50 DEGREES AND -30 .GE. BETA .LE. 30
C     DEGREES.  IF A VARIABLE PASSES OUTSIDE A BOUNDARY, SET THAT
C     VARIABLE EQUAL TO THAT LIMIT AND ISSUE A MESSAGE TO THE
C     SCREEN AND CONTINUE TO EXECUTE.
c
c      IF(U(1) .GT. 50.) WRITE(6,*) 'ALPHA > 50 DEGREES, CONTINUE
TO RUN'
c      IF(U(1) .LT. -8.) WRITE(6,*) 'ALPHA < -8 DEGREES, CONTINUE
TO RUN'
c     IF(U(2) .GT. 30.) WRITE(6,*) 'BETA > 30 DEGREES, CONTINUE TO
RUN'
c      IF(U(2) .LT. -30.) WRITE(6,*)'BETA < -30 DEGREES, CONTINUE
TO RUN'
C
C
c      WRITE(*,*)'ALPHA,BETA,P,Q=',U(1),U(2),U(3),U(4)
c      WRITE(*,*)'R,THETA,PHI,VELOCITY=',U(5),U(6),U(7),U(8)
c
      CALL COEFF(U,PAR,n)
C
      CALL FUNX(n,U,FF)
```

```
c
      do 13 i=1,n
      f(i,nxt)=FF(i)
 13   continue
c
C
c      WRITE(*,*) 'F1,F2= ',FF(1),FF(2)
C      WRITE(11,*) 'F1,F2= ',FF(1),FF(2)
c      WRITE(*,*) 'F3,F4= ',FF(3),FF(4)
C      WRITE(11,*) 'F3,F4= ',FF(3),FF(4)
c      WRITE(*,*) 'F5,F6= ',FF(5),FF(6)
C      WRITE(11,*) 'F5,F6= ',FF(5),FF(6)
c      WRITE(*,*) 'F7,F8= ',FF(7),FF(8)
C      WRITE(11,*) 'F7,F8= ',FF(7),FF(8)
C
C
      RETURN
      END

      SUBROUTINE FUNX(NDIM,U,F)
C     ---------- ---------
C
C     SUBROUTINE FUNX EVALUATES THE NDIM EQUATIONS GIVEN THE
C     STATE VECTOR U.
C
C     NDIM- THE DIMENSION OF THE PROBLEM
C     U   - THE VECTOR OF STATES ALPHA, BETA, ... (INPUT)
C     F   - THE VECTOR RESULT OF FUNCTION EVALUATIONS (OUTPUT)
C
      IMPLICIT DOUBLE PRECISION (A-H,O-Z)
      COMMON /SEIZE/ CX,CY,CZ,CLM,CMM,CNM
      COMMON /KS/ K1,K5,K7,K8,K9,K10,K12,K13,K14,K15,K16,K17
      DOUBLE PRECISION K1,K5,K7,K8,K9,K10,K12,K13,K14,K15,K16,K17
      DIMENSION U(NDIM),F(NDIM)
C
C     SET TRIGONOMETRIC RELATIONSHIPS OF THE STATES ALPHA, BETA,
C     THETA, AND PHI AND THEN SET P, Q, R, AND VTRFPS
C
C      WRITE(6,*) 'ENTERED FUNX'
c      IWRITE=1
C                          I F ( I W R I T E . E Q . 1 ) W R I T E ( 6 , * ) '
K1,5,7,8,9,10,12-17=',K1,K5,K7,K8,
C     +                                 K9,K10,K12,K13,K14,K15,K16,K17
C      IF(IWRITE.EQ.1)WRITE(6,*)'FUNX U(1)-U(8)=',  1),U(2),U(3),
C     +    U(4),U(5),U(6),U(7),U(8)
C
      DEGRAD=57.29577951D 00
C
      CA=DCOS(U(1)/DEGRAD)
      SA=DSIN(U(1)/DEGRAD)
      CB=DCOS(U(2)/DEGRAD)
      SB=DSIN(U(2)/DEGRAD)
```

```
      CTHE=DCOS(U(6)/DEGRAD)
      STHE=DSIN(U(6)/DEGRAD)
      CPHI=DCOS(U(7)/DEGRAD)
      SPHI=DSIN(U(7)/DEGRAD)
C
      P=U(3)
      Q=U(4)
      R=U(5)
      VTRFPS=1000.D 00*U(8)
C
C     SET THE GRAVITATIONAL CONSTANT, FT/SEC
C
      G=32.174D 00
C
C    THE FOLLOWING SYSTEM OF NONLINEAR DIFFERENTIAL EQUATIONS
C    GOVERN AIRCRAFT MOTION
C
C    UPDATED FOR PROPER DEGREE-RADIAN UNITS AND PROPERLY
C    SCALED VELOCITY EQUATION:  7 JUN 88
C
C   F(1)=ALPHA-DOT
C
  1   F(1)=Q+(-(K1*VTRFPS*CX-G*STHE/VTRFPS+R*SB)*SA+(K1*VTRFPS
     +          *CZ+(G*CTHE*CPHI/VTRFPS)-P*SB)*CA)/CB
      F(1)=F(1)*DEGRAD
C
C
C   F(2)=BETA-DOT
C
  2   F(2)=-((K1*VTRFPS*CX-G*STHE/VTRFPS)*SB+R)*CA+(K1*VTRFPS*CY
     +  +G*CTHE*SPHI/VTRFPS)*CB-((K1*VTRFPS*CZ+G*CTHE*CPHI/VTRFPS)
     +   *SB-P)*SA
      F(2)=F(2)*DEGRAD
C
C
WRITE(6,*)'K1,CX,CY,CZ,F(2),G,SB,CB,CA,SA,SPHI,CPHI,CTHE,STHE',
C                      +
K1,CX,CY,CZ,F(2),G,SB,CB,CA,SA,SPHI,CPHI,CTHE,STHE
C
C   F(3)=P-DOT
C
  3   F(3)=-K12*Q*R+K13*P*Q+K14*(CLM+K7*CNM)*VTRFPS*VTRFPS
C
C
C   F(4)=Q-DOT
C
  4   F(4)=K8*VTRFPS*VTRFPS*CMM+K9*P*R+K10*(R*R-P*P)
C
C
C   F(5)=R-DOT
C
  5   F(5)=K15*P*Q-K16*Q*R+K17*VTRFPS*VTRFPS*(K5*CLM+CNM)
```

```
C
C
C   F(6)=THETA-DOT
C
  6   F(6)=Q*CPHI-R*SPHI
      F(6)=F(6)*DEGRAD
C
C
C   F(7)=PHI-DOT
C
  7   F(7)=P+Q*(STHE/CTHE)*SPHI+R*(STHE/CTHE)*CPHI
      F(7)=F(7)*DEGRAD
C
C
C   F(8)=VTRFPS-DOT  (SCALED BY A FACTOR OF 1000)
C
  8   F(8)=U(8)*((K1*VTRFPS*CX-G*STHE/VTRFPS)*CA*CB+(K1*VTRFPS*CY
                                                              +
+G*CTHE*SPHI/VTRFPS)*SB+(K1*VTRFPS*CZ+G*CTHE*CPHI/VTRFPS)*SA*CB)
C
C
C      WRITE(6,*) 'LEAVING FUNX'
c                        W R I T E ( 6 , * ) ' l v    f u n x
F=',F(1),F(2),F(3),F(4),F(5),F(6),F(7),F(8)
      RETURN
      END
C
C
C
c
c
      subroutine haming(nxt)
c
c     haming is a fourth order predictor-corrector algorithm
c       for the integration of systems of ordinary differential
equations
c     the common block /ham/ contains most of the variables:
c        x is the independent variable, the 'time'
c        y contains 4 copies of the state vector, with
c              n odes being integrated
c        f contains the calculated equations of motion
c        errest is a truncation error estimate
c        n is the number of odes
c        h is the integration timestep
c     nxt assumes the values 1,2,3,4,1,2,3,4,..., and points to
c     the current value of the state vector
c
c     the user must supply a subroutine 'rhs(nxt)' which
c     calculates the equations of motion f(i,nxt) from the
c     state vector y(i,nxt)
c
c     to initialize haming, the initial conditions must be stored
```

```
c     in y(i,1), i=1,n ; x,n, and h must be initialized, and
c     then haming is called with nxt=0.  If haming returns with
c     nxt=1, initialization is successful.  If nxt=0 still, haming
c     did not initialize (h is usually too big)
c
      common /ham/ x,y(12,4),f(12,4),errest(12),n,h
      double precision x,y,f,errest,h,xo,tol,hh
      tol = 1.0d-12
c     branch on nxt: startup or propagating?
      if(nxt) 190,10,200
c
c     haming initialization:  4 point picard iteration
c
   10 xo = x
      hh = h/2.0
      call rhs(1)
      do 40 l = 2,4
      x = x + hh
      do 20 i = 1,n
   20 y(i,l) = y(i,l-1) + hh*f(i,l-1)
      call rhs(l)
      x = x + hh
      do 30 i = 1,n
   30 y(i,l) = y(i,l-1) + h*f(i,l)
   40 call rhs(l)
      jsw = -10
   50 isw = 1
      do 120 i = 1,n
      hh = y(i,1) + h*( 9.0*f(i,1) + 19.0*f(i,2) - 5.0*f(i,3)
     1     + f(i,4) ) / 24.0
      if( dabs( hh - y(i,2)) .lt. tol ) go to 70
      isw = 0
   70 y(i,2) = hh
      hh = y(i,1) + h*( f(i,1) + 4.0*f(i,2) + f(i,3))/3.0
      if( dabs( hh-y(i,3)) .lt. tol ) go to 90
      isw = 0
   90 y(i,3) = hh
      hh = y(i,1) + h*( 3.0*f(i,1) + 9.0*f(i,2) + 9.0*f(i,3)
     1     + 3.0*f(i,4) ) / 8.0
      if( dabs(hh-y(i,4)) .lt. tol ) go to 110
      isw = 0
  110 y(i,4) = hh
  120 continue
      x = xo
      do 130 l = 2,4
      x = x + h
  130 call rhs(l)
      if(isw) 140,140,150
  140 jsw = jsw + 1
      if(jsw) 50,280,280
  150 x = xo
      isw = 1
```

```
      jsw = 1
      do 160 i = 1,n
  160 errest(i) = 0.0
      nxt = 1
      go to 280
  190 jsw = 2
      nxt = iabs(nxt)
c
c     haming propagation section
c
  200 x = x + h
      npl = mod(nxt,4) + 1
      go to (210,230),isw
  210 go to (270,270,270,220),nxt
  220 isw = 2
c
c     permute indices
c
  230 nm2 = mod(npl,4) + 1
      nml = mod(nm2,4) + 1
      npo = mod(nml,4) + 1
c
c     predictor
c
      do 240 i = 1,n
      f(i,nm2) = y(i,npl) + 4.0*h*( 2.0*f(i,npo) - f(i,nml)
     1     + 2.0*f(i,nm2) ) / 3.0
  240 y(i,npl) = f(i,nm2) - 0.925619835*errest(i)
      call rhs(npl)
c
c     corrector
c
      do 250 i = 1,n
      y(i,npl) = ( 9.0*y(i,npo) - y(i,nm2) + 3.0*h*( f(i,npl)
     1     + 2.0*f(i,npo) - f(i,nml) ) ) / 8.0
      errest(i) = f(i,nm2) - y(i,npl)
  250 y(i,npl) = y(i,npl) + 0.0743801653 * errest(i)
      go to (260,270),jsw
  260 call rhs(npl)
  270 nxt = npl
  280 return
      end
c
*******************************************************************
*******
      SUBROUTINE COEFF(U,NDIM)
*******************************************************************
*******
C  Last Edited:  30 May 90 by J.Beck

C  This subroutine computes the aerodynamic force and moment
```

```
C   coefficients to be used in subroutine FUNX.  It was taken
directly
C  from Dan Baumann's program D2ICC.  The only changes made were to
C   incorporate the CONSTANT common block, to change the control
surface
C  deflections from parameters to states (i.e., DSTBD=U(13) rather
than
C  DSTBD=PAR(1)), to remove PAR from the argument list, to use the
1988
C  data base control surface deflection names (DSTBD, DAILD, DTALD,
and
C  DRUDD), and to use the differential tail deflection state rather
than
C   .3*DAILD.
C=================================================================
*******
      IMPLICIT DOUBLE PRECISION (A-H,O-Z)
      DIMENSION U(NDIM)
      COMMON /ACDATA/ BWING,CWING,SREF,RHO,RMASS,THRUST
      COMMON /SEIZE/ CX,CY,CZ,CLM,CMM,CNM

C   THE PRIMARY SOURCE OF THESE COEFFICIENT EQUATIONS IS SUBROUTINE

C    ARO10 FROM MCAIR CODE USED IN THE F15 BASELINE SIMULATOR.

C   MOST OF THE COEFFICIENTS USED IN THE EQUATIONS WERE COMPUTED
C   USING SAS WITH RAW DATA FROM THE F15 SIMULATOR DATA TABLES.

C   THIS SUBROUTINE IS CALLED BY THE DRIVER PROGRAM FOR THE AUTO
C   SOFTWARE.  IT MERELY TAKES INPUTS ON THE A/C STATE AND CONTROL

C   SURFACE POSITIONS AND RETURNS THE APPROPRIATE AERO COEFFICIENTS

C    CX, CY, CZ, CL, CM, AND CM.

C    22 July 1990- Due to the fact that this is a merger of a later
C    subroutine to an earlier version, some of the complexity of
C    the later version has to be taken out. In this case it C
involves restating certian constants.

C     GRAVITATIONAL CONSTANT
      G=32.174

C     DEGREE TO RADIAN CONVERSION
      DEGRAD=57.2957795131

C     PI
      PI=3.14159265360

C   INPUTS TO THIS SUBROUTINE

C   AL      - ANGLE OF ATTACK, DEG
```

```
C   BETA     - SIDESLIP ANGLE, DEG
C   DDA      - AILERON DEFLECTION ANGLE, DEG
C   DELEDD   - DIFFERENTIAL TAIL DEFLECTION ANGLE, DEG
C   DELESD   - SYMMETRICAL TAIL DEFLECTION ANGLE, DEG
C   DRUDD    - RUDDER DEFLECTION, POSITIVE TRAILING EDGE LEFT, DEG

C   P        - ROLL RATE, RAD/SEC
C   Q        - PITCH RATE, RAD/SEC
C   R        - YAW RATE, RAD/SEC
C   THRUST   - TOTAL ENGINE THRUST, POUNDS
C   VTRFPS   - TRUE AIRSPEED, FT/SEC

C   INTERMEDIATE VARIABLES USED IN THIS SUBROUTINE

C   ABET     - ABSOLUTE VALUE OF BETA, DEG
C   ARUD     - ABSOLUTE VALUE OF RUDDER DEFLECTION, DEG
C   BWING    - WING SPAN, FEET
C   CA       - COSINE RAL (RAL IN RADIANS)
C   CD       - COEFFICIENT OF DRAG
C   CL       - BASIC LIFT COEFFICIENT
C   CWING    - MEAN AERODYNAMIC CHORD, FEET
C   DAHD     - DIFFERENTIAL ELEVATOR DEFLECTION, DEG
C   DAHLD    - LEFT AILERON DEFLECTION, DEG
C   DAHRD    - RIGHT AILERON DELFECTION, DEG
C   DELEDR   - DIFFERENTIAL TAIL DEFLECTION ANGLE, RAD
C   DELESR   - SYMMETRIC TAIL DEFLECTION ANGLE, RAD
C   QBARS    - DYNAMIC PRESSURE TIMES WING REFERENCE AREA, LBF
C   RABET    - ABSOLUTE VALUE OF BETA, RADIANS
C   RAL      - ABSOLUTE VALUE OF ALPHA, RADIANS
C   RARUD    - ABSOLUTE VALUE OF RUDDER, RADIANS
C   SA       - SINE RAL (RAL IN RADIANS)

C   OUTPUTS FROM THIS SUBROUTINE

C   CX       - BASIC AXIAL FORCE COEFFICIENT, BODY AXIS, + FORWARD

C   CY       - BASIC SIDE FORCE COEFFICIENT, BODY AXIS, + RIGHT
C   CZ       - BASIC NORMAL FORCE COEFFICIENT, BODY AXIS, + DOWN
C   CLM      - BASIC ROLLING MOMENT COEFFICIENT, BODY AXIS, + R WING
C                DOWN
C   CMM      - BASIC PITCHING MOMENT COEFFICIENT, BODY AXIS, + NOSE
                 UP
C   CNM      - BASIC YAWING MOMENT COEFFICIENT, BODY AXIS, + NOSE
                 RIGHT

C    ANGLES USED IN CALCULATING CL, CLLDB, ..., ARE IN RADIANS.
C    THIS IS BECAUSE RADIANS WERE USED IN THE CURVE FITTING PROGRAM
C    TO OBTAIN THE COEFFICIENTS OF THE ALPHA, BETA, ..., TERMS IN
C    THE FOLLOWING EQUATIONS.

C   MOMENT REFERENCE CENTER WAS SET IN AR010 PROGRAM AS:
```

```
C      DATA CMCGR /.2565/, CNCGR /.2565/

C    THE AERO STABILITY DATA WAS TAKEN REFERENCED TO THESE CG
C    LOCATIONS.  THE MOMENTS OF INERTIA AND OTHER AIRCRAFT DATA
C    ARE FOR A CLEAN CONFIGURATION TEST AIRCRAFT WITH A CG AT
C    THE SAME CG.  AS A RESULT, THERE IS NO 'CG OFFSET' TO BE
C    COMPUTED.

       AL=U(1)
       BETA=U(2)
       P=U(3)
       Q=U(4)
       R=U(5)
       THETA=U(6)
       PHI=U(7)
       VTRFPS=U(8)*1000.
       DSTBD=U(9)
       DAILD=U(10)
       DTALD=U(11)
       DRUDD=U(12)

       QBARS=.5*RHO*VTRFPS*VTRFPS*SREF
       CO2V=CWING/(2.*VTRFPS)
       BO2V=BWING/(2.*VTRFPS)
       QSB=BWING*QBARS
       ARUD=ABS(DRUDD)
       RARUD=ARUD/DEGRAD
       RAL=AL/DEGRAD
       ABET=ABS(BETA)
       RABET=ABET/DEGRAD
       RBETA=BETA/DEGRAD
       DAILA=ABS(DAILD)
       DSTBR=DSTBD/DEGRAD

C*********************************************************************
C
C
C
C     NEW SECTION OF CODE - 1) ALL THE AERODYNAMIC COEFFICIENTS IN
C                              THIS VERSION OF THE DRIVER PROGRAM
C                              ARE TAKEN DIRECTLY FROM THE 1988
C                             F15 AEROBASE (0.6 MACH, 20000 FEET)
C
C                            2) THIS SECTION SUMMARIZES THE
C                             AERODYNAMIC COEFFICIENTS AS TO WHAT
C                              THEY ARE AND HOW THEY ARE USED.
C                                THE FIRST ACCRONYM IS THE JOVIAL
C                              NAME OF THE AERODYNAMIC COEFFICIENT
C                              (CFX1,ETC), THE SECOND ACCRONYM IS
C                              THE F15 AEROBASE CODE OR CTAB NAME
C                              (ATAB15, ETC).  A BRIEF DEFINITION
```

```
C                                OF THE AERODYNAMIC COEFFICIENT IS
C                               ALSO PROVIDED.
C
C                                 3) THERE IS ALSO A SECTION THAT C
                                PROVIDES A TABLE OF CONVERSIONS C
                              BETWEEN WHAT THE VARIABLE IS CALLED C
                              IN THE ORIGINAL SECTION OF THIS C
                           PROGRAM       AND   ITS   NAME   IN   THE   1988
C                                F15 AEROBASE. FOR THE SAKE OF C
                               CONTINUITY THE ORIGINAL PROGRAM NAME C
                               IS USED AND THE 1988 F15 AEROBASE C
                               NAME IS PROVIDED AS BOOK KEEPING
C                                   INFORMATION.
C
C
C*****************************************************************
C
C
C  CFX = FORCE IN STABILITY AXIS X DIRECTION (CD IN BODY AXIS)
C        (FUNCTION OF CL OR CFZ1)
C  CFX = CFX1 + CXRB + STORE INCREMENTS + CXDSPD + DCXLG + DCD
C
C  CFX1 = ATAB15 = PERFORMANCE DRAG COEFFICIENT - CD
C  CXRB = ATAB22 = DELTA CD DUE TO CG (=0.0)
C CXDSPD = ATAB27 = DELTA CD DUE TO SPEEDBRAKE (NORMALLY = 0.0436)
C                    SET TO 0 SINCE THIS STUDY IS CONCERNED
C                    WITH HIGH ANGLES
C                  OF ATTACK PHENOMENON (>40 DEGREES) AND BECAUSE

C                    THE SPEEDBRAKE WILL NOT DEPLOY AT ANGLES OF
C                    ATTACK GREATER THAN 15 DEGREES.
C  DCXLG = ATAB19 = DELTA CD DUE TO REYNOLD'S NUMBER  (=-0.0005)
C  DCD = BTAB03 = DELTA CD DUE TO 2-PLACE CANOPY (F15B) (=0.0005)
C       ******* NOTE THAT DCXLG AND DCD CANCEL EACH OTHER *******
C
C
C*****************************************************************
C
C
C
C  CFY = FORCE IN BODY AXIS Y DIRECTION
C  CFY = CFY1*EPA02 + CYDAD*DAILD + [CYDRD*DRUDD*DRFLX5]*EPA43
C       +[CYDTD*DTFLX5 + DTFLX6]*DTALD + CFYP*PB + CFYR*RB
C       +CYRB + STORE INCREMENTS + DCYB*BETA
C
C  CFY1  = ATAB16 = BASIC SIDE FORCE COEFFICIENT - CY(BETA)
C  EPA02 = ATAB21 = BETA MULTIPLIER TABLE
C   CYDAD  =  ATAB75  =  SIDE  FORCE  COEFFICIENT  DUE  TO  AILERON
C                  DEFLECTION
C  DAILD           = AILERON DEFLECTION (DEG)
C CYDRD = ATAB69 = SIDE FORCE COEFFICIENT DUE TO RUDDER DEFLECTION
```

```
C  DRUDD           = RUDDER DEFLECTION  (DEG)
C  DRFLX5 = ATAB88 = FLEX MULTIPLIER ON CYDRD (=0.89)
C   EPA43  =  ATAB30  =  MULTIPLIER  ON  CNDR,  CLDR,  CYDR  DUE  TO
C                    SPEEDBRAKE
C                    (=1.0)
C  CYDTD = ATAB72 = SIDE FORCE COEFFICIENT DUE TO DIFFERENTIAL TAIL

C                    DEFLECTION - CYDDT
C  DTFLX5 = ATAB10 = FLEX MULTIPLIER ON CYDTD (=0.975)
C  DTFLX6 = ATAB77 = FLEX INCREMENT TO CYDTD (=0.0)
C  DTALD           = DIFFERENTIAL TAIL DEFLECTION (DEG) WHICH IS
C                     DIRECTLY PROPORTIONAL TO AILERON DEFLECTION
C                    AND IS PRIMARILY USED TO ASSIST IN ROLLING THE
C                    F-15B (DTALD=0.3*DAILD)
C  CFYP = ATAB13 = SIDE FORCE COEFFICIENT DUE TO ROLL RATE (CYP)
C  PB              = (PEOBB*SPAN)/(2*VILWF)
C                     PEOBB = ROLL RATE IN RAD/SEC = P
C                     SPAN = WING SPAN = 42.8 FEET = BWING
C                     VILWF = VELOCITY IN FT/SEC = VTRFPS
C  CFYR = ATAB07 = SIDE FORCE COEFFICIENT DUE TO YAW RATE (CYR)
C  RB              = (REOBB*SPAN)/(2*VILWF)
C                     REOBB = YAW RATE IN RAD/SEC = R
C  CYRB = ATAB93 = ASSYMETRIC CY AT HIGH ALPHA (ANGLE OF ATTACK)

C  DCYB           = 0.0  THERE IS NO INCREMENT DELTA CYB (SIDE C
               FORCE) DUE TO A 2-PLACE CANOPY ON THE F15B.  C
               THIS IS BECAUSE THE SAME CANOPY IS USED ON BOTH C
               THE BASELINE F15A AND THE F15B.  THE SIDEFORCE C
               IS THE SAME FOR BOTH VERSIONS OF THE F15 AND C
               ALREADY INCLUDED IN THE BASIC SIDE FORCE (CFY1).
C                   THE TWO PLACE CANOPY IS MOUNTED DIFFERENTLY C
               HOWEVER, SO THERE IS A DIFFERENCE IN YAWING AND C
               ROLLING MOMENT. (SEE DCNB AND DCLB)
C
C
C*****************************************************************
C
C
C
C  CFZ = FORCE IN STABILITY AXIS Z DIRECTION (CL IN BODY AXIS)
C  CFZ = CFZ1 + CZDSPD + STORE INCREMENTS + DCL*BETA

C
C
C  CFZ1 = ATAB17 = BASIC LIFT COEFFICIENT - CL
C  CZDSPD = ATAB26 = DELTA CL DUE TO SPEEDBRAKE
C                     SET TO 0 DUE TO THE REASONS GIVEN ABOVE IN
C                    CXDSPD
C  DCL = BTAB01 = DELTA CL DUE TO 2-PLACE CANOPY (F15B) (=0.0)
C
C
C*****************************************************************
```

```
C
C
C
C  CML = TOTAL ROLLING MOMENT COEFFICIENT IN BODY AXIS
C  CML = CML1*EPA02 + CLDAD*DAILD + [CLDRD*DRUDD*DRFLX1]*EPA43 +
C        [CLDTD*DTFLX1 + DTFLX2]*DTALD + CMLP*PB + CMLR*RB +
C        STORE INCREMENTS + CLDSPD + DCLB*BETA
C
C
C  CML1 = ATAB01 = BASIC ROLLING MOMENT COEFFICIENT - CL(BETA)
C  EPA02 = ATAB21 = BETA MULTIPLIER TABLE
C  CLDAD = ATAB73 = ROLL MOMENT COEFFICIENT DUE TO AILERON C
                DEFLECTION
C                    -(CLDA)
C  DAILD             = AILERON DEFLECTION (DEG)
C  CLDRD = ATAB67 = ROLLING MOMENT COEFFICIENT DUE TO RUDDER
C                    DEFLECTION  -(CLD)
C  DRUDD             = RUDDER DEFLECTION (DEG)
C  DRFLX1 = ATAB80 = FLEX MULTIPLIER ON CLDRD (=0.85)
C   EPA43  =  ATAB30  =  MULTIPLIER  ON  CNDR,  CLDR,  CYDR  DUE  TO
C                    SPEEDBRAKE
C                    (=1.0)
C  CLDTD = ATAB70 = ROLL MOMENT COEFFICIENT DUE TO DIFFERENTIAL
C                    TAIL DEFLECTION - CLDD
C  DTFLX1 = ATAB04 = FLEX MULTIPLIER ON CLDTD (=0.975)
C  DTFLX2 = ATAB84 = FLEX INCREMENT TO CLDTD (=0.0)
C  DTALD             = DIFFERENTIAL TAIL DEFLECTION (DEG) WHICH IS
C                      DIRECTLY PROPORTIONAL TO AILERON DEFLECTION
C                     AND IS PRIMARILY USED TO ASSIST IN ROLLING THE
C                     F-15B
C                     (DTALD = 0.3*DAILD)
C  CMLP = ATAB02 = ROLL DAMPING DERIVATIVE -CLP
C  PB             = (PEOBB*SPAN)/(2*VILWF)
C                    PEOBB = ROLL RATE IN RAD/SEC = P
C                    SPAN = WING SPAN = 42.8 FEET = BWING
C                    VILWF = VELOCITY IN FT/SEC = VTRFPS
C CMLR = ATAB11 = ROLLING MOMENT COEFFICIENT DUE TO YAW RATE - CLR

C  RB             = (REOBB*SPAN)/(2*VILWF)
C                   REOBB = YAW RATE IN RAD/SEC = R
C  CLDSPD = ATAB29 = DELTA CL DUE TO SPEEDBRAKE
C                     SET TO 0 DUE TO THE REASONS GIVEN ABOVE IN
C                    CXDSPD
C  DCLB = BTAB04 = INCREMENT DELTA CLB (ROLLING MOMENT) DUE TO C
            2-PLACE
C                   CANOPY FROM PSWT 499
C
C
C*****************************************************************
C
C
C
```

```
C  CMM = TOTAL PITCHING MOMENT COEFFICIENT IN STABILITY AXIS
C        (BODY AXIS - AS WELL)
C  CMM = CMM1 + CMMQ*QB + STORE INCREMENTS + CMDSPD + DCM
C
C  CMM1 = ATAB03 = BASIC PITCHING MOMENT COEFFICIENT - CM
C  CMMQ = ATAB05 = PITCH DAMPING DERIVATIVE - CMQ
C  QB            = (QEOBB*MAC)/(2*VILWF)
C                  QEOBB = PITCH RATE IN RAD/SEC = Q
C                  MAC = MEAN AERODYNAMIC CHORD = 15.94 FEET = C
C                WING
C                  VILWF = VELOCITY IN FT/SEC = VTRFPS
C  CMDSPD = ATAB25 = DELTA CM DUE TO SPEEDBRAKE
C                   SET TO 0 DUE THE REASONS GIVEN ABOVE IN CXDSPD
C  DCM = BTAB02 = DELTA CM DUE TO 2-PLACE CANOPY (F15B)  (=0.0)
C
C
C*****************************************************************
C
C
C
C  CMN = TOTAL YAWING MOMENT COEFFICIENT IN BODY AXIS
C  CMN = CMN1*EPA02 + CNDAD*DAILD + [CNDRD*DRUDD*DRFLX3]*EPA43
C        +[CNDTD*DTLX3 + DTFLX4]*DTALD + CMNP*PB + CMNR*RB + CNP
C        +DCNB2*EPA36 + STORE INCREMENTS + CNDSPD + DCNB*BETA
C
C
C  CMN1 = ATAB12 = BASIC YAWING MOMENT COEFFICIENT  - CN (BETA)
C  EPA02 = ATAB21 = BETA MULTIPLIER TABLE
C  CNDAD = ATAB74 = YAW MOMENT COEFFICIENT DUE TO AILERON
C                   DEFLECTION -CNDA
C  DAILD =        = AILERON DEFLECTION (DEG)
C  CNDRD = ATAB68 = YAWING MOMENT COEFFICIENT DUE TO RUDDER
C                   DEFLECTION -CNDR
C  DRUDD          = RUDDER DEFLECTION (DEG)
C  DRFLX3 = ATAB85 = FLEX MULTIPLIER ON CNDRD
C  EPA43 = ATAB30 =  MULTIPLIER ON CNDR, CLDR, CYDR DUE TO C
C                SPEEDBRAKE
C  CNDTD = ATAB71 = YAWING MOMENT COEFFICIENT DUE TO DIFFERENTIAL
C                   TAIL
C                   DEFLECTION - CNDDT
C  DTFLX3 = ATAB08 = FLEX MULTIPLIER ON CNDTD
C  DTFLX4 = ATAB09 = FLEX INCREMENT ON CNDTD  (=0.0)
C  DTALD =         = DIFFERENTIAL TAIL DEFLECTION (DEG) WHICH IS
C                    DIRECTLY PROPORTIONAL TO AILERON DEFLECTION
C                    AND IS PRIMARILY USED TO ASSIST IN ROLLING
C                    THE F-15B (DTALD = 0.3*DAILD)
C  CMNP = ATAB06 = YAWING MOMENT COEFFICIENT DUE TO ROLL RATE - CNP
C  PB            = (PEOBB*SPAN)/(2*VILWF)
C                  PEOBB=ROLL RATE IN RAD/SEC = P
C                  SPAN = WING SPAN = 42.8 FT = BWING
C                  VILWF = VELOCITY IN FT/SEC = VTRFPS
C  CMNR = ATAB14 = YAW DAMPING DERIVATIVE - CNR
```

```
C  RB              = (REOBB*SPAN)/(2*VILWF)
C                    REOBB = YAW RATE IN RAD/SEC = R
C  CNRB = ATAB86 = ASSYMETRIC CN AT HIGH ALPHA
C  DCNB2 = ATAB44 = DELTA CNB WITH STABILATOR EFFECT - DELCNB C
              (=0.0)
C  EPA36 = ATAB94 = MULTIPLIER ON DCNB2  (=BETA)
C  CNDSPD = ATAB28 = DELTA CN DUE TO SPEEDBRAKE
C                      SET TO 0 DUE TO THE REASONS GIVEN ABOVE IN
C                    CXDSPD
C  DCNB = BTAB05 = INCREMENT DELTA CNB (YAWING MOMENT) DUE TO
C                  2-PLACE CANOPY (F15B)
C
C
C*****************************************************************
C
C
C
C  MISCELLANEOUS COEFFICIENTS AND NAME CONVERSION TABLE
C
C
C       1988 F15                ORIGINAL
C       AEROBASE NAME           PROGRAM NAME          DEFINITION
C       *************           ************          **********
C
C       AL77D                   AL                ANGLE OF ATTACK
C                                                       (DEG)
C       BE77D                   BETA              SIDESLIP ANGLE
C                                                       (DEG)
C       BE77D                   RBETA             SIDESLIP ANGLE
C                                                       (RAD)
C       BO77D                   ABET              ABSOLUTE VALUE OF
C                                                    SIDESLIP ANGLE
C                                                       (DEG)
C       DAILA                   DAILA             ABSOLUTE VALUE OF
C                                                 AILERON DEFLEC-
C                                                    TION (DEG)
C       DAILD                   DDA               AILERON DEFLEC-
C                                                    TION (DEG)
C       DRUABS                  ARUD              ABSOLUTE VALUE OF
C                                                  RUDDER DEFLEC-
C                                                  TION (DEG)
C       DRUABS                  RARUD             ABSOLUTE VALUE OF
C                                                  RUDDER DEFLEC-
C                                                  TION (RAD)
C       DRUDD                   DRUDD             RUDDER DEFLECTION
C                                                  (DEG)
C       DSTBD                   DELESD(R)         AVERAGE
C                                                  STABILATOR
C                                                  DEFLECTION
C                                                  DEG (RAD)
C       DTALD                   DELEDD(R)         DIFFERENTIAL TAIL
C                                                  DEFLECTION
```

```
C                                                          DEG (RAD)
C
C
C
C
C
C
C
      PB=(P*BWING)/(2*VTRFPS)
      QB=(Q*CWING)/(2*VTRFPS)
      RB=(R*BWING)/(2*VTRFPS)
C
C   THE F-15B AERO DATA TABLES DO NOT CONTAIN STABILITY COEFFICIENT
C    DATA FOR BETA AND RUDDER DEFLECTION ,DRUDD, LESS THAN 0
C    DEGREES.  THE ABSOLUTE VALUE OF BETA, ABET, AND THE ABSOLUTE
C    VALUE OF RUDDER DEFLECTION, ARUDD, ARE USED IN THE FOLLOWING
C    EQUATIONS.  IN RADIANS THESE PARAMETERS ARE RABET AND RARUD,
C    RESPECTIVELY.  IN SOME CASES THE COEFFICIENT IS MULTIPLIED BY
C    A -1 FOR PARAMETER VALUES LESS THAN ZERO.
C
C    EPA02 IS A MULTIPLIER THAT ADJUSTS THE PARTICULAR COEFFICIENT
C    IT IS WORKING ON (CFY1,CML1,CMN1) BY CHANGING THAT PARTICULAR
C    COEFFICIENTS SIGN (POSITIVE OR NEGATIVE) DEPENDENT ON THE SIGN
C    OF THE SIDESLIP ANGLE (BETA).  IF BETA IS NEGATIVE THEN
C    EPA02=-1.0.  IF BETA IS POSITIVE THEN EPA02=1.0.  SINCE THIS
C    FUNCTION IS DISCONTINUOUS AT THE ORIGIN A CUBIC SPLINE HAS
C    BEEN EMPLOYED TO REPRESENT THIS FUNCTION IN ORDER THAT
C    AUTO CAN RUN.
C
C    Revised 15 Jun 90 - Combined three IF statements into
IF-THEN-ELSE.
      IF(BETA.LE.-1.0)THEN
        EPA02S=-1.00
      ELSEIF(BETA.GE.1.0)THEN
        EPA02S=1.00
      ELSE
        EPA02S=-1.00+(1.5*((BETA+1.0)**2))-(0.5*((BETA+1.0)**3))
      ENDIF
C
C    Revised 15 Jun 90 - Combined three IF statements into
IF-THEN-ELSE.
      IF(BETA.LE.-5.0)THEN
        EPA02L=-1.00
      ELSEIF(BETA.GE.5.0)THEN
        EPA02L=1.00
      ELSE

EPA02L=-1.00+(0.06*((BETA+5.0)**2))-(0.004*((BETA+5.0)**3))
      ENDIF
C
C
C
C
```

```
C
C
C*****************************************************************
C
C

      CFZ1=-0.00369376+(3.78028702*RAL)+(0.6921459*RAL*RAL)-(5.0005867
     +*(RAL**3))+(1.94478199*(RAL**4))+(0.40781955*DSTBR)+(0.10114579
     +*(DSTBR*DSTBR))
C
      CFZ=CFZ1
C
C
C*****************************************************************
C
C
C
C
C
      CL=CFZ1/57.29578
C
C     THIS CONVERSION OF CFZ1 TO CL IS AN ARTIFACT FROM THE
C     CURVE FITTING PROCESS WHERE ALL THE INDEPENDENT VARIABLES
C     WERE ANGLES THAT WERE CONVERTED FROM DEGREES TO RADIANS.
C     IT JUST SO HAPPENED THAT FOR CFX1 ONE OF THE VARIABLES
C     WAS NOT AN ANGLE BUT A DIMENSIONLESS COEFFICIENT.
C
C
      CFX1=0.01806821+(0.01556573*CL)+(498.96208868*CL*CL)
     +-(14451.56518396*(CL**3))+(2132344.6184755*(CL**4))
C
C     TRANSITIONING FROM LOW AOA DRAG TABLE TO HIGH AOA DRAG TABLE
C
      CFX2=0.0267297-(0.10646919*RAL)+(5.39836337*RAL*RAL)
     +-(5.0086893*(RAL**3))+(1.34148193*(RAL**4))+
     +(0.20978902*DSTBR)+(0.30604211*(DSTBR**2))+0.09833517
C
      A1=20.0/DEGRAD
      A2=30.0/DEGRAD
      A12=A1+A2
      BA=2.0/(-A1**3+3.*A1*A2*(A1-A2)+A2**3)
      BB=-3.*BA*(A1+A2)/2.
      BC=3.*BA*A1*A2
      BD=BA*A2**2*(A2-3.*A1)/2.
      F1=BA*RAL**3+BB*RAL**2+BC*RAL+BD
      F2=-BA*RAL**3+(3.*A12*BA+BB)*RAL**2-
     +    (BC+2.*A12*BB+3.*A12**2*BA)*RAL+
     +    BD+A12*BC+A12**2*BB+A12**3*BA
C
      IF (RAL .LT. A1) THEN
C
        CFX=CFX1
```

```
C
      ELSEIF (RAL .GT. A2) THEN
C
        CFX=CFX2
C
      ELSE
C
        CFX=CFX1*F1+CFX2*F2
C
      ENDIF
C
C
C*****************************************************************
*****
C
C
      DTFLX5=0.975
      DRFLX5=0.89
C
      CFY1=-0.05060386-(0.12342073*RAL)+(1.04501136*RAL*RAL)
     +-(0.17239516*(RAL**3))-(2.90979277*(RAL**4))
     ++(3.06782935*(RAL**5))-(0.88422116*(RAL**6))
     +-(0.06578812*RAL*RABET)-(0.71521988*RABET)-(0.00000475273
     +*(RABET**2))-(0.04856168*RAL*DSTBR)-(0.05943607*RABET*DSTBR)+
     +(0.02018534*DSTBR)
C
      IF (RAL .LT. .52359998) THEN
C
      CFYP=0.014606188+(2.52405055*RAL)-(5.02687473*(RAL**2))
     +-(106.43222962*(RAL**3))+(256.80215423*(RAL**4))
     ++(1256.39636248*(RAL**5))
     +-(3887.92878173*(RAL**6))-(2863.16083460*(RAL**7))+
     +(17382.72226362*(RAL**8))-(13731.65408408*(RAL**9))
      ENDIF
C
      IF ((RAL .GE. .52359998) .AND. (RAL .LE. .610865)) THEN
C

CFYP=0.00236511+(0.52044678*(RAL-0.52359998))-(12.8597002*(RAL-
     +0.52359998)**2)+(75.46138*(RAL-0.52359998)**3)
      ENDIF
C
      IF (RAL .GT. 0.610865) THEN
C
      CFYP=0.0
      ENDIF
C
      IF (RAL .LT. -0.06981) THEN
C
      CFYR=0.35
      ENDIF
C
```

```
      IF ((RAL .GE. -0.06981) .AND. (RAL .LT. 0.0)) THEN
C
      CFYR=0.34999999+(35.4012413*(RAL+0.06981)**2)-(493.33441162*
     +(RAL+0.06981)**3)
      ENDIF
C
      IF ((RAL .GE. 0.0) .AND. (RAL .LE. 0.523599)) THEN
C
      CFYR=0.35468605-(2.26998141*RAL)+(51.82178387*RAL*RAL)
     +-(718.55069823*(RAL**3))
     ++(4570.00492172*(RAL**4))-(14471.88028351*(RAL**5))+
     +(22026.58930662*(RAL**6))-(12795.99029404*(RAL**7))
      ENDIF
C
      IF ((RAL .GT. 0.523599) .AND. (RAL .LE. 0.61087)) THEN

C

CFYR=0.00193787+(1.78332496*(RAL-0.52359903))-(41.63198853*(RAL-
     +0.52359903)**2)+(239.97909546*(RAL-0.52359903)**3)
      ENDIF
C
      IF (RAL .GT. 0.61087) THEN
C
      CFYR=0.0
      ENDIF
C
      IF (RAL .LT. 0.55851) THEN
C
      CYDAD=-0.00020812+(0.00062122*RAL)+(0.00260729*RAL*RAL)
     ++(0.00745739*(RAL**3))-(0.0365611*(RAL**4))
     +-(0.04532683*(RAL**5))+(0.20674845*(RAL**6))
     +-(0.13264434*(RAL**7))-(0.00193383*(RAL**8))
      ENDIF
C
      IF ((RAL .GE. 0.55851) .AND. (RAL .LT. 0.61087)) THEN
C
      CYDAD=0.00023894+(0.00195121*(RAL-0.55851001))+(0.02459273
     +*(RAL-0.55851001)**2)-(0.1202244*((RAL-0.55851001)**3))
      ENDIF
C
      IF (RAL .GE. 0.61087) THEN
C
      CYDAD=0.27681285-(2.02305395*RAL)+(6.01180715*RAL*RAL)
     +-(9.24292188*(RAL**3))+(7.59857819*(RAL**4))
     +-(2.8565527*(RAL**5))+(0.25460503*(RAL**7))
     +-(0.01819815*(RAL**9))
      ENDIF
C
C
C     IF (RAL .LE. 0.0) THEN
C     EPA43=1.0
```

```
C      ENDIF
C      IF (RAL .GT. 0.0 AND .LE. 0.6283185) THEN
C      0.6283185 RADIANS = 36 DEGREES
C      EPA43=0.9584809+(4.13369452*RAL)-(18.31288396*RAL*RAL)+
C     +(19.5511456*(RAL**3))-(1.09295946*RAL*DSPBD)+(0.17441033*
C     +DSPBD*DSPBD)
C      ENDIF
C      IF (RAL .GT. 0.6283185) THEN
       EPA43=1.0
C      ENDIF
C
C*************************************************************
C           *  NOTE - THE PARAMETER EPA43 IS A MULTIPLIER ON RUDDER
C           *
C           *  EFFECTIVENESS DUE TO SPEEDBRAKE.  THIS TABLE IS ALSO
C           *
C           *  LIMITED TO 36 DEG AOA.  HOWEVER, THERE IS NO AERODY
C           *
C           *  NAMIC EFFECT FOR ANGLES OF ATTACK LESS THAN 16 DEG,
C           *
C           *  AND THE SPEEDBRAKE IS AUTOMATICALLY RETRACTED AT AOA
C           *
C           *  GREATER THAN 15 DEG.  THEREFORE, THIS TABLE SHOULD
C           *
C           *  NOT BE NECESSARY FOR THE ORDINARY OPERATION OF THE
C           *
C           *  AIRCRAFT
C           *
C
C*************************************************************
C
       CYDRD=0.00310199+(0.00119963*RAL)+(0.02806933*RAL*RAL)
      +-(0.12408447*(RAL**3))-(0.12032121*(RAL**4))
      ++(0.79150279*(RAL**5))-(0.86544347*(RAL**6))
      ++(0.27845115*(RAL**7))+(0.00122999*RAL*RARUD)+(0.00145943
      +*RARUD)-(0.01211427*RARUD*RARUD)+(0.00977937*(RARUD**3))
C
       CYDTD=-0.00157745-(0.0020881*RAL)+(0.00557239*RAL*RAL)
      +-(0.00139886*(RAL**3))+(0.04956247*(RAL**4))
      +-(0.0135353*(RAL**5))-(0.11552397*(RAL**6))
      ++(0.11443452*(RAL**7))-(0.03072189*(RAL**8))-(0.01061113*
      +(RAL**3)*DSTBR)-(0.00010529*RAL*RAL*DSTBR*DSTBR)
      +-(0.00572463*RAL*DSTBR*DSTBR)
      ++(0.01885361*RAL*RAL*DSTBR)-(0.01412258*RAL*(DSTBR**3))
      +-(0.00081776*DSTBR)+(0.00404354*(DSTBR**2))-
      +(0.00212189*(DSTBR**3))+(0.00655063*(DSTBR**4))
      ++(0.03341584*(DSTBR**5))
C
       RALY1=0.6108652
       RALY2=90.0/DEGRAD
       RBETY1=-0.0872665
       RBETY2=0.1745329
```

```
C
      AY=0.164
      ASTARY=0.95993
      BSTARY=0.087266
C
      ZETAY=(2.0D0*ASTARY-(RALY1+RALY2))/(RALY2-RALY1)
      ETAY=(2.0D0*BSTARY-(RBETY1+RBETY2))/(RBETY2-RBETY1)
C
      X=(2.0D0*RAL-(RALY1+RALY2))/(RALY2-RALY1)
      Y=(2.0D0*RBETA-(RBETY1+RBETY2))/(RBETY2-RBETY1)
C

      FY=((5.0D0*(ZETAY**2))-(4.0D0*ZETAY*X)-1.0D0)*(((X**2)-1.0D0)
     +**2)*(1.0D0/(((ZETAY**2)-1.0D0)**3))
C

GY=((5.0D0*(ETAY**2))-(4.0D0*ETAY*Y)-1.0D0)*(((Y**2)-1.0D0)**2)
     +*(1.0D0/(((ETAY**2)-1.0D0)**3))
C
      CYRB=AY*FY*GY
C
      IF (RAL .LT. 0.6108652) THEN
C
      CYRB=0.0
      GOTO 500
      ENDIF
C
      IF ((RBETA .LT. -0.0872665) .OR. (RBETA .GT. 0.1745329)) THEN
C
      CYRB=0.0
      GOTO 500
      ENDIF
C
 500  CFY=(CFY1*EPA02L)+(CYDAD*DAILD)+(CYDRD*DRUDD*DRFLX5*EPA43)+

     +((CYDTD*DTFLX5)*DTALD)+(CFYP*PB)+(CFYR*RB)
     ++CYRB
C
C
C*****************************************************************
C
C
      DTFLX1=0.975
      DRFLX1=0.85
C
      CML1=-0.00238235-(0.04616235*RAL)+(0.10553168*RAL*RAL)
     ++(0.10541585*(RAL**3))-(0.40254765*(RAL**4))
     ++(0.32530491*(RAL**5))-(0.08496121*(RAL**6))
     ++(0.00112288*(RAL**7))-(0.05940477*RABET*RAL)-
     +(0.07356236*RABET)-(0.00550119*RABET*RABET)+(0.00326191
     +*(RABET**3))
C
```

```
      IF (RAL .LT. 0.29671) THEN
C
      CMLP=-0.24963201-(0.03106297*RAL)+(0.12430631*RAL*RAL)
     +-(8.95276618*(RAL**3))+(100.33109929*(RAL**4))
     ++(275.70069578*(RAL**5))-(1178.83425699*(RAL**6))
     +-(2102.66811522*(RAL**7))+(2274.89785551*(RAL**8))
      ENDIF
C
      IF ((RAL .GE. 0.29671) .AND. (RAL .LT. 0.34907)) THEN
C
      CMLP=-0.1635261-(3.77847099*(RAL-0.29671001))+(147.47639465
     +*(RAL-0.29671001)**2)-(1295.94799805*(RAL-0.29671001)**3)
      ENDIF
C
      IF (RAL .GE. 0.34907) THEN
C
      CMLP=-1.37120291+(7.06112181*RAL)-(13.57010422*RAL*RAL)
     ++(11.21320850*(RAL**3))
     +-(4.26789425*(RAL**4))+(0.6237381*(RAL**5))
      ENDIF
C
      IF (RAL .LT. 0.7854) THEN
C
      CMLR=0.03515391+(0.59296381*RAL)+(2.27456302*RAL*RAL)
     +-(3.8097803*(RAL**3))
     +-(45.83163842*(RAL**4))+(59.31669213*(RAL**5))+
+(194.29237485*(RAL**6))-(393.22969953*(RAL**7))+(192.20860739*
     +(RAL**8))
      ENDIF
C
      IF ((RAL .GE. 0 7854) .AND. (RAL .LE. 0.87266)) THEN
C
      CMLR=0.0925579071-(0.6000000238*(RAL-0.7853999734))
     ++(1.3515939713*((RAL-0.7853999734)**2))
     ++(29.0733299255*((RAL-0.7853999734)**3))
      ENDIF
C
      IF (RAL .GT. 0.87266) THEN
C
      CMLR=-311.126041+(1457.23391042*RAL)-(2680.19461944*RAL*RAL)+
+(2361.44914738*(RAL**3))-(893.83567263*(RAL**4))+(68.23501924*
     +(RAL**6))-(1.72572994*(RAL**9))
      ENDIF
C
      CLDAD=0.00057626+(0.00038479*RAL)-(0.00502091*RAL*RAL)
     ++(0.00161407*(RAL**3))+(0.02268829*(RAL**4))
     +-(0.03935269*(RAL**5))+(0.02472827*(RAL**6))
     +-(0.00543345*(RAL**7))+(0.0000007520348*DSTBR*RAL)+
     +(0.000000390773*DSTBR)
C
```

```
      CLDRD=0.00013713-(0.00035439*RAL)-(0.00227912*RAL*RAL)
     ++(0.00742636*(RAL**3))+(0.00991839*(RAL**4))
     +-(0.04711846*(RAL**5))+(0.046124*(RAL**6))
     +-(0.01379021*(RAL**7))+(0.00003678685*RARUD*RAL)+
     +(0.00001043751*RARUD)-(0.00015866*RARUD*RARUD)+(0.00016133
     +*(RARUD**3))
C
      CLDTD=0.00066663+(0.00074174*RAL)+(0.00285735*RAL*RAL)
     +-(0.02030692*(RAL**3))-(0.00352997*(RAL**4))
     ++(0.0997962*(RAL**5))-(0.14591227*
     +(RAL**6))+(0.08282004*(RAL**7))
     +-(0.0168667*(RAL**8))+(0.00306142*(RAL**3)*DSTBR)
     +-(0.00110266*RAL*RAL*(DSTBR**2))+(0.00088031*RAL*
     +(DSTBR**2))-(0.00432594*RAL*RAL*DSTBR)-
     +(0.00720141*RAL*(DSTBR**3))
     +-(0.00034325*DSTBR)+(0.00033433*(DSTBR**2))+(0.00800183
     +*(DSTBR**3))-(0.00555986*(DSTBR**4))-(0.01841172*(DSTBR**5))
C
      IF (RAL .LT. 0.0) THEN
C
      DCLB=-0.00006
      ENDIF
C
      IF ((RAL .GE. 0.0) .AND. (RAL .LE. 0.209434)) THEN
C
      DCLB=-0.00006+(0.0041035078*RAL*RAL)-(0.0130618699*(RAL**3))
      ENDIF
C
      IF (RAL .GT. 0.209434) THEN
C
      DCLB=0.0
      ENDIF
C
C
      CML=(CML1*EPA02S)+(CLDAD*DAILD)+(CLDRD*DRUDD*DRFLX1*EPA43)+

     +((CLDTD*DTFLX1)*DTALD)+(CMLP*PB)+(CMLR*RB)+(DCLB*BETA)
C
C
C*****************************************************************
C
C
      CMM1=0.00501496-(0.08004901*RAL)-(1.03486675*RAL*RAL)
     +-(0.68580677*(RAL**3))+(6.46858488*(RAL**4))
     +-(10.15574108*(RAL**5))+
     +(6.44350808*(RAL**6))-(1.46175188*(RAL**7))
     ++(0.24050902*RAL*DSTBR)
     +-(0.42629958*DSTBR)-(0.03337449*DSTBR*DSTBR)
     +-(0.53951733*(DSTBR**3))
C
      IF (RAL .LE. 0.25307) THEN
C
```

```
       CMMQ=-3.8386262+(13.54661297*RAL)+(402.53011559*RAL*RAL)
      +-(6660.95327122*(RAL**3))-(62257.89908743*(RAL**4))
      ++(261526.10242329*(RAL**5))
      ++(2177190.33155227*(RAL**6))-(703575.13709062*(RAL**7))-
      +(20725000.34643054*(RAL**8))-(27829700.53333649*(RAL**9))
       ENDIF
C
       IF ((RAL .GT. 0.25307) .AND. (RAL .LT. 0.29671)) THEN
C
       CMMQ=-8.4926528931-(2705.3000488281*(RAL-0.2530699968))
      ++(123801.5*(RAL-0.2530699968)**2)
      +-(1414377*(RAL-0.2530699968)**3)
       ENDIF
C
       IF (RAL .GE. .29671) THEN
C
       CMMQ=47.24676075-(709.60757056*RAL)+(3359.08807193*RAL*RAL)-
      +(7565.32017266*(RAL**3))+(8695.1858091*(RAL**4))
      +-(4891.77183313*(RAL**5))+(1061.55915089*(RAL**6))
       ENDIF
C
       CMM=CMM1+(CMMQ*QB)
C
C
C*****************************************************************

       DTFLX3=0.975
       DRFLX3=0.89
C
C
       CMN1=0.01441512+(0.02242944*RAL)-(0.30472558*(RAL**2))
      ++(0.14475549*(RAL**3))
      ++(0.93140112*(RAL**4))-(1.52168677*(RAL**5))+
      +(0.90743413*(RAL**6))-(0.16510989*(RAL**7))
      +-(0.0461968*(RAL**8))
      ++(0.01754292*(RAL**9))-(0.17553807*RAL*RABET)+
      +(0.15415649*RAL*RABET*DSTBR)
      ++(0.14829547*(RAL**2)*(RABET**2))
      +-(0.11605031*(RAL**2)*RABET*DSTBR)
      +-(0.06290678*(RAL**2)*(DSTBR**2))
      +-(0.01404857*(RAL**2)*(DSTBR**2))
      ++(0.07225609*RABET)-(0.08567087*(RABET**2))
      ++(0.01184674*(RABET**3))
      +-(0.00519152*RAL*DSTBR)+(0.03865177*RABET*DSTBR)
      ++(0.00062918*DSTBR)
C
       CNDRD=-0.00153402+(0.00184982*RAL)-(0.0068693*RAL*RAL)
      ++(0.01772037*(RAL**3))
      ++(0.03263787*(RAL**4))-(0.15157163*(RAL**5))+(0.18562888

+*(RAL**6))-(0.0966163*(RAL**7))+(0.01859168*(RAL**8))+(0.0002587
```

```
     +*RAL*DSTBR)-(0.00018546*RAL*DSTBR*RBETA)-(0.00000517304*RBETA)

     +-(0.00102718*RAL*RBETA)-(0.0000689379*RBETA*DSTBR)-(0.00040536
          +*RBETA*RARUD)-(0.00000480484*DSTBR*RARUD)
          +-(0.00041786*RAL*RARUD)
          ++(0.0000461872*RBETA)+(0.00434094*(RBETA**2))
          +-(0.00490777*(RBETA**3))
          ++(0.000005157867*RARUD)+(0.00225169*RARUD*RARUD)-(0.00208072
          +*(RARUD**3))
C
           IF (RAL .LT. 0.55851) THEN
C
           CMNP=-0.00635409-(1.14153932*RAL)+(2.82119027*(RAL**2))+
          +(54.4739579*(RAL**3))-(140.89527667*(RAL**4))-(676.73746128*

          +(RAL**5))+(2059.18263976*(RAL**6))+(1579.41664748*(RAL**7))

          +-(8933.08535712*(RAL**8))+(6806.54761267*(RAL**9))
           ENDIF
C
           IF ((RAL .GE. 0.55851001) .AND. (RAL .LE. 0.61087)) THEN
C
           CMNP=-.07023239+(1.085815*(RAL -0.55851))
          ++(8.852651*((RAL-.55851)**2))-(192.6093*((RAL-0.55851)**3))
           ENDIF
C
           IF (RAL .GT. 0.61087) THEN
C
           CMNP=-71.03693533+(491.32506715*RAL)
          +-(1388.11177979*(RAL**2))+
          +(2033.48621905*(RAL**3))
          +-(1590.91322362*(RAL**4))+(567.38432316*(RAL**5))
          +-(44.97702536*(RAL**7))+(2.8140669*(RAL**9))
           ENDIF
C
C
C
           IF (RAL .LE. -.069813) THEN
C
           CMNR= -0.2805
           ENDIF
C
           IF ((RAL .GT. -.069813) .AND. (RAL .LT. 0.0)) THEN
C
           CMNR=-0.2804999948+(35.9903717041*(RAL+.0698129982)**2)
          +-(516.1574707031*(RAL+.0698129982)**3)
           ENDIF
C
           IF ((RAL .GE. 0.0) .AND. (RAL .LE. 0.78539801)) THEN
C
           CMNR=-.28071511-(2.52183924*RAL)+(68.90860031*(RAL**2))
```

```
     +-(573.23100511*(RAL**3))+(2009.08725005*(RAL**4))
     +-(3385.15675307*(RAL**5))
     ++(2730.49473149*(RAL**6))-(848.12322034*(RAL**7))
      ENDIF
C
      IF ((RAL .GT. 0.78539801) .AND. (RAL .LT. 0.95993102)) THEN
C
CMNR=-0.1096954+(0.52893072*(RAL-0.78539801))-(6.09109497*(RAL-
     +0.78539801)**2)+(17.47834015*(RAL-0.78539801)**3)
      ENDIF
C
      IF (RAL .GE. 0.95993102) THEN
C
      CMNR=-0.11
      ENDIF
C
      CNDTD=0.00058286+(0.0007341*RAL)-(0.00746113*RAL*RAL)
     +-(0.00685223*(RAL**3))
     ++(0.03277271*(RAL**4))-(0.02791456*(RAL**5))
     ++(0.00732915*(RAL**6))
     ++(0.00120456*RAL*DSTBR)-(0.00168102*DSTBR)+(0.0006462*
     +DSTBR*DSTBR)
C
      CNDAD=0.00008228887-(0.00014015*RAL)-(0.0013493*RAL*RAL)+
     +(0.00020487*(RAL**3))+(0.00561241*(RAL**4))
     +-(0.00634392*(RAL**5))

++(0.00193323*(RAL**6))-(2.05815E-17*(RAL*DAILA))+(3.794816E-17*
     +(DAILA**3))
C
      DCNB=-2.500E-4
C
      RALN1=0.69813
      RALN2=90.0/DEGRAD
      RBETN1=-0.174532
      RBETN2=0.34906
C
      AN=0.034
      ASTARN=1.0472
      BSTARN=0.087266
C
      ZETAN=(2.0D0*ASTARN-(RALN1+RALN2))/(RALN2-RALN1)
      ETAN=(2.0D0*BSTARN-(RBETN1+RBETN2))/(RBETN2-RBETN1)
C
      XN=(2.0D0*RAL-(RALN1+RALN2))/(RALN2-RALN1)
      YN=(2.0D0*RBETA-(RBETN1+RBETN2))/(RBETN2-RBETN1)
C
      FN=((5.0D0*(ZETAN**2))-(4.0D0*ZETAN*XN)-1.0D0)*
     +(((XN**2)-1.0D0)**2)/(((ZETAN**2)-1.0D0)**3)
C
```

```
      GN=((5.0D0*(ETAN**2))-(4.0D0*ETAN*YN)-1.0D0)*
     +(((YN**2)-1.0D0)**2)/(((ETAN**2)-1.0D0)**3)
C
      CNRB=AN*FN*GN
C
      IF (RAL .LT. 0.69813) THEN
C
      CNRB=0.0
      GOTO 1000
      ENDIF
C
      IF ((RBETA .LT. -0.174532) .OR. (RBETA .GT. 0.34906)) THEN
C
      CNRB=0.0
      GOTO 1000
      ENDIF
C
C
C
 1000 CMN=(CMN1*EPA02S)+(CNDAD*DAILD)+((CNDRD*DRUDD*DRFLX3)*EPA43)+
     +((CNDTD*DTFLX3)*DTALD)+(CMNP*PB)+(CMNR*RB)+(DCNB*BETA)
     ++CNRB
C
C
C**********************************************************************
C
C
      CX=CFZ*SIN(RAL)-CFX*COS(RAL)+THRUST/QBARS
      CY=CFY
      CZ=-(CFZ*COS(RAL)+CFX*SIN(RAL))
      CLM=CML
      CMM=CMM+THRUST*(0.25/12.0)/(QBARS*CWING)
C
C   THE (0.25/12.0) IS THE OFFSET OF THE THRUST VECTOR FROM THE CG
C
      CNM=CMN
C
C    RETURN CX, CY, CZ, CLM, CMM, CNM TO CALLING PROGRAM.
C
C
C       IWRITE=0
C       IF(IWRITE.EQ.1) WRITE(6,*)' CX,CY,CZ,CLM,CMM,CNM=',
C      +                            CX,CY,CZ,CLM,CMM,CNM
C
C       WRITE(6,*) ' END OF SUB COEFF U(1,2,3)=',U(1),U(2),U(3)
C       WRITE(6,*)'LEAVING COEFF'
      RETURN
      END
```

# APPENDIX D

# T-38A STRIP CHART DATA

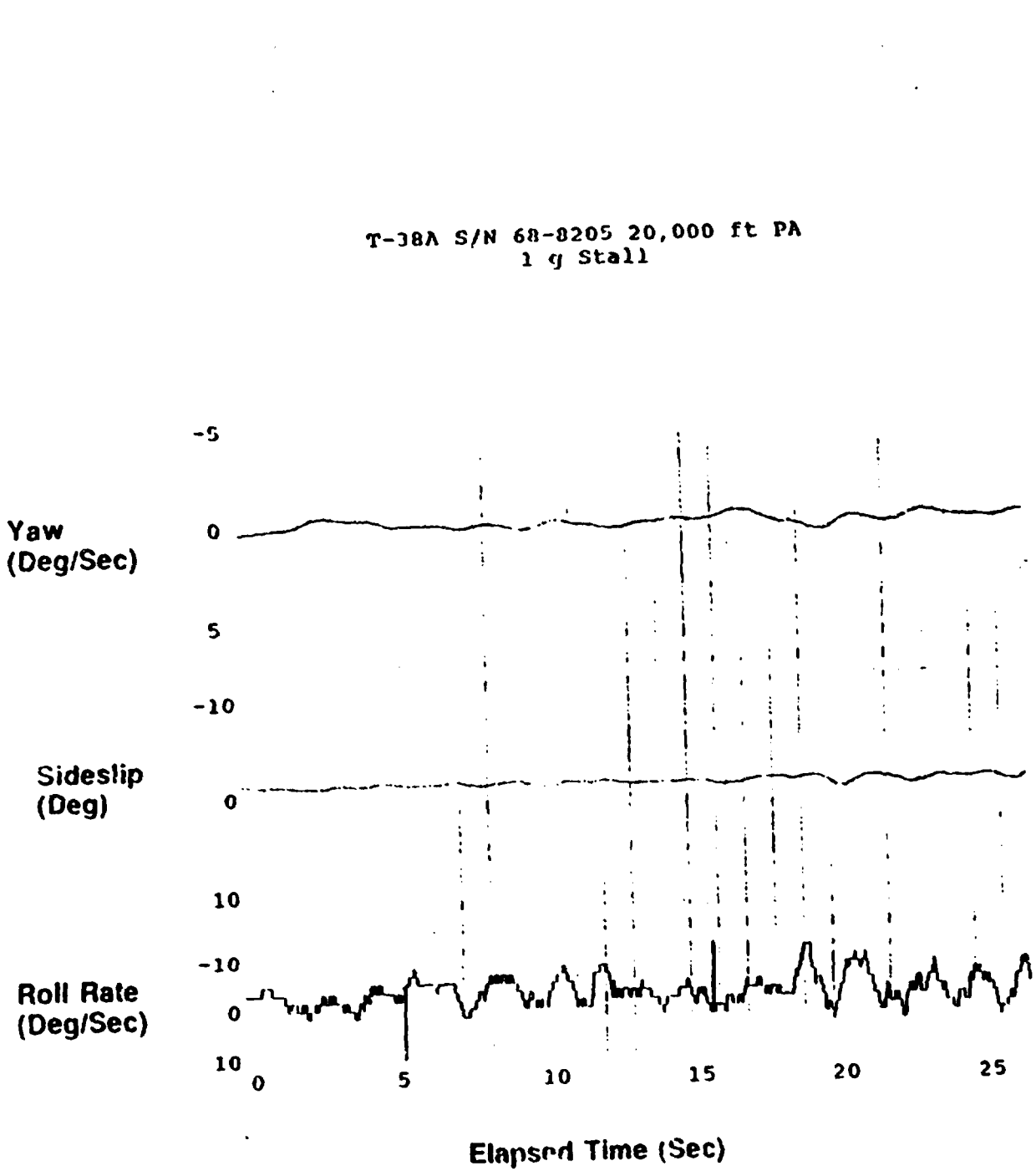


Figure 29. Sideslip, Roll and Yaw Rate of Wing Rock

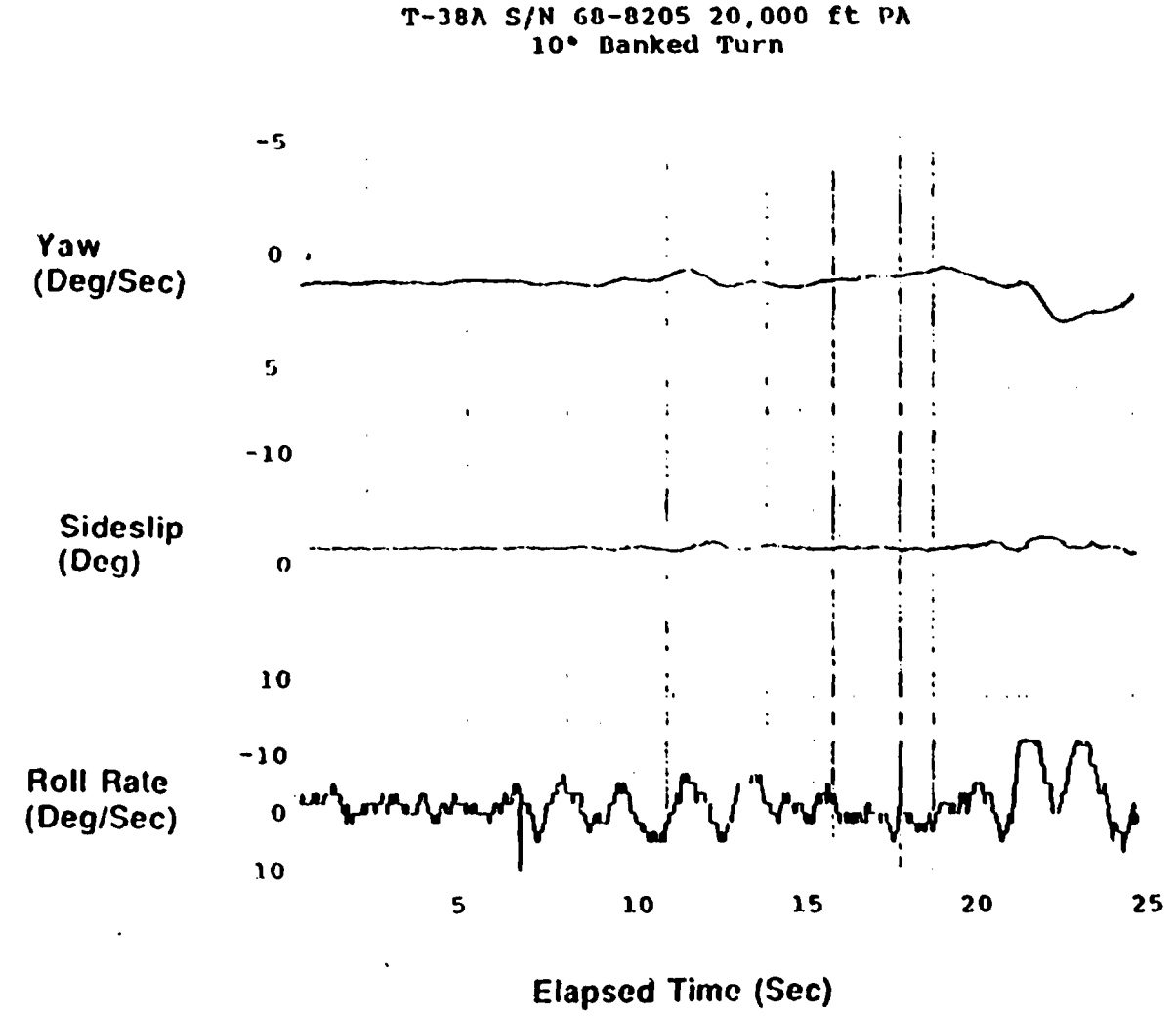


Figure 30. Sideslip, Roll and Yaw Rate of Wing Rock

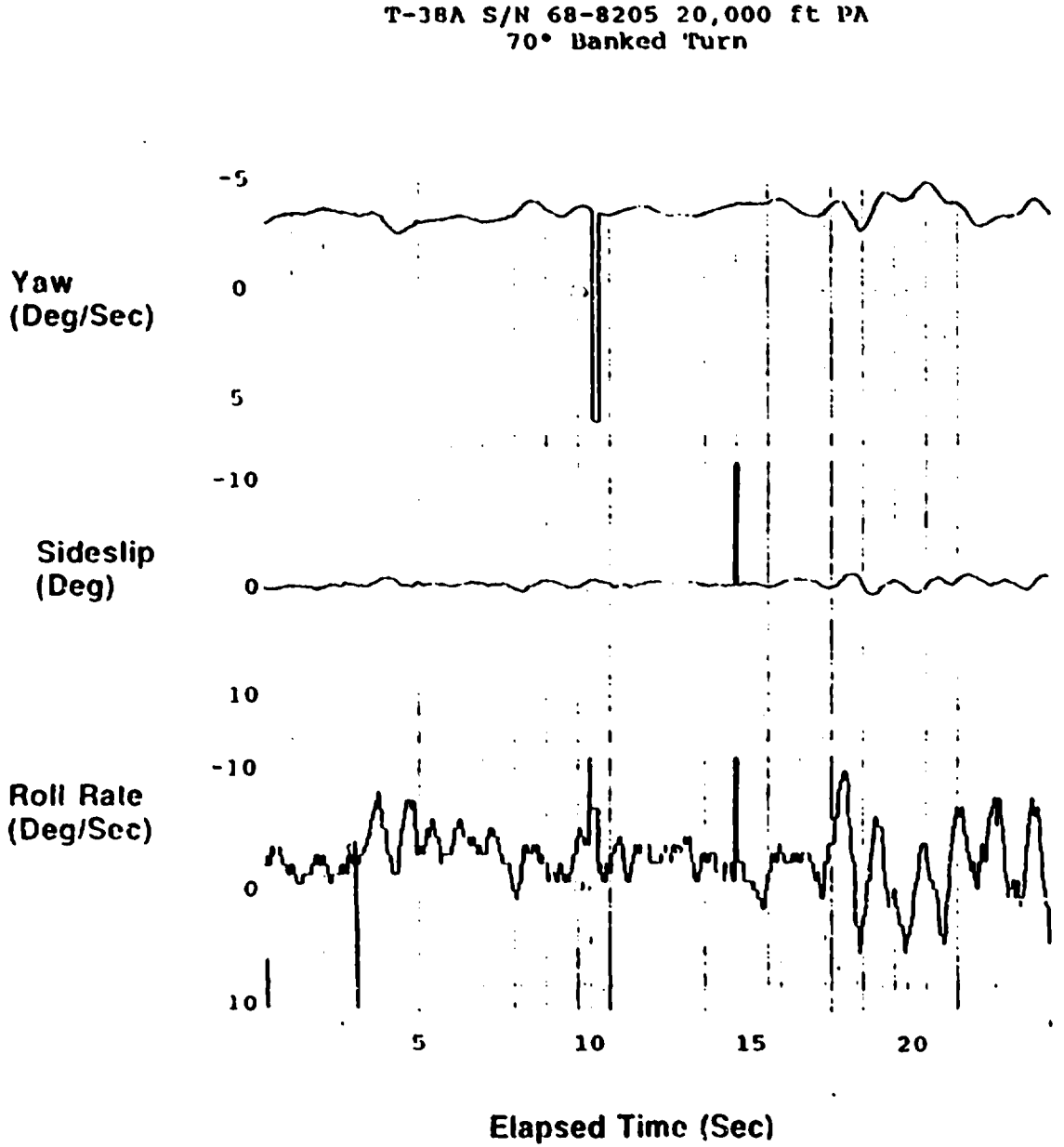


Figure 31. Sideslip, Roll and Yaw Rate of Wing Rock

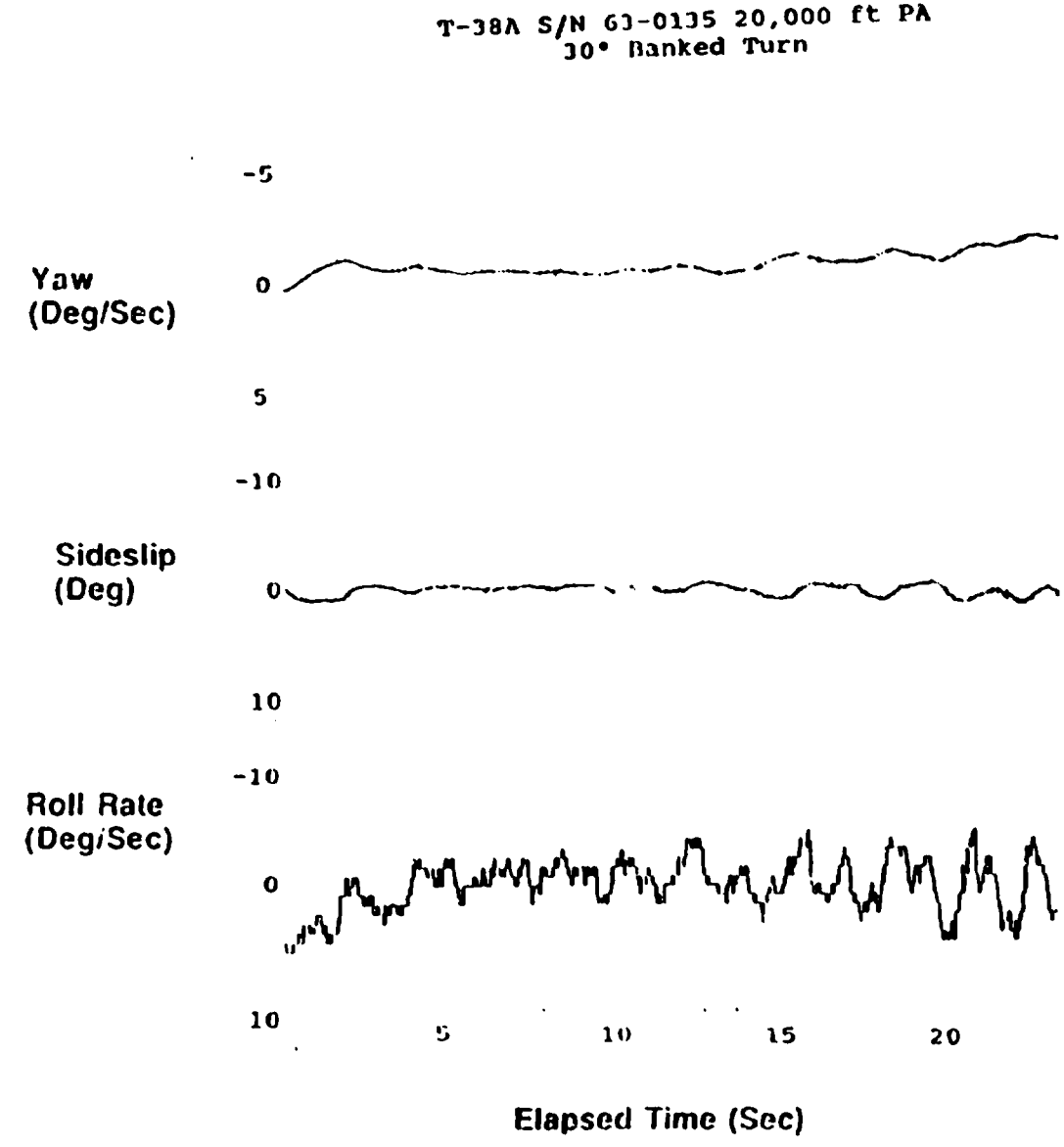


Figure 32. Sideslip, Roll and Yaw Rate of Wing Rock

# APPENDIX E
# F-15D TABULATED FLIGHT TEST DATA

**Table E1**
**F-15D Wing Rock Onset Summary**

| MANEUVER | WING ROCK ONSET AOA (UNITS) | MACH |
|---|---|---|
| 1 G STALL | 26 | 0.32 |
| 10° AOB TURN | 26 | 0.32 |
| 30° AOB TURN | 26 | 0.35 |
| 70° AOB TURN | 26 | 0.44 |
| SYMMETRIC PULLUP | 30 | 0.60 |

**Table E2**
**F-15 D Wing Rock Limit Cycles - 1 G Stall**

| UNITS AOA | WING ROCK LIMIT CYCLES - DEG AOB EXCURSIONS | | | | | | | |
|---|---|---|---|---|---|---|---|---|
| | NO WING ROCK LIMIT CYCLE OBSERVED | ±.5° | ±1° | ±2° | ±5° | ±10° | ±15° | ±25° |
| 24 | x | | | | | | | |
| 25 | x | x | | | | | | |
| 26 | | | xx | | | | | |
| 27 | | | xx | | | | | |
| 28 | x | | x | x | | | | |
| 30 | | | | x | xxx x | | | |
| 32 | | | | | x | x | | |
| 33 | | | | | x | x | | |
| 34 | | | | | | x | xx | |
| 35 | | | | | | | x | |
| 36 | | | | | | | x | x |
| 37 | | | | | | | x | x |
| 38 | | | | | | | | x |
| 40 | | | | | | | x | |

X = ONE OBSERVED WING ROCK LIMIT CYCLE

**Table E3**
**F-15D Wing Rock Limit Cycles - 10° AOB TURN**

| UNITS AOA | NO WING ROCK LIMIT CYCLE OBSERVED | WING ROCK LIMIT CYCLES - DEG AOB EXCURSIONS | | | |
|---|---|---|---|---|---|
| | | ±.5° | ±1° | ±7° | ±10° |
| 25 | x | | | | |
| 26 | | xx | | | |
| 27 | | x | xx | | |
| 29 | | | x | | |
| 31 | | | | | x |
| 32 | | | | x | |

X = ONE OBSERVED WING ROCK LIMIT CYCLE

**Table E4**
**F-15D Wing Rock Limit Cycles - 30° AOB TURN**

| UNITS AOA | NO WING ROCK LIMIT CYCLE OBSERVED | WING ROCK LIMIT CYCLES - DEG AOB EXCURSIONS | | | | | | |
|---|---|---|---|---|---|---|---|---|
| | | ±.5° | ±1° | ±2° | ±3° | ±4° | ±5° | ±15° |
| 25 | x | | | | | | | |
| 26 | | x | | | | | x | |
| 27 | | | x | | | | x | |
| 28 | | | x | | | | x | |
| 29 | | | | | x | | | |
| 32 | | | | x | | | x | |
| 33 | | | | | | x | | |
| 38 | | | | | | | | x |

X = ONE OBSERVED WING ROCK LIMIT CYCLE

**Table E5**
**F-15D Wing Rock Limit Cycles - 70° AOB TURN**

| UNIT AOA | NO WING ROCK LIMIT CYCLE OBSERVED | WING ROCK LIMIT CYCLES - DEG AOB EXCURSIONS | | | | | | | | | |
|---|---|---|---|---|---|---|---|---|---|---|---|
| | | ±.5 | ±1 | ±1.5 | ±2 | ±3 | ±4 | ±5 | ±7 | ±10 | ±12 |
| 25 | x | | | | | | | | | | |
| 26 | | xx | xx | x | | | | | | | |
| 27 | | x | xx | | | | | | | | |
| 28 | | x | xxx | x | x | | | | | | |
| 30 | | | x | xx | x | | | | | | |
| 31 | | | xx | | | | | x | | | |
| 32 | | | | | | x | x | xx | | x | |
| 34 | | | | | x | x | | x | x | | |
| 35 | | | | | x | | | | | | |
| 36 | | | | | | x | x | x | | | x |
| 38 | | | | | | | | | | | x |
| 39 | | | | | | | | | | | x |

X = ONE OBSERVED WING ROCK LIMIT CYCLE

**Table E6**
**F-15D Wing Rock Onset- SYMMETRIC PULLUP**

| UNITS AOA | NUMBER OF OBSERVED WING ROCK ONSETS |
|---|---|
| 29 | 0 |
| 30 | 3 |
| 31 | 1 |

# APPENDIX F

# FLIGHT TEST TECHNIQUES

## FLIGHT TEST TECHNIQUES

### General

The aircraft was trimmed to steady level flight at 20,000 feet PA with 29.92 set in the altimeter and feet off the rudder pedals. Extreme care was given to eliminate all lateral rolling tendencies and ensure the ball was centered in the front cockpit turn and slip indicator. The roll CAS was then disengaged and the process repeated. These actions were taken to guarantee any subsequent aircraft rolling motions were the result of only aerodynamic forces. In the front cockpit, the Heads Up Display was placed in the Attitude Directional Indicator (ADI) mode to obtain the greatest amount of flight information.

### 1 g Stall

The aircraft was trimmed at 20,000 ft PA and 25 units AOA as described above. The throttles and pitch rate were then smoothly modulated to establish a 1 kt/sec bleed rate. This bleed rate was then held until 30 units AOA. This condition was maintained for 10 seconds to observe the F-15D flight characteristics. The AOA was then increased by two cockpit unit increments and the observation process repeated until the onset of wing rock was observed. After the onset of wing rock, the AOA was increased in one to two unit increments, as conditions allowed, and the observation process repeated. The AOA was incrementally increased in this manner until a central AOA of 40 units was achieved or the bottom of the data band was exited. The control stick was centered to eliminate lateral inputs. At each stabilized AOA value, the magnitude of the wing rock was measured by observing the bank angle oscillations on the ADI. The ADI was also used to determine the pitch angles at which wing rock was occurring. The wing rock period, when possible, was also measured from the ADI. The front cockpit AOA indicator was used to measure the wing rock AOA and excursions. Airspeed and altitude were taken from the front cockpit main instruments.

### 10 Degree Bank Turn

The F-15D was trimmed at 20,000 ft PA and 25 units AOA in steady level flight. A 10 degree bank turn was then established with aileron and the control stick centered after the input. The AOA was then increased in the same manner as during the 1 g Stall test point and the aircraft wing rock characteristics observed. The process was repeated in both directions.

**30 Degree Bank Turn**

The F-15D was trimmed at 21,000 ft PA and 25 units AOA in steady level flight. A 30 degree bank was established with aileron and the control stick subsequently centered. AOA was increased as described above and the F-15D wing rock characteristics observed. The test was repeated in both directions.

**70 Degree Bank Turn**

The aircraft was trimmed at 23,000 ft PA above the data band at 25 units AOA. A 70 degree bank turn was established and AOA allowed to increase. Power was modulated to minimize sink rate. Because of the sink rate and narrow data bank, the AOA was not stopped at intermittent values, but rather increased up to the onset of wing rock. The wing rock characteristics of the aircraft were then observed and recorded at this and higher AOA values. The process was terminated upon exiting the data band. The maneuver was then repeated in the opposite direction.

**Symmetric Pullup**

To complete the symmetric pullup maneuver, the aircraft was trimmed to steady level flight at 23,000-24,000 ft PA and Mach=0.6. This corresponded to approximately 275 KCAS. The aircraft was then pulled to a set AOA and airspeed was allowed to increase to maintain 0.6 mach until the aircraft exited the data band. Any wing rock characteristics were recorded. This maneuver was repeated for each AOA tested, with a single AOA captured for each maneuver.

# APPENDIX G

# TEST POINT SUMMARY
# &
# DATA TOLERANCE

**Table G1**
**Test Point Summary**

| TEST PT. | TRIM CONDITION | MANEUVER | STABILIZED AOA[1] (COCKPIT UNITS) | G | BLEED RATE KT/SEC | REMARK |
|---|---|---|---|---|---|---|
| 1 | 20K, .25 CPU AOA | 1 G Stall | 30,32,34,36,38,40 | 1 | 1 | Roll CAS off |
| 2 | 20K, .25 CPU AOA | 10 deg banked turn | 30,34,38 | 1 | 2-4 | Roll CAS off |
| 3 | 20K, .25 CPU AOA | 30 deg banked turn | 30,34,38 | 1.2 | 2-4 | Roll CAS off |
| 4 | 20K, .25 CPU AOA | 70 deg banked turn | 30,34,38 | 2.9 | 2-4 | Roll CAS off |
| 5 | 20K, M=0.6 | Symmetric pullup | N/A | 6 | 2-4 | Roll CAS off |

NOTES: 1. F-15 will be temporarily stabilized at these angles at attack to study wing rock onset and limit cycle behavior. T-38 was be stabilized at different angles of attack that was determined in the initial phases of this program.

**Table G2**
**Data Tolerances**

| PARAMETER | TOLERANCE |
|---|---|
| Altitude | ± 2000' |
| AOA | ± 1 degree |
| Bank Angle | ± 2 degrees |
| Mach Number | ± 0.02 |

## BIBLIOGRAPHY


1. Nguyen,L.T., Gilbert, W.P., Gera, J., Iliff, K.W., Enevoldson, E.K., Carr, P.C. "Application of High-alpha Control System Concepts to a Variable Sweep Fighter Airplane." NASA Tactical Aircraft Research and Technology, Vol. 1, Part 1. 1980

2. Nguyen, L.T. and Ross, A.J. "Some Observations Regarding Wing Rock Oscillations At Higl. Angles of Attack." AIAA Paper 88-4371-CP Aug. 1988.

3. "Manoeuvre Limitations of Combat Aircraft." AGARD AR-155A, Aug. 1979.

4. Lusby, W.A. and Hanks, N.J. T-38A Category II Stability and Control Tests. AFFTC-TR-61-15. Edwards AFB CA: HQ AFFTC, August 1961. (AD-263411)

5. Hsu, C.H. and Lan, C.E. "Theory of Wing Rock." Journal of Aircraft, Vol.22, No.10 1985.

6. Ericson, L.E."Various Sources of Wing Rock." Journal of Aircraft, Vol.27, No.6 1990

7. Air Force Flight Test Center. F-15A Approach-to-Stall/Stall/Post-Stall Evaluation. AFFTC-TR-75-32. Edwards AFB CA: HQ AFFTC, January 1976 (AD-B045115)

8. Croom, M.A., Whipple, R.D., et al. "High-Alpha Flight Dynamics Research on the X-29 Configuration Using Dynamic Model Test Techniques." SAE Paper 881420. October 1988.

9. Roskam, J. Airplane Flight Dynamics. Roskam Aviation and Engineering Corporation, Ottawa KS. 1979.

10. Baumann, Capt Daniel D. F-15B High Angle-of-Attack Phenomena and Spin Prediction Using Bifurcation Analysis. MS Thesis, AFIT/GAE/ENY/89D-01. School of Engineering, Air Force Institute of Technology (AU), Wright-Patterson AFB OH, December 1989.

11. Dodel, E. and Kernevez,J.P. Software for Continuation Problems in Ordinary Differential Equations with Applications.
California Institute of Technology, Pasadena, CA.

12. Barth, Capt Thomas J. Determination of High Angle-of-Attack Phenomena and Spin Prediction Using Bifurcation Analysis. MS Thesis, AFIT/GAE/AA/87D-01. School of Engineering, Air Force Institute of Technology (AU), Wright-Patterson AFB, OH, December 1987.

13. Beck, Capt Jeffrey A. Bifurcation Analysis of a Model Fighter Aircraft with Control Augmentation. MS Thesis, AFIT/GAE/ENY/89D-01. School of Engineering, Air Force Institute of Technology (AU), Wright-Patterson AFB, OH, December, 1989.

14. McDonnell, Capt Robert J. Investigation of the High Angle of Attack Dynamics of the F-15B Using Bifurcation Analysis. MS Thesis, AFIT/GAE/ENY/90D-16. School of Engineering, Air Force Institute of Technology (AU), Wright-Patterson AFB, OH, December, 1990.

15. Ross, A.J. "Lateral Stability at High Angles of Attack, Particularly Wing Rock." AGARD-CP-260, 1978.

16. Johnston, D.E., Mitchell, D.G. and Myers, T.T. Investigation of High Angle-of-Attack Maneuver-Limiting Factors. AFWAL-TR-80-3141. December 1980.

17. Planeaux, J.B, Beck, J.A., and Baumann, D.D. "Bifurcation Analysis of a Model Fighter Aircraft with Control Augmentation." AIAA Paper AIAA-90-2863 August 1990.

18. Davison, M., Lockhart, P., and Mlnarik, R. F-15D Wing Rock Investigation, USAFTPS unpublished report, December 1991.

19. Hwang,C. and Pi, W.S. "Some Observations on the Mechanism of Wing Rock." Journal of Aircraft, Vol. 16, No. 4, 1979

20. Sedeyel, R., From Equilibrium to Chaos: Practical Bifurcation And Stability Analysis. New York: Elsiver Press, 1988.

21. Davison, M., Lockhart, P. and Mlnarik, R. Project Wing Rock Test Plan, November, 1991.

22. USAF Series F-15A/B/C/D Aircraft Flight Manual, TO 1F-15A-1, 15 January 1984

23. McDonnell Aircraft Company. F/TF-15 Stability Derivatives, Mass, and Inertia Characteristics Flight Test Basis, Part I, Mass and Inertia Characteristics, Report No. MDC A4172.

24. Carrol, J.V. and Merha, R.K., "Bifurcation Analysis of Nonlinear Aircraft Dynamics", AIAA Paper 82-4254, Journal of Guidance and Control, 5:529-536 (Sept-Oct 1982).

## VITA

Captain Michael T. Davison was born in Mansfield, Massachusetts on 11 August 1964. He graduated from Mansfield High School in June 1982. He attended the University of Oklahoma, at Norman, Oklahoma, majoring in Aerospace Engineering. He received his Bachelor of Science in Aerospace Engineering (with Special Distinction) on 9 May 1987. Upon graduation, he received his commission through USAF Reserve Officer Training Program (ROTC). He was then assigned to the Ballistic Missile Office where he worked on the third stage of the Small Intercontential Ballistic Missile (SICBM). In 1989, Captain Davison was selected for the Joint Air Force Institute of Technology- Test Pilot School (AFIT/TPS) Program. He entered AFIT in September 1989 and after completing the course work at Wright-Patterson began the Flight Test Engineering course at the USAF Test Pilot School in January 1991. He graduated from the Test Pilot School in December 1991 and upon completion of the AFIT/TPS thesis project received a Master of Science degree in Aeronautical Engineering from the Air Force Institute of Technology.

# REPORT DOCUMENTATION PAGE

Form Approved
OMB No. 0704-0188



| 1. AGENCY USE ONLY (Leave blank) | 2. REPORT DATE | 3. REPORT TYPE AND DATES COVERED |
|---|---|---|
| | February 1992 | Final April 1991-February 1992 |

**4. TITLE AND SUBTITLE**
An Examination of Wing Rock in the F-15

**5. FUNDING NUMBERS**

**6. AUTHOR(S)**
Davison, Michael T. Capt, USAF

**7. PERFORMING ORGANIZATION NAME(S) AND ADDRESS(ES)**
AFIT/ENY
WPAFB, Oh, 45433

**8. PERFORMING ORGANIZATION REPORT NUMBER**

**9. SPONSORING/MONITORING AGENCY NAME(S) AND ADDRESS(ES)**
USAFTPS/ED
Edwards AFB CA 93523

**10. SPONSORING/MONITORING AGENCY REPORT NUMBER**

**11. SUPPLEMENTARY NOTES**

**12a. DISTRIBUTION/AVAILABILITY STATEMENT**
Distribution Unlimited

**12b. DISTRIBUTION CODE**

**13. ABSTRACT** *(Maximum 200 words)*

Wing rock in the F-15 was examined both analytically and experimentally. Using a previously developed model for the F-15, bifurcati. . analysis and continuation techniques were used to map out the periodic wing rock solutions and the equilibrum solutions leading up to wing rock. This was done for four manuvers; a 1 g stall, rudder sweeps, constant bank turns and a symmetric pullup. To supplement this research, time history simulations were used to examine the time history of wing rock. A study of stability derivatives was also done, to determine the critical parameters in wing rock. Bifurcation was also used to study candidate feedback architectures used to supress wing rock. It was found that feeding back roll rate was effective in delaying wing rock onset and supressing the subisiquent motion, but this made the aircraft more departure prone.

The results of the 1 g stall, constant bank turns, and the symmetric pullup were experimentally tested through flight test. Wing rock onset differed 4 degrees AOA from predicted in all manuvers but the symmetricpullup, where the flight mach number correlated with the computer model's flight condition. Wing rock was found to be highly random and non periodic, directly contradicting computer predictions and prior research.

| 14. SUBJECT TERMS | 15. NUMBER OF PAGES |
|---|---|
| High AOA Stability and Control F-15 Wing Rock, Stability Derivatives Stall | 168 |
| | 16. PRICE CODE |

| 17. SECURITY CLASSIFICATION OF REPORT | 18. SECURITY CLASSIFICATION OF THIS PAGE | 19. SECURITY CLASSIFICATION OF ABSTRACT | 20. LIMITATION OF ABSTRACT |
|---|---|---|---|
| Unclassified | Unclassified | Unclassified | Unlimited |

## GENERAL INSTRUCTIONS FOR COMPLETING SF 298

The Report Documentation Page (RDP) is used in announcing and cataloging reports. It is important that this information be consistent with the rest of the report, particularly the cover and title page. Instructions for filling in each block of the form follow. It is important to ***stay within the lines*** to meet ***optical scanning requirements***

**Block 1.** Agency Use Only *(Leave blank)*.

**Block 2.** Report Date. Full publication date including day, month, and year, if available (e.g. 1 Jan 88). Must cite at least the year.

**Block 3.** Type of Report and Dates Covered. State whether report is interim, final, etc. If applicable, enter inclusive report dates (e.g. 10 Jun 87 - 30 Jun 88).

**Block 4.** Title and Subtitle. A title is taken from the part of the report that provides the most meaningful and complete information. When a report is prepared in more than one volume, repeat the primary title, add volume number, and include subtitle for the specific volume. On classified documents enter the title classification in parentheses.

**Block 5.** Funding Numbers. To include contract and grant numbers; may include program element number(s), project number(s), task number(s), and work unit number(s). Use the following labels:

| | | | |
|---|---|---|---|
| C | - Contract | PR | - Project |
| G | - Grant | TA | - Task |
| PE | - Program Element | WU | - Work Unit Accession No. |

**Block 6.** Author(s). Name(s) of person(s) responsible for writing the report, performing the research, or credited with the content of the report. If editor or compiler, this should follow the name(s).

**Block 7.** Performing Organization Name(s) and Address(es). Self-explanatory.

**Block 8.** Performing Organization Report Number. Enter the unique alphanumeric report number(s) assigned by the organization performing the report.

**Block 9.** Sponsoring/Monitoring Agency Name(s) and Address(es). Self-explanatory.

**Block 10.** Sponsoring/Monitoring Agency Report Number. *(If known)*

**Block 11.** Supplementary Notes. Enter information not included elsewhere such as: Prepared in cooperation with...; Trans. of...; To be published in.... When a report is revised, include a statement whether the new report supersedes or supplements the older report.

**Block 12a.** Distribution/Availability Statement. Denotes public availability or limitations. Cite any availability to the public. Enter additional limitations or special markings in all capitals (e.g. NOFORN, REL, ITAR).

- **DOD** - See DoDD 5230.24, "Distribution Statements on Technical Documents."
- **DOE** - See authorities.
- **NASA** - See Handbook NHB 2200.2.
- **NTIS** - Leave blank.

**Block 12b.** Distribution Code.

- **DOD** - Leave blank.
- **DOE** - Enter DOE distribution categories from the Standard Distribution for Unclassified Scientific and Technical Reports.
- **NASA** - Leave blank.
- **NTIS** - Leave blank.

**Block 13.** Abstract. Include a brief *(Maximum 200 words)* factual summary of the most significant information contained in the report.

**Block 14.** Subject Terms. Keywords or phrases identifying major subjects in the report.

**Block 15.** Number of Pages. Enter the total number of pages.

**Block 16.** Price Code. Enter appropriate price code *(NTIS only)*.

**Blocks 17. - 19.** Security Classifications. Self-explanatory. Enter U.S. Security Classification in accordance with U.S. Security Regulations (i.e., UNCLASSIFIED). If form contains classified information, stamp classification on the top and bottom of the page.

**Block 20.** Limitation of Abstract. This block must be completed to assign a limitation to the abstract. Enter either UL (unlimited) or SAR (same as report). An entry in this block is necessary if the abstract is to be limited. If blank, the abstract is assumed to be unlimited.